

Characterization of inducible

SYK knockout mice

Dissertation

zur Erlangung des akademischen Grades des Doktors der
Naturwissenschaften (Dr. rer. nat.)

an der

Universität Konstanz

Mathematisch-Naturwissenschaftliche Sektion

Fachbereich Biologie

vorgelegt von

Dipl. Biochem. Eva Wex

Tag der mündlichen Prüfung: 23.02.2011

1. Referent: Prof. Dr. Florian Gantner

2. Referent: Prof. Dr. Marcel Leist

For my parents

I. ABSTRACT

Spleen tyrosine kinase (SYK) is a key mediator of immunoreceptor signalling in inflammatory cells. Thus, interfering with the function of SYK by genetic deletion or pharmacological inhibition might influence a variety of allergic and autoimmune processes. Since conventional SYK knockout mice are not viable, studies addressing the effect of SYK deletion in adult animals have been limited. To further explore *in vivo* functions of SYK inducible SYK knockout mice were generated. These mice harbour a floxed *Syk* gene and a tamoxifen-inducible Cre recombinase under the control of the ubiquitously active *Rosa26*-promoter. This study shows that treatment of mice with tamoxifen led to the deletion of SYK in all organs analyzed. Long-term SYK deletion induced in adult mice reduced B cell counts and slightly improved mechanical bone properties. Furthermore, SYK deletion reduced inflammatory responses in mast cell-driven animal models, including models of passive cutaneous anaphylaxis and ovalbumin-induced lung eosinophilia, but had no effect on the migration of macrophages or neutrophils in models of MCP-1-, cigarette smoke- and lipopolysaccharide-induced lung inflammation, as well as in a model of thioglycollate-induced peritonitis. Therefore, the inducible SYK knockout mice presented here provide a valuable tool to further explore the role of SYK *in vivo*.

II. TABLE OF CONTENTS

I. ABSTRACT	I
II. TABLE OF CONTENTS.....	II
III. ABBREVIATIONS	VII
IV. AIM OF THE STUDY	IX
1. INTRODUCTION	1
1.1. Domain structure of SYK	1
1.2. Function of SYK	3
1.3. Distinct function of SYK in different cell types	5
1.3.1. Function of SYK in B cells	6
1.3.2. Function of SYK in mast cells	7
1.3.3. Function of SYK in neutrophils.....	8
1.3.4. Function of SYK in macrophages.....	10
1.3.5. Function of SYK in osteoclasts	11
1.4. Conditional Gene Targeting	12
2. MATERIALS AND METHODS	14
2.1. Materials	14
2.1.1. Reagents	14
2.1.2. Antibodies.....	14
2.1.3. Buffers and cell culture media	16
2.2. Animals.....	17
2.3. Methods.....	17
2.3.1. Animal housing and handling.....	17
2.3.2. Generation of inducible SYK knockout mice	17

2.3.3. Tamoxifen induction of knockout	17
2.3.4. Analysis of knockout efficiency	18
2.3.4.1. PCR analysis of genomic DNA	18
2.3.4.2. Western blot analysis of tissue samples	18
2.3.4.3. Quantitative real-time PCR	19
2.3.5. <i>In vitro</i> assays	20
2.3.5.1. B cells	20
2.3.5.1.1. Staining of B and T cells in whole blood	20
2.3.5.1.2. Isolation of splenic B cells	20
2.3.5.1.3. Intracellular staining of SYK for flow cytometric analysis	20
2.3.5.1.4. Calcium assay with splenic B cells	21
2.3.5.1.5. Anti-IgM-induced CD25 and CD69 expression on splenic B cells	21
2.3.5.2. Bone marrow-derived mast cells	22
2.3.5.2.1. Preparation of mouse bone marrow-derived mast cells	22
2.3.5.2.2. Calcium assay with mouse bone marrow-derived mast cells	22
2.3.5.2.3. Histamine release assay with mouse bone marrow-derived mast cells	22
2.3.5.2.4. Stimulation of mouse bone marrow-derived mast cells for Western blotting	23
2.3.5.3. Splenocytes	23
2.3.5.3.1. CD23 staining of splenocytes	23
2.3.5.3.2. IL-3-induced cytokine release from splenocytes	23
2.3.5.4. Neutrophils	24
2.3.5.4.1. Chemotaxis assay using primary neutrophils	24
2.3.5.5. Osteoclasts	24
2.3.5.5.1. <i>In vitro</i> generation of osteoclasts and functional analysis	24

2.3.6. <i>In vivo</i> studies	25
2.3.6.1. IgE-induced passive cutaneous anaphylaxis.....	25
2.3.6.2. Ovalbumin-induced pulmonary eosinophilia	26
2.3.6.3. Thioglycollate-induced sterile peritonitis.....	27
2.3.6.4. Lipopolysaccharid-induced pulmonary inflammation.....	27
2.3.6.5. Cigarette smoke-induced pulmonary inflammation	27
2.3.6.6. MCP-1-induced lung inflammation	28
2.3.6.7. Treatment of animals for bone analysis.....	29
2.3.7. Bone analysis	29
2.3.7.1. Tartrate-resistant acid phosphatase and alkaline phosphatase staining of humeri	29
2.3.7.2. Microcomputed tomography (μ CT) analysis of cortical and trabecular bone	30
2.3.7.3. Mechanical tests	30
2.3.8. Total and differential cell count.....	31
2.3.9. Statistical analysis	31
3. RESULTS.....	32
3.1. Generation of tamoxifen-inducible SYK knockout mice	32
3.1.1. Principle and proof of concept	32
3.1.2. Establishment of a tamoxifen treatment protocol for short-term SYK deletion	33
3.1.3. Short-term SYK deletion has no negative impact on the health status of iSYKKO mice	34
3.1.4. SYK expression recurs with time – Development of a tamoxifen-treatment protocol for long-term SYK deletion	35
3.2. Function of SYK in B cells	37
3.2.1. Long-term SYK deletion leads to a gradual reduction of B lymphocytes in blood	37
3.2.2. Calcium signalling in B cells is dependent on the activity of SYK.....	39
3.2.3. CD69 and CD25 expression is inhibited in SYK negative B cells <i>in vitro</i>	40

3.3. Function of SYK in mast cells.....	41
3.3.1. SYK deleted bone marrow cells differentiate normally into mature BMMCs <i>in vitro</i> but do not respond to FcεRI cross-linking.....	41
3.3.2. Pharmacological inhibition of SYK abrogates FcεRI-triggered signal transduction in mBMMCs....	43
3.3.3. Deletion and pharmacological inhibition of SYK reduces the IgE-induced passive cutaneous anaphylaxis (PCA) reaction	45
3.3.4. SYK deletion reduces pathology in a model of ovalbumin-induced pulmonary eosinophilia in a therapeutic and prophylactic setting	46
3.3.4.1. Therapeutic setup	47
3.3.4.2. Prophylactic setup.....	49
3.3.5. Pharmacological inhibition of SYK reduces ovalbumin-induced pulmonary eosinophilic inflammation in a therapeutic setup	51
3.4. Combined effect of reduced B cell counts and inhibition of mast cell function	52
3.4.1. Long-term SYK deletion improves pathology but leads to increased IgE levels in a model of ovalbumin-induced lung eosinophilia.....	52
3.4.2. Total CD23 expression on spleen cells is reduced after long-term SYK deletion.....	55
3.5. Function of SYK in splenocytes	56
3.5.1. IL-3-induced cytokine production from primary splenocytes is defective after deletion or pharmacological inhibition of SYK	56
3.6. Function of SYK in neutrophils.....	58
3.6.1. SYK deletion results in increased chemotactic activity of SYK negative neutrophils <i>in vitro</i>	58
3.6.2. SYK is not required <i>in vivo</i> for the migration of neutrophils in models of thioglycollate-induced sterile peritonitis and LPS- or CS-induced pulmonary inflammation	59
3.7. Function of SYK in macrophages.....	60
3.7.1. SYK deletion has no influence on cell recruitment in models of MCP-1 and cigarette smoke-induced monocytic lung inflammation	60
3.8. Function of SYK in osteoclasts	62

3.8.1. <i>In vitro</i> differentiation and function is inhibited in SYK negative osteoclasts	62
3.8.2. Pharmacological inhibition of SYK activity concentration-dependently inhibits osteoclast differentiation and function <i>in vitro</i>	64
3.8.3. SYK deletion leads to reduced TRACP 5b and CTX-I levels in the serum of SYK knockout mice	66
3.8.4. Osteoblast and osteoclast numbers in humeri are not affected after 18 weeks of SYK deletion ..	67
3.8.5. Cortical thickness of femora is increased in female mice after 18 weeks of SYK deletion	68
3.8.6. Changes in trabecular parameters are only seen in female SYK knockout mice after 18 weeks of SYK deletion	69
3.8.7. Maximum torsional strength and energy to failure are increased in the femora of female iSYKKO ^{-/-} mice	74
4. DISCUSSION.....	75
4.1. Tamoxifen-inducible SYK deletion	75
4.2. Function of SYK in B cells	76
4.3. Function of SYK in mast cells.....	77
4.4. Combined effect of reduced B cell counts and inhibition of mast cell function	79
4.5. Function of SYK in splenocytes	81
4.6. Function of SYK in neutrophils.....	82
4.7. Function of SYK in macrophages.....	84
4.8. Function of SYK in osteoclasts	84
5. SUMMARY	88
6. ZUSAMMENFASSUNG	90
7. REFERENCES	92
8. ACKNOWLEDGEMENTS	103
9. PUBLICATIONS.....	104

III. ABBREVIATIONS

BALF	bronchoalveolar lavage fluid
BCR	B cell receptor
BSA	bovine serum albumin
DAP12	DNAX-activation protein 12
CBL	Casitas B cell lymphoma
COPD	chronic obstructive pulmonary disease
CS	cigarette smoke
DNP-BSA	2,4-dinitrophenyl bovine serum albumin
FBS	fetal bovine serum
FcεR	Fc receptor for IgE
FcεRI	high affinity IgE receptor
FcγR	Fc receptor for IgG
FcRγ	Fc receptor γ-chain
FEV ₁	forced expiratory volume in one second
fMLP	N-formyl-methionyl-leucyl-phenylalanine
GPCR	G protein coupled receptor
iSYKKO	inducible SYK knockout
IL	interleukin
i.p.	intraperitoneal
iSYKKO ^{-/-}	tamoxifen-treated inducible SYK knockout mice
iSYKKO ^{+/+}	vehicle-treated inducible SYK knockout mice
ITAM	immunoreceptor tyrosine-based activation motif
KC	keratinocyte-derived cytokine
LAT	linker for activation of T cells
LDS	lithium dodecyl sulfate
LPS	lipopolysaccharide
MAPK	mitogen-activated protein kinase

MCP-1	monocyte chemotactic protein-1
M-CSF	macrophage colony-stimulating factor
μ CT	microcomputed tomography
mBMMCs	mouse bone marrow derived mast cells
NF- κ B	nuclear factor κ B
NK cell	natural killer cell
OVA	ovalbumin
PCA	passive cutaneous anaphylaxis
PI3K	phosphoinositide 3-kinases
PLC γ	phospholipase C γ
p.o.	per os
RA	rheumatoid arthritis
RANKL	receptor activator for nuclear factor κ B ligand
ROS	reactive oxygen species
SH2	SRC homology 2
SFK	SRC family kinases
SFO	sun flower oil
SLP-65	SRC homology 2 domain-containing leukocyte protein of 65 kDa
SYK	spleen tyrosine kinase
TBS	Tris buffered saline
TCR	T cell receptor
TM	tamoxifen
TRAP	tartrate-resistant acid phosphatase
WBC	white blood cell
WT	wild type
ZAP-70	zeta-chain-associated protein kinase 70

IV. AIM OF THE STUDY

The non-receptor tyrosine kinase SYK has been implicated in signal transduction downstream of cell surface receptors in many cells of hematopoietic and non-hematopoietic origin. Altered SYK expression and activity were found to be involved in the pathogenesis of a diverse pattern of malignancies including peripheral T-cell lymphomas, systemic lupus erythematosus and B cell lymphomas. However, knowledge of the role of SYK *in vivo* is limited since germ-line deleted SYK knockout mice are not viable. Thus, the main goal of this study was to provide an *in vivo* model to explore the consequences of a long-term pharmacotherapy targeting SYK.

For this purpose a tamoxifen-inducible SYK knockout mouse strain was generated allowing the induced deletion of SYK in adult mice in all cells of the body, thereby circumventing developmental issues observed in germ-line deleted SYK knockout mice. In a first set of experiments tamoxifen-induction protocols were established that guaranteed a prominent and sustained knockout of the target gene while keeping tamoxifen exposure as low as possible. Using these protocols SYK deletion was induced and physiological parameters were monitored to determine whether the deletion of SYK has an impact on the general health status of adult mice both after short- and long-term SYK deletion. To verify and further elucidate the role of SYK in the pathogenesis of allergic and inflammatory processes both, *in vitro* and *in vivo*, cells of vehicle- or tamoxifen-treated animals were isolated and analyzed and a variety of disease-related animal models were conducted.

1. INTRODUCTION

1.1. Domain structure of SYK

Spleen tyrosine kinase (SYK) is a 72 kDa protein containing two N-terminal SRC homology 2 (SH2) domains followed by a C-terminal tyrosine kinase domain and a short COOH-terminal extension (1). SYK contains multiple tyrosine residues that play an important role in the regulation of SYK activity. Throughout this thesis amino acid numbers are enumerated as in mouse SYK.

In general SH2 domains are involved in the regulation and binding of proteins and participate in substrate recognition. The two SYK SH2 domains specifically bind to dual-phosphorylated immunoreceptor tyrosine-based activating motifs (ITAM) which are found in immunoreceptor-associated transmembrane adapters or in the cytoplasmic tail of the ligand binding receptor chain itself. ITAMs typically have the consensus sequence [D/E]xxYxx[L/I]_{x(6-8)}Yxx[L/I] (one-letter code for amino acids with x representing any amino acid) (2). SYK is able to transduce signals downstream of several different immunoreceptors with different numbers of amino acids spaced between the two tyrosine residues within the ITAM motif. This ability is due to the fact that the tandem SH2 domains of SYK display high conformational flexibility enabling them to evaluate the distance between phosphotyrosines and to adjust their relative orientation to fit that spacing (3).

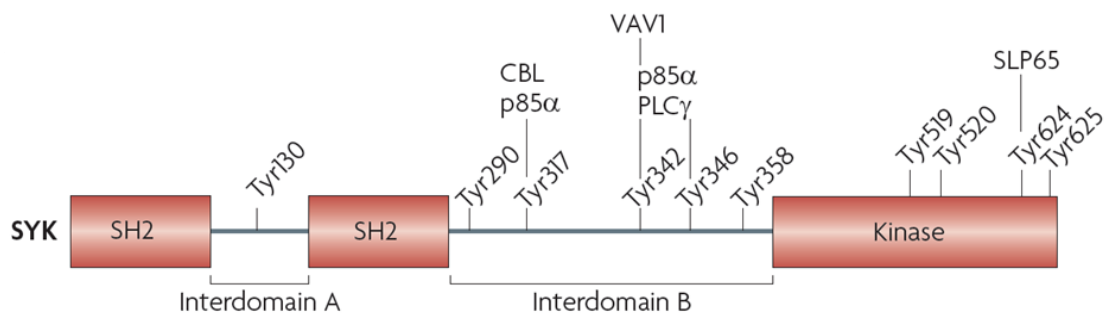


Fig. 1: The domain structure of SYK with tyrosine residues shown to be sites of autophosphorylation. Proteins that bind to phosphorylated tyrosines are indicated above the respective tyrosine residues. Amino acids are enumerated as in mouse SYK. (Copied from Mocsai *et al.* (4).)

The SH2 domains of SYK are separated by a region called interdomain A, which is highly conserved between different species and contains one autophosphorylation site (Tyr130) (Fig. 1). Tyr130 is phosphorylated upon activation of the B cell receptor (BCR) (5). This leads to the dissociation of SYK from the phosphorylated ITAMs of the BCR complex (6,7). Mutation studies of Tyr130 to glutamic acid led to decreased ITAM binding and increased kinase activity, supporting an inhibitory role of interdomain A (6).

The second SH2 domain and the kinase domain of SYK are separated by a region called interdomain B or 'linker region'. The interdomain B contains multiple tyrosines which, when phosphorylated, act as docking sites for the direct binding of downstream effector molecules. For example, phosphorylated Tyr317 is a binding site for the ubiquitin ligase CBL, which is involved in the regulation of SYK activity through its ubiquitylation and degradation (8). Furthermore, phosphorylated Tyr317, Tyr342 and Tyr346 serve as binding sites for the SH2 domains of the p85 α subunit of the phosphoinositide 3-kinases (PI3K) (9). Phosphorylated Tyr342 further serves as a docking site for the SH2 domain of VAV1 (10) and phosphorylated Tyr342 and Tyr346 bind to the SH2 domains of phospholipase C γ 1 (PLC γ 1) (11). Within its linker region SYK also contains a 23 amino acid insert which is not found in SYKB, which is an alternatively spliced form of SYK (12) and ZAP-70, the SYK equivalent expressed in T cells and natural killer cells (13). The role of this 23 amino acid insert is only poorly understood but experiments have shown that it executes at least two functions. First, the insert contains a signal sequence which is required for the nuclear translocation of SYK (14), and second, the insert is responsible for the higher binding affinity of SYK to phosphorylated ITAMs compared to ZAP-70 and SYKB (15).

The SYK kinase domain has a K_m (Michaelis constant) for ATP of $\sim 10 \mu\text{M}$ (16) and contains autophosphorylation sites (Tyr519 and Tyr520) that are essential for the induction of SYK activity (1,17).

C-terminal to the catalytic domain lie two tyrosine residues, Tyr624 and Tyr625, which give rise to gain-of-function mutants when mutated to phenylalanine (18). The mechanism by which these C-terminal tyrosines mediate their inhibitory effect is not known but might

involve the binding of a phosphatase which dephosphorylates SYK or the participation of these tyrosines in the stabilization of an autoinhibitory conformation. Furthermore, Tyr624 binds to the SH2 domain of SLP-65 (also known as BLNK) which is an important adapter in signalling events downstream of the BCR (19).

1.2. Function of SYK

SYK was long considered as a tyrosine kinase exclusively involved in signal transduction downstream of adaptive immune receptors in leukocytes. However, recent observations demonstrated the involvement of SYK in a variety of biological functions, including cellular adhesion, degranulation, innate immune recognition, osteoclast maturation and function, and platelet activation even in cells outside the hematopoietic lineage (4).

SYK plays a pivotal role in the regulation of signals downstream of classical immunoreceptors, such as Fc receptors (FcRs), B cell receptors (BCRs), T-cell receptors (TCRs) and NK receptors, in a multitude of different cell types including B cells, mast cells, neutrophils, macrophages, and osteoclasts. Independent of the particular cell type, pathways involving the activation of SYK downstream of ITAM-bearing receptor complexes share common characteristics and can be summarized as follows: ligation of an immunoreceptor results in the activation of receptor-associated SRC family kinases (SFKs), such as Lyn and Fyn, which are critical regulators of immunoreceptor signalling (20,21). SRC kinases increase their own activity through autophosphorylation (22) and subsequently phosphorylate the tyrosine residues in the ITAM motifs located in the cytoplasmic domains of immunoreceptor-associated transmembrane adapters or, in the case of FcγRIIA, in the ligand binding receptor chain itself. Through interaction with the tandem SH2 domains of SYK the dual-phosphorylated ITAMs recruit SYK to the activated receptor complex (23). Binding of SYK results in conformational changes in the SYK protein which lead to an increase in SYK kinase activity (24,25). Activated SYK is tyrosine-phosphorylated, predominantly due to autophosphorylation which further increases its own kinase activity and creates docking sites for downstream signalling molecules (1).

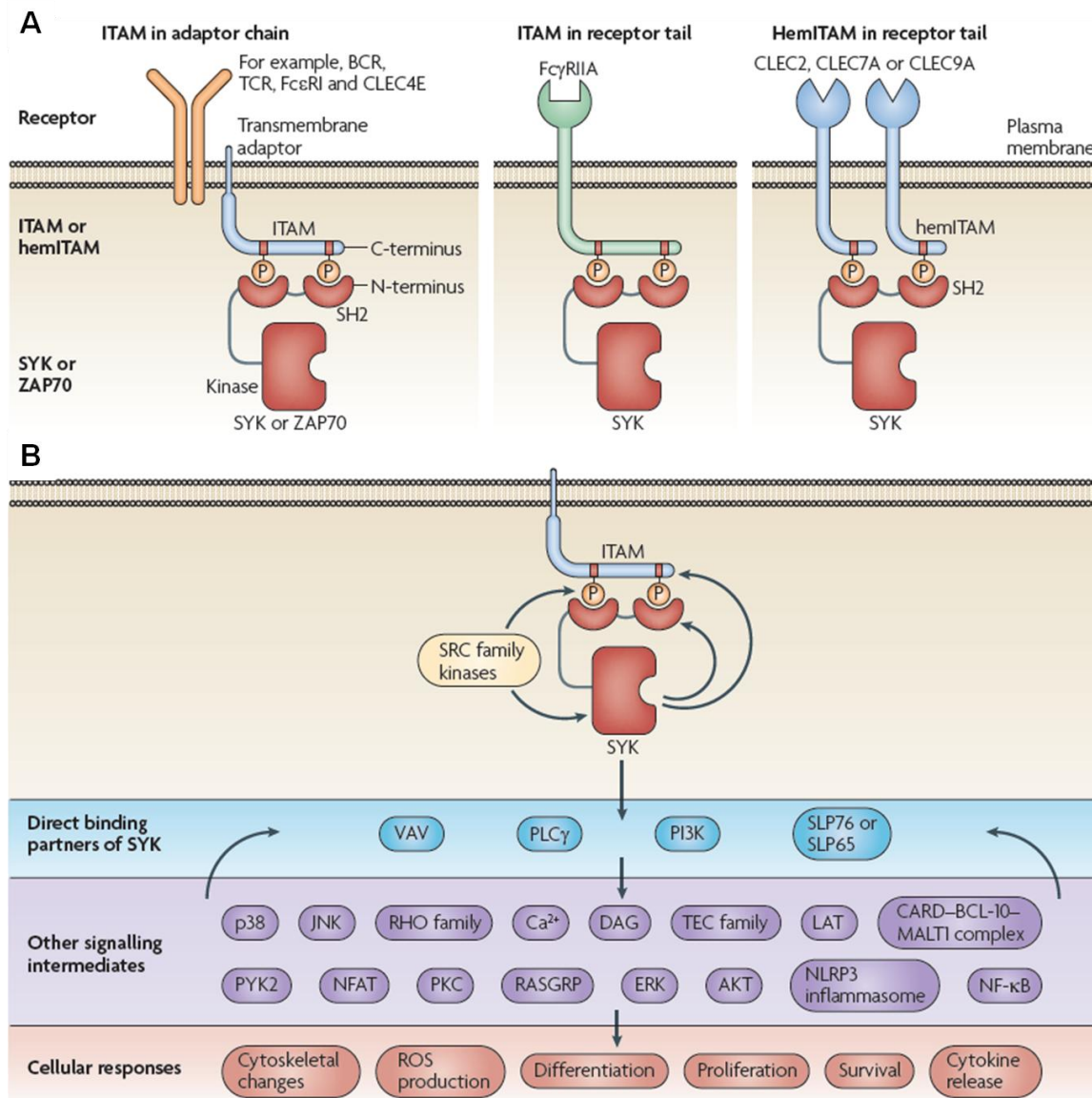


Fig. 2: General mechanism of SYK-mediated signalling. (A) Binding of tandem SH2 domains to dual-phosphorylated tyrosine residues recruits SYK or ZAP-70 to activated cell surface receptors. The two phosphorylated tyrosine residues are either located in a single immunoreceptor tyrosine-based activation motif (ITAM) or in two hemITAMs on two separate receptor peptide chains. (B) General scheme of signal transduction through SYK. (Copied from Mocsai *et al.* (4).)

Through the binding and phosphorylation of downstream targets and through the recruitment of additional SH2-containing adapter proteins SYK invokes multiple downstream signalling pathways, including phosphoinositide 3-kinases (PI3K), Ras signalling pathways,

mitogen-activated protein kinase (MAPK), phospholipase C γ 2 (PLC γ 2) and nuclear factor- κ B (NF- κ B) activation, eventually leading to cytoskeletal rearrangements, degranulation, cytokine release, ROS production, altered gene transcription, differentiation, proliferation and survival (4). In addition to its function in signalling events downstream of classical immunoreceptors, SYK has also been shown to mediate signalling by receptors that do not contain conventional ITAM motifs, including integrins (26), C-type lectins (27) and chemokine receptors (28). However, in these cases ITAM-containing adapter proteins have been found that mediate the interaction between the receptor and SYK. In neutrophils, macrophages and osteoclasts DAP12 and the FcR γ -chain (FcR γ) have been identified as the transmembrane adapter molecules that link β 2 integrin signalling to SYK activation (29). The FcR γ -chain has also been demonstrated to be the adapter protein that links IL-3 receptor signalling to SYK activation in basophils (28). Hence, the participation of SYK in signalling events downstream of receptors, that do not contain ITAM motifs, suggests the possibility that SYK is involved in a variety of biological processes that have not been recognized previously.

1.3. Distinct function of SYK in different cell types

SYK is involved in a variety of biological functions in numerous cell types. While this thesis focuses on the role of SYK in B cells, mast cells, basophils, neutrophils, macrophages and osteoclasts altered SYK expression and activity were found to be the reason for a diverse group of malignancies in a host of different cell types. In T lymphocytes, for example, SYK plays an important role in signalling events downstream of the T cell receptor and higher amounts of SYK expression and activity were associated with the pathogenesis of peripheral T-cell lymphomas or systemic lupus erythematosus (30,31). Furthermore, the strong expression of SYK in mammary glands prompted research into its potential role in mammary carcinogenesis. Numerous studies about the role of SYK in breast cancer have been conducted, however with conflicting outcomes. While some hypothesised that SYK expression is down-regulated in breast cancer others could not confirm this finding (32,33).

1.3.1. Function of SYK in B cells

B cells are an essential element of the adaptive immune response. Besides their role as antigen presenting cells they function in the production of antibodies eventually developing into memory B cells. Differentiation and activation of B cells both depend on signalling from the B cell receptor (BCR). The BCR found on mature B cells is a multiprotein structure. It consists of an antigen-binding subunit, the membrane immunoglobulin (mIg), and a signalling subunit, which is a disulfide-linked heterodimer of the Ig α (CD79a) and Ig β (CD79b) proteins (34). Both Ig α and Ig β contain an immunoreceptor tyrosine-based activation motif (ITAM) within their cytoplasmic tail that initiates signal transduction following BCR aggregation (35). Thus, recognition of an extracellular antigen leads to cross linking of the BCR and with it to the activation of a cascade of intracellular effector molecules including SYK. While the SRC-family kinase Lyn predominantly phosphorylates the ITAM contained in the Ig α -chain, SYK phosphorylates and binds to tyrosine residues present in the ITAM of the Ig α - and Ig β -chains (36). Through the phosphorylation of adapter proteins like SLP-65 (also known as BLNK) SYK further amplifies the signal and activates downstream signalling cascades (19). Thus, in the absence of SYK, few if any signals are sent following BCR clustering preventing most downstream BCR signalling. Accordingly, a marked block in B cell development at the transitions from pro-B cells to pre-B cells and from immature to mature B cells was observed in SYK-deficient embryos (37,38).

Antigen-independent phosphorylation of SYK has been observed in a variety of common B cell malignancies, including follicular lymphoma, diffuse large B cell lymphoma, mantle cell lymphoma and B cell chronic lymphocytic leukemia (39). Furthermore, the oral SYK inhibitor fostamatinib (also known as R406 which is the biologically active component of the prodrug R788) has shown preliminary evidence of clinical activity in patients with chronic lymphocytic leukemia (40) indicating that deregulated SYK activity might contribute to the pathogenesis of those diseases. Additionally, SLP-65 acts as a tumour suppressor in pre-B cells by limiting the pre-B cell proliferation and promoting B cell differentiation (41).

B cells also play a pivotal role in the pathogenesis of autoimmune and allergic diseases. In autoimmune diseases, like rheumatoid arthritis, B cells contribute to the inflammatory response by processing autoantigen and presenting it to T cells, as well as by producing cytokines and autoantibodies (42). Allergic disorders, such as asthma, are accompanied by elevated IgE levels which are produced and released by B cells in response to T_H2 cytokines, such as IL-4 and IL-13. Thus, limiting the activity of SYK downstream of the BCR and as such the activity of downstream signalling molecules might be a reasonable starting point to cure those diseases.

1.3.2. Function of SYK in mast cells

Under physiologic conditions mast cells play a key role in host defence against bacteria and parasites, but under pathological conditions they contribute to allergy and autoimmunity. Mast cells reside at strategic sites such as the skin and the vascular and mucosal barriers and constitutively express large amounts of the high-affinity Fc receptor for IgE (FcεRI) on their surface. The FcεRI receptor is a heterotetramer consisting of one IgE-binding α-subunit, one β-subunit and two γ-chains. Both, the β- and the γ-chains contain ITAM motifs located within their cytoplasmic tails (43). Since the FcεRI has no intrinsic enzymatic activity, the activation of non-receptor protein tyrosine kinases, like SYK, is essential for mast cell signalling (44).

Allergic disorders including allergic asthma, allergic rhinitis, anaphylaxis and atopic dermatitis, are characterized by hypersensitive immune responses, mediated by IgE to foreign antigens. Cross linking of receptor-bound IgE by an antigen on the surface of mast cells initiates FcεRI receptor activation, resulting in the recruitment of SYK which eventually leads to degranulation, altered gene transcription and the de-novo synthesis of cytokines and lipid mediators (45). This massive release of mediators from mast cells in response to antigen exposure occurs within minutes after allergen challenge and mediates the early allergic response, characterized by increased vascular permeability, smooth muscle contraction and the initial influx of inflammatory cells. The late allergic response, which

includes chronic inflammation and tissue remodelling is carried out mainly by cytokines and chemokines that trigger the recruitment of neutrophils, macrophages, eosinophils and T helper 2 (T_H2) cells. In addition to their involvement in classical IgE-mediated allergies, increased numbers of mast cells have also been found in the synovial tissues and fluids of patients with rheumatoid arthritis contributing to the processes of inflammation and matrix degradation (46). Thus, deletion or pharmacological inhibition of SYK will block FcεRI-mediated mast cell activation, providing a therapeutic platform for the treatment of malignancies such as asthma and rheumatoid arthritis.

1.3.3. Function of SYK in neutrophils

Neutrophils constitute the first line of host defence against infections. They dominate the early stages of inflammation and set the stage for repair of tissue damage by macrophages. Under pathological conditions neutrophils are involved in both allergic and inflammatory reactions.

Neutrophils express a diverse repertoire of receptors on their surface, including G-protein coupled receptors (GPCRs), leukocyte-specific CD18 integrins and three classes of Fcγ receptors (FcγRI, FcγRII, and FcγRIII) which are involved in neutrophil responses, including chemotaxis, adhesion, oxidative burst, degranulation and phagocytosis.

Neutrophils are directed to the site of inflammation through the release of chemokines which function by signalling through G-protein coupled receptors (GPCRs). The role of SYK in GPCR signalling is controversial. While some studies have demonstrated the involvement of SYK in signalling events downstream of GPCRs (47-50), others failed to find activation of SYK in response to GPCR ligation (51,52). A more recent *in vivo* study using bone marrow chimeras with a *Syk*^{-/-} hematopoietic system demonstrated normal respiratory burst, degranulation and migration of neutrophils in response to the bacterial peptide fMLP indicating that SYK does not play a major functional role in chemokine signalling in neutrophils (53).

CD18 integrins, are members of the β₂ integrin family. They function as phagocytic receptors

for bacterial uptake and killing and are critical in neutrophil spreading and adhesion during migration, as well as in the release of reactive oxygen species (ROS) and exocytosis of secondary granules. The signalling pathways downstream of CD18 integrins are mediated by the phosphorylation of the ITAM-bearing transmembrane adapters, DAP12 and Fc γ R, and by members of the SRC tyrosine kinase, again leading to SH2-mediated recruitment and activation of SYK (29). SYK is known to be phosphorylated and activated upon β_2 integrin-mediated adhesion and previous data indicated that SYK is constitutively associated with the cytoplasmic tail of CD18 (54-56). The *in vivo* loss of SYK in neutrophils results in reduced clearance of *Staphylococcus aureus* (57), thus proving that SYK is indispensable for CD18-mediated leukocyte activation. *In vitro* studies showed that SYK negative neutrophils fail to undergo respiratory burst and degranulation in response to pro-inflammatory stimuli while adherent to immobilized integrin (54) and that SYK-deficient neutrophils are incapable of generating reactive oxygen intermediates in response to Fc γ R clustering (58). In contrast, the role of SYK in integrin-mediated neutrophil migration is controversial. One study demonstrated a fundamental role of SYK in integrin-mediated neutrophil recruitment (59), whereas another showed that the integrin-dependent *in vitro* or *in vivo* migration of SYK negative neutrophils is not impaired (54).

SYK is not involved in the differentiation of neutrophils, since SYK negative neutrophils isolated from the bone marrow of mouse radiation chimeras do not show developmental defects (58).

Many pathological lung conditions are characterized by neutrophil-dominated inflammation. In COPD, for example, neutrophils are the most abundant inflammatory cell type present in the bronchial wall, bronchial lumen, lung parenchyma, and submucosal glands (60). Furthermore, the incidence of neutrophils in lung and blood of smokers and ex-smokers correlates with the rate of decline in FEV₁ (61). In addition, neutrophils were detected in bronchial biopsy samples obtained during the allergen-induced late asthmatic response (62). In patients with rheumatoid arthritis the release of nitric oxide, reactive oxygen intermediates and pro-inflammatory cytokines from neutrophils and macrophages,

which is triggered by SYK, leads to irreversible joint damage and initiates an inflammatory response (63). Thus, the use of small molecule SYK kinase inhibitors, interacting with the ATP-binding site of SYK, could, by limiting the action of neutrophils, conceivably treat these disorders. In this regard, a phase 2 study using the SYK inhibitor fostamatinib disodium (a prodrug of R406) demonstrated reduced disease activity in patients with rheumatoid arthritis (64). However, one of the key challenges in the treatment of these chronic diseases is to manipulate neutrophil function in a way that does not compromise protection against bacterial and fungal infections.

1.3.4. Function of SYK in macrophages

Macrophages are mononuclear phagocytes derived from monocytic precursors in the blood and bone marrow. They are key effector cells of innate immunity and participate in host defence through a variety of mechanisms. As phagocytes they protect the body from invading pathogens and ingest debris as well as apoptotic and dead cells. Besides their function in the uptake of perturbing objects, they are important sources of pro- and anti-inflammatory cytokines. Being one of the most active secretory cell type in the body, macrophages release a wide range of mediators that regulate inflammation, adaptive immunity, and homeostasis (65,66).

Like neutrophils, macrophages also express Fc γ receptors and β_2 integrins on their surfaces which are involved in the clearance of immune complexes and opsonized pathogens. Apart from phagocytosis, cross-linking of Fc γ receptors and integrins on the surface of mononuclear cells trigger functions such as cell migration, antibody-dependent cell-mediated cytotoxicity, generation of respiratory burst, and production of inflammatory mediators and cytokines. Signal propagation downstream of Fc γ receptors and β_2 integrins is mediated by SYK (67). Thus, *in vitro* treatment of human peripheral blood monocytes with SYK antisense oligodeoxynucleotides suppresses Fc γ R-mediated phagocytosis (68). Furthermore, studies using the murine macrophage cell line RAW264.7 demonstrated that SYK is essential for proper reorganization of the actin cytoskeleton in response to CX3CL1, a

chemotactic factor for monocytes, and is therefore required for cell chemotaxis to CX3CL1 *in vitro* (69). Additionally, similar to the situation in neutrophils, macrophages lacking the ITAM-containing adapter proteins, DAP12 and FcR γ , are defective in integrin-mediated responses (29). However, in macrophages loss of DAP12 alone is sufficient to impair integrin signalling indicating that an interaction between the SYK SH2 domains and the ITAM of DAP12 is required for signalling downstream of integrins in macrophages (29). As such SYK plays a central role in host defence by monocytes.

However, activation of macrophages is not always desirable. Evidence has accumulated demonstrating that lung injury, following inhalation of irritants, is not only due to direct effects of the chemical, but also indirectly to the actions of inflammatory mediators released by infiltrating macrophages (66). Following exposure to toxic agents, macrophages can become hyperresponsive, resulting in dysregulated release of mediators that exacerbate acute tissue injury and promote the development of chronic diseases such as COPD, fibrosis and cancer (70). In COPD macrophage numbers in lung tissue are increased and cigarette smoke further activates those macrophages to release inflammatory mediators, such as TNF- α , IL-8, and LTB $_4$, leading to diffuse persistent inflammation and remodelling of the airways and lung parenchyma (71). As such, targeting SYK might be an appropriate way in the treatment of diseases characterized by dysregulated macrophage activation.

1.3.5. Function of SYK in osteoclasts

Osteoclasts are multinucleated bone-resorbing cells of the myeloid lineage generated by the fusion of mononuclear progenitors of the monocyte/macrophage family. *In vitro* osteoclast differentiation is under the control of two hematopoietic factors, macrophage colony-stimulating factor (M-CSF) and receptor activator of NF κ B ligand (RANKL) (72). Stimulation of osteoclast progenitor cells with M-CSF and RANKL leads to the activation of signalling molecules including the two ITAM-bearing adapter proteins, Dap12 and FcR γ , which signal through SYK (73). These adapters are required for normal bone homeostasis since mice lacking both proteins develop osteopetrosis with a severe defect in osteoclast differentiation (74).

Besides its proposed role in osteoclastogenesis SYK is also important for osteoclast function *in vitro* and *in vivo* (75,76). Both, the $\alpha\beta3$ integrin, the most abundantly expressed integrin in osteoclasts, and c-Fms, the transmembrane receptor for M-CSF, play a pivotal role in cytoskeletal remodelling and actin ring formation, a prerequisite for bone resorption (77,78). Both receptor types collaborate in organizing the osteoclast cytoskeleton by sharing the same effector molecule, Dap12 (76,78). Thus, activation of both, $\alpha\beta3$ integrin and c-Fms, leads to the phosphorylation of Dap12. Activated Dap12 in turn induces the recruitment of several SH2-domain-containing proteins, including SYK, which initiates a signalling cascade leading to cytoskeletal organization (77,78). The requirement of SYK in this process is supported by the fact that SYK negative osteoclasts fail to organize their cytoskeleton, leading to a complete arrest of their bone resorptive capacity *in vitro* (75). Furthermore, an increased skeletal mass in SYK deficient embryos has been described (76). Inhibiting the capability of osteoclasts to resorb bone might be an effective treatment in a variety of disorders. Rheumatoid arthritis, for example, is often complicated by generalized osteopenia, as osteoclasts of patients with rheumatoid arthritis exhibit increased resorptive activity (79). Inhibition of SYK might also be an appropriate treatment for the therapy of osteoporosis since the underlying mechanism is an imbalance between bone formation and bone destruction, and as such, inhibiting osteoclast function might positively impact the severity of symptoms.

1.4. Conditional Gene Targeting

The analysis of gene function based on the generation of mutant mice by homologous recombination in embryonic stem cells is limited if gene disruption is embryonic lethal. In these cases conditional gene targeting is the method of choice (80). One possible system relies on the inducible activation of a bacterial enzyme, the Cre recombinase. Cre targets a specific DNA sequence, the loxP site, and deletes a segment of DNA flanked by two loxP sequences (81). Several possibilities exist to render the Cre recombinase inducible. One possible way is to fuse Cre to the ligand binding domain of a hormone receptor (82). In this

study a chimeric protein consisting of the Cre recombinase fused to the mutated form of the ligand binding domain of the human oestrogen receptor, abbreviated as CreER^{T2}, was used (83). Modification of the ligand binding domain assures that the fusion protein is efficiently activated after administration of the synthetic oestrogen-like agonist tamoxifen, but not in response to endogenous levels of oestrogen. In the absence of tamoxifen CreER^{T2} is retained in the cytoplasm. Only after the binding of tamoxifen the fusion protein is able to enter the nucleus and to delete the DNA sequence located between the loxP sites. Furthermore, the Cre-loxP recombination system does not only allow to set the time of gene deletion, but also to limit gene deletion to distinct cell types or tissues by choosing tissue-specific promoters, that drive the expression of the Cre recombinase. As such, the Cre-loxP system provides a sophisticated tool to analyze the effect of gene deletion in cases where conventional gene deletion has reached its limitations.

However, despite providing several new experimental possibilities, inducible knockout strains also exhibit several shortcomings, that have to be taken into account when working with them. First, efficiency of the induced deletion of a target gene might differ between tissues and always has to be monitored thoroughly. Second, the ligand that induces Cre activation might impact the outcome of the study. Thus, it is necessary to carefully titrate the dose of ligand to achieve a prominent and sustained knockout of the target gene while keeping the exposure to the exogenous ligand as low as possible. Furthermore, it is necessary to include the appropriate controls, e.g. wild type animals that have been treated with the ligand only, to be able to differentiate between effects that are direct consequences of the gene deletion and effects that have been triggered by the exogenous ligand.

2. MATERIALS AND METHODS

2.1. Materials

2.1.1. Reagents

DNP-BSA was purchased from Invitrogen (Eugene, Oregon). Tamoxifen, sun flower oil and Evans Blue were purchased from Sigma-Aldrich Corporation (St. Louis, MO). The SYK inhibitors BAY61-3606 and R406 were synthesized at Boehringer Ingelheim Pharma GmbH & Co. KG (Biberach, Germany). Recombinant mouse IL-3 and recombinant mouse KC were purchased from R&D systems (Minneapolis, MN). The ionophore A23187 was from Calbiochem (La Jolla, CA). The mouse IL-4, IL-5 and IL-6 ELISA sets were purchased from BD (San Diego, CA). The OVA-specific IgE and IgG1 ELISAs were home-made and the antibodies used are indicated in the table below. Triton X-100 was purchased from Serva (Heidelberg, Germany). The histamine ELISA was from Beckman Coulter Immunotech (Marseille, France). The mouse TRACP 5b ELISA was from Immunodiagnostic Systems Ltd (Baldon, Tyne and Wear, UK) and the mouse CTX-I ELISA was from Cusabio Biotech Co. Ltd (Wuhan, China).

2.1.2. Antibodies

Name	Source	Catalogue number	Lot number
Primary antibodies used for Western blotting			
AKT	Cell Signaling Technology	4691	7
Phospho-AKT (Ser473)	Cell Signaling Technology	4058	17
Phospho-AKT (Thr308)	Cell Signaling Technology	2965	3
β -Actin (C4)	Santa Cruz Biotechnology	sc-47778	L1508
ERK	Cell Signaling Technology	9102	18
Phospho-ERK (Thr202/Tyr204)	Cell Signaling Technology	9101	23
LAT	Cell Signaling Technology	9166	1
Phospho-LAT (Tyr191)	Cell Signaling Technology	3584	1
PLCy1	Santa Cruz Biotechnology	sc-58407	I0607
Phospho-PLCy1 (Tyr783)	Cell Signaling Technology	2821	3

Phospho-p38 MAPK (Thr180/Tyr182)	Cell Signaling Technology	9215	1
SLP-76	BD Biosciences	610736	45372
Phospho-SLP-76 (Tyr128)	BD Biosciences	558367	33664
SYK (SYK-01)	Santa Cruz Biotechnology	sc-51703	L0309
SYK (N-19)	Santa Cruz Biotechnology	sc-1077	B1406
Secondary antibodies used for Western blotting			
Peroxidase-conjugated donkey anti-mouse IgG	Jackson ImmunoResearch Laboratories	715-035-150	46232
Peroxidase-conjugated mouse anti-rabbit IgG	Jackson ImmunoResearch Laboratories	211-032-171	65905
Fluorescent-labelled antibodies used for flow cytometry			
APC-conjugated CD3e	BD Biosciences	553066	60549
PE-conjugated CD23	BD Biosciences	553139	32502
FITC-conjugated Fc ϵ RI	eBioscience	11-5898-85	E030644
PE-conjugated c-Kit	BD Biosciences	553355	95988
PE-conjugated SYK (N-19)	Santa Cruz Biotechnology	sc-1077 PE	I1608
PE-Cy [™] 7-conjugated CD45R/B220	BD Biosciences	552772	10894
CD19, CD25, CD69 cocktail	BD Biosciences	558064	55171
Antibody used for the sensitization of mBMMCs			
anti-DNP IgE	Sigma-Aldrich	D8406	
Antibody used for the stimulation of B cells			
Goat anti-mouse IgM	Dianova	115-005-020	82406
Antibodies used for OVA-specific IgE ELISA			
Mouse anti-Ovalbumin IgE	Serotec	MCA2259	0707
Biotin Rat anti-Mouse IgE	BD Biosciences	553419	23320
Antibodies used for OVA-specific IgG1 ELISA			
Mouse anti-Ovalbumin IgG1	Sigma	A6075	M047254
Biotin Rat anti-Mouse IgG1	BD Biosciences	553441	22582

2.1.3. Buffers and cell culture media

TBS (pH 7.5)	10 mM Tris 150 mM NaCl
TBS-T	TBS containing 0.05% (v/v) Tween 20
Blocking buffer	5% (w/v) non-fat dry milk powder in TBS
ACK lysing buffer	155 mM NH ₄ Cl 10 mM KHCO ₃ 0.1 mM EDTA
FACS buffer	PBS (pH 7.2) 0.1% (w/v) BSA
Assay buffer	PBS (pH 7.2) 0.5% (w/v) BSA 2 mM EDTA
Mast cell medium	RPMI medium 1640 10% (v/v) FBS 55 μM β-mercaptoethanol 100 U/ml penicillin 100 μg/ml streptomycin 5 ng/ml recombinant mouse IL-3
Osteoclast medium	Minimum essential medium (MEM) 10% (v/v) FBS 100 U/ml penicillin 100 μg/ml streptomycin

2.2. Animals

BALB/c mice were purchased from Charles River Laboratories (Kisslegg, Germany).

2.3. Methods

2.3.1. Animal housing and handling

Mice were housed in isolated ventilated cages under a 12-hour light-dark cycle and received food and water *ad libitum*. All animal experimentation was conducted in accordance with German national guidelines and legal regulations.

2.3.2. Generation of inducible SYK knockout mice

C57BL/6 -mice heterozygous for a *Syk* gene carrying an exon 2 flanked by two loxP sites (*Syk^{fl/+}*) were obtained from Alexander Tarakhovsky (Rockefeller University) (21) and bred to homozygous *Syk^{fl/fl}* mice. These mice were crossed with homozygous *Rosa26CreER^{T2}* mice (B6D2F1 background, TaconicArtemis Pharmaceuticals GmbH Cologne, Germany). Double homozygous F1 inducible SYK knockout (*Syk^{fl/fl}Rosa26CreER^{(T2)+/+}* = iSYKKO) and wild type (WT) mice were interbred to expand the colony and F2 animals were used for the experiments. For a detailed description on the generation of the *Syk^{fl/+}* mice readers are referred to the original publication by Saijo *et al.* (21).

2.3.3. Tamoxifen induction of knockout

For short-term experiments SYK knockout was induced by the oral administration of 20 mg/kg tamoxifen in 9% (v/v) ethanol in sun flower oil (application volume: 4 ml/kg) on 5 consecutive days. Animals in vehicle-treated control groups received 9% (v/v) ethanol in sun flower oil (application volume: 4 ml/kg) on 5 consecutive days. For long-term knockout studies animals were initially treated on 5 consecutive days by oral administration of tamoxifen or vehicle as mentioned above. To guarantee a sustained knockout of SYK, oral administration of tamoxifen was repeated every six weeks on 3 consecutive days. Vehicle

treatment was repeated accordingly. During p.o. application health status and body weight was checked every day. When p.o. treatment was concluded health status and body weight of animals were monitored twice per week. Throughout this thesis vehicle-treated inducible SYK knockout mice were designated as iSYKKO^{+/+} and tamoxifen-treated inducible SYK knockout mice were designated as iSYKKO^{-/-} mice.

2.3.4. Analysis of knockout efficiency

2.3.4.1. PCR analysis of genomic DNA

For isolation of genomic DNA from tissue samples the QIAamp[®] DNA Mini Kit (Qiagen, Hilden, Germany) was used following the manufacturer's protocol. To confirm the knockout of exon 2 of *Syk*, PCR analysis (FP: 5'-GCCCGTTCTGTGCCTACTGG-3', RP: 5'-GCTGGTTCCTTTT CCTTCC-3') was performed using the PCR Core Kit (Roche, Mannheim, Germany) and 250 ng of isolated genomic DNA. Cycle conditions were 94°C for 3 min, 30 cycles of 94°C for 45 sec, 58°C for 1 min, 72°C for 2 min followed by a final elongation at 72°C for 5 min. PCR fragments were separated on a 1% (w/v) agarose gel.

2.3.4.2. Western blot analysis of tissue samples

Tissue samples were homogenized in Tissue Extraction Reagent I[®] (Invitrogen, Carlsbad, CA) containing Protease and Phosphatase Inhibitor Cocktail (Thermo Scientific, Rockford, IL) for 40 seconds at 6.5 m/s using a FastPrep[®]-24 instrument (MP Biomedicals, Solon, OH). After centrifugation for 5 min at 10,000 rpm (10,600 x g) in a Eppendorf Microcentrifuge (Model 5417 R) the supernatants were either stored at -80°C or directly solubilised in 1 x LDS Sample Buffer (Invitrogen). After addition of NuPAGE[®] Sample Reducing Agent (Invitrogen) samples were heated to 70°C for 10 minutes and run on 4-12% Bis-Tris gels (Invitrogen) at 200 V for 60 min. Proteins were electroblotted onto a PVDF-membrane (Millipore, Bedford, MA) at 100 V for 60 min using a Mini-PROTEAN[®] II electrophoresis cell (Bio-Rad Laboratories, Hercules, CA) and Tris/Glycine transfer buffer (Bio-Rad Laboratories). Membranes were blocked with blocking buffer for 30 minutes and subsequently probed for

one hour with the respective primary antibody and for 30 min with the respective secondary antibody. All primary antibodies, apart from the β -Actin antibody, were diluted 1:1,000 in blocking buffer. The β -Actin antibody was diluted 1:10,000 in blocking buffer. All secondary antibodies were diluted 1:5,000 in blocking buffer. After each antibody incubation step the membranes were washed 4 x 10 min with TBS-T. Membranes were developed using Western Lightning™ Chemiluminescence Reagent *Plus* (Perkin Elmer, Waltham, MA).

2.3.4.3. Quantitative real-time PCR

Total RNA was isolated from whole blood using PAXgene Blood RNA Tubes® and the PAXgene Blood RNA Kit® (PreAnalytix, Hombrechtikon, Switzerland) following the manufacturer's protocol. Reverse transcription was conducted using the High Capacity cDNA Reverse Transcription Kit® (Applied Biosystems, Foster City, CA) according to the manufacturer's protocol. Quantitative Real-Time PCR was carried out using the QuantiFast Probe PCR Kit® (Qiagen, Hilden, Germany) and a custom-made *Syk* specific primer/probe set (FP: 5'-CTCATCAGGGAATATGTGAAACAGA-3', RP: 5'-TGGCTGATGATGGCTTGCT-3', Probe: 5'-FAM/CTGGAACCTTCAGGGCCAGGCTCT/TAMRA-3'). Mouse GAPDH (Applied Biosystems, part number: 4352339E, VIC®/MGB Probe, primer limited) was used as endogenous control. Cyclor conditions were 50°C for 2 min, 95°C for 5 min, 40 cycles of 95°C for 10 sec and 60°C for 1 min. The PCR reactions were run in triplicates. All reactions were carried out on 96-well plates using an ABI PRISM 7700 Sequence Detection System (Applied Biosystems) and analyzed using ABI PRISM 7000 SDS Software (version 1.1). Quantification of real-time PCR experiments was based on the comparative $\Delta\Delta C_t$ method described by Livak and Schmittgen (84) with relative expression levels being calculated as $2^{-\Delta\Delta C_t}$.

2.3.5. *In vitro* assays

2.3.5.1. B cells

2.3.5.1.1. Staining of B and T cells in whole blood

EDTA-anticoagulated blood samples were collected by puncture of the retrobulbar venous plexus of short-term anaesthetised mice. B and T lymphocytes were stained by incubating 100 µl of whole blood with 0.1 µg of PE-CyTM7-conjugated CD45R/B220 and APC-conjugated CD3e antibodies, respectively, for 30 min at room temperature. The stained samples were treated for 10 minutes with BD FACSTM Lysing Solution (BD Biosciences, San Jose, CA) which lysed erythrocytes under gently hypotonic conditions. Before flow cytometric analysis cells were washed twice with FACS buffer. Samples were analyzed on a LSR II flow cytometer (BD).

2.3.5.1.2. Isolation of splenic B cells

For generation of single-cell suspensions freshly isolated spleens were squeezed through a sterile nylon mesh (pore size: 100 µm) and flushed with assay buffer. For the isolation of untouched B cells the commercially available B Cell Isolation Kit (Miltenyi Biotec, Bergisch Gladbach, Germany) was used following the manufacturer's protocol. Purity of B cell isolations was checked by flow cytometric analysis using the PE-CyTM7-conjugated CD45R/B220 antibody. For this purpose 0.5×10^6 freshly isolated B cells were stained with 0.1 µg of PE-CyTM7-conjugated CD45R/B220 antibody in FACS buffer. After incubation for 30 min at 4°C cells were washed with FACS buffer and analyzed on a LSR II flow cytometer (BD).

2.3.5.1.3. Intracellular staining of SYK for flow cytometric analysis

Splenic B cells from vehicle- or tamoxifen-treated iSYKKO mice were isolated as mentioned above. 0.2×10^6 freshly isolated B cells were stained for 20 min at 4°C with 50 ng of PE-CyTM7-conjugated CD45R/B220 antibody diluted in FACS buffer. Afterwards cells were fixed and permeabilized for 20 min at 4°C with BD Cytofix/CytopermTM solution (BD Biosciences,

San Diego, CA). To analyze SYK expression cells were incubated for 20 min at 4°C with PE-conjugated SYK antibody diluted in BD Perm/Wash™ buffer. Subsequently cells were washed twice with BD Perm/Wash™ buffer and analyzed on a LSR II flow cytometer (BD).

2.3.5.1.4. Calcium assay with splenic B cells

Splenic B cells from either vehicle- or tamoxifen-treated iSYKKO mice were isolated as mentioned above and resuspended at 1.25×10^6 cells/ml in Hank's Balanced Salt Solution without calcium and magnesium containing 0.1% (w/v) BSA. Cells were loaded with fluo-4 AM (Invitrogen) by incubating the cell suspension with a final concentration of 2 μ M of the cell-permeant green-fluorescent calcium indicator for 45 minutes at 37°C. Afterwards cells were washed and resuspended to a concentration of 1.25×10^6 cells/ml in Hank's Balanced Salt Solution with calcium and magnesium containing 0.1% (w/v) BSA. To determine calcium flux cells were either directly stimulated with increasing concentrations of goat anti-mouse IgM (final concentration of 5, 10, 20 and 40 μ g/ml) or pre-treated for 30 minutes with increasing concentrations of R406 (final concentration of 0.01, 0.03, 0.1, 0.3, 1, 3, 10 μ M) and then stimulated with goat anti-mouse IgM (final concentration of 20 μ g/ml). Calcium influx was determined using FLIPR^{TETRA} (Molecular Devices) (excitation 485 nm, emission 525 nm) with a read time of 120 s.

2.3.5.1.5. Anti-IgM-induced CD25 and CD69 expression on splenic B cells

Splenic B cells from either vehicle- or tamoxifen-treated iSYKKO mice were isolated as mentioned above. Cells were resuspended at a concentration of 0.5×10^7 cells/ml in RPMI1640 medium containing 10% (v/v) FBS. 100 μ l of the cell suspension were added to each well of a 96-well microtiter plate. Goat anti-mouse IgM was added to a final concentration of 20 μ g/ml. After 18 hours in a CO₂-incubator (37°C, 5% CO₂) cells were stained according to the manufacturer's protocol using 10 μ l of the commercially available Mouse B Lymphocyte Activation Antibody Cocktail (BD Biosciences, San Diego, CA) and analyzed on the LSR II flow cytometer (BD).

2.3.5.2. Bone marrow-derived mast cells

2.3.5.2.1. Preparation of mouse bone marrow-derived mast cells

After treatment with either vehicle or tamoxifen, 8-15 week old female iSYKKO mice were sacrificed with pentobarbital (i.p. 400 mg/kg) (Merial GmbH, Hallbergmoos, Germany). Long bones were removed and flushed with 2% (v/v) FBS in PBS. Red blood cells were lysed by incubating bone marrow cells with ACK lysing buffer for 1 min. Cells were cultured at 1×10^6 cells/ml in mast cell medium. Medium was replaced three times a week. After 4 weeks of culture expression levels of FcεRIα and c-Kit were analyzed on a BD LSR II flow cytometer. Cell populations co-expressing both markers >90% were used for functional assays.

2.3.5.2.2. Calcium assay with mouse bone marrow-derived mast cells

mBMMCs, isolated from the bone marrow of either iSYKKO^{+/+} or iSYKKO^{-/-} mice, were seeded at 1×10^6 cells/ml in mast cell medium and sensitized with anti-DNP IgE (1 μg/ml) overnight. Cells were loaded with 2 μM fluo-4 AM (Invitrogen) by incubation with the calcium indicator for 45 minutes at 37°C. To stimulate calcium influx cells were incubated with increasing concentrations of DNP-BSA (1, 3, 10, 30, 100, 300 and 1000 ng/ml). To test the SYK inhibitors, BAY61-3606 and R406, cells were pre-incubation for 2 min with the inhibitor of interest (final concentration of 0.01, 0.03, 0.1, 0.3, 1, 3, 10 μM) and subsequently stimulated with DNP-BSA at a final concentration of 30 ng/ml. Calcium influx was determined using FLIPR^{TETRA} (Molecular Devices) (excitation 485 nm, emission 525 nm) with a read time of 120 s.

2.3.5.2.3. Histamine release assay with mouse bone marrow-derived mast cells

mBMMCs were seeded at 1×10^6 cells/ml in mast cell medium and sensitized with anti-DNP-IgE (1 μg/ml) overnight. After washing, cells were incubated for 30 minutes with either BAY61-3606 or R406 (final concentration of 0.01, 0.03, 0.1, 0.3, 1, 3, 10 μM) followed by the

activation of the FcεRI with 30 ng/ml DNP-BSA for 30 minutes. Triton X-100 (final concentration of 0.2%) or calcium ionophore A23187 (final concentration of 2 μM) were added as positive controls. Histamine content in supernatants was measured by ELISA (Beckman Coulter Immunotech, Marseille, France).

2.3.5.2.4. Stimulation of mouse bone marrow-derived mast cells for Western blotting

mBMMCs were seeded at 1×10^6 cells/ml in mast cell medium and sensitized with anti-DNP-IgE (1 μg/ml) overnight. After washing twice with mast cell medium, cells were incubated for 30 minutes with either BAY61-3606 or R406 (1 μM) followed by stimulation with DNP-BSA (100 ng/ml) for 10 minutes. Cells were lysed in 1 x LDS Sample Buffer containing Sample Reducing Agent, Protease and Phosphatase Inhibitor Cocktail (Thermo Scientific). Western blot analysis was performed as described above (see 2.3.4.2.).

2.3.5.3. Splenocytes

2.3.5.3.1. CD23 staining of splenocytes

Single-cell suspensions of freshly isolated spleens were generated as described for the isolation of untouched B cells. 0.5×10^6 spleen cells were double-stained using 0.1 μg of PE-conjugated CD23 antibody and 0.1 μg of PE-Cy™7-conjugated CD45R/B220, respectively. After antibody incubation for 30 min at 4°C cells were washed with FACS buffer and analyzed on a LSR II flow cytometer (BD).

2.3.5.3.2. IL-3-induced cytokine release from splenocytes

Single-cell suspensions of freshly isolated spleens were generated as described for the isolation of untouched B cells. Splenocytes were resuspended in RPMI1640 medium supplemented with 10% (v/v) FBS, 100 U/ml penicillin, 100 μg/ml streptomycin and 55 μM β-Mercaptoethanol. 0.5×10^6 cells were added to each well of a 96-well plate and treated with different concentrations of recombinant mouse IL-3 (final concentration of 0.03 or 10 ng/mL) and the SYK inhibitor R406 resuspended in DMSO (final concentration of 0.1, 0.3 and

1 μM). After incubation for either 24 or 72 hours in a CO_2 -incubator (37°C , 5% CO_2) supernatants were collected and stored at -20°C until sampled for cytokines using commercially available ELISA kits.

2.3.5.4. Neutrophils

2.3.5.4.1. Chemotaxis assay using primary neutrophils

Neutrophils contained in the peritoneal exudates of iSYKKO^{+/+} or iSYKKO^{-/-} mice four hours after thioglycollate-treatment (see 2.3.6.3.) were used for the experiments. Cells were resuspended to 1×10^6 cells/ml in ice-cold Hank's Balanced Salt Solution containing calcium, magnesium and 0.1% (w/v) BSA. Recombinant mouse keratinocyte-derived cytokine (KC) was resuspended in the same buffer at different concentrations and placed in the lower chamber of a 96-well cell migration system with a $5.0 \mu\text{m}$ porous polycarbonate membrane. $80 \mu\text{l}$ of cell suspension was placed in the upper chamber and incubated for two hours in a CO_2 -incubator. The number of viable cells that had migrated into the lower chamber was determined using the CellTiter-Glo[®] Luminescent Cell Viability Assay (Promega, Madison, WI).

2.3.5.5. Osteoclasts

2.3.5.5.1. *In vitro* generation of osteoclasts and functional analysis

Ten days after the last vehicle or tamoxifen application animals were sacrificed with pentobarbital (i.p. 400 mg/kg) (Merial GmbH) and femora and tibiae of wild type or inducible SYK knockout mice were isolated. For the profiling of the SYK inhibitor, R406, bone marrow cells isolated from the long-bones of female BALB/c mice were used. Bone marrow was extracted with PBS containing 2% (v/v) FBS. After lysis of red blood cells for one minute with ACK lysing buffer cells were cultured in osteoclast medium for one day. Non-adherent cells were cultured with osteoclast medium containing 20 ng/ml murine M-CSF in Petri dishes for 4 days. Cells were washed with PBS and lifted using a cell scraper. A total of $1 \times$

10^5 cells per well were cultured in 200 μ l of osteoclast medium with 100 ng/ml RANKL and 80 ng/ml murine M-CSF in 96-well tissue culture plates with addition of fresh media every 3 days. Cells were fixed and stained for TRAP activity after 9 days in culture using a commercially available kit (Acid Phosphatase, Leukocyte (TRAP) Kit, Sigma-Aldrich). For the quantification of resorption pits, cells were cultured on calcium phosphate-coated quartz slides (BD BioCoat™ Osteologic™ MultiTest Slides). After 9 days of culture cells were removed and resorption pit formation was visualized using von Kossa staining. Images were captured using a Zeiss AxioCam MRm attached to a Zeiss Axiovert 25 microscope. Images of TRAP-stained osteoclasts (Fig. 37 and 39) were taken using the 20x objective. Images of von Kossa-stained calcium phosphate-coated quartz slides (Fig. 38 and 39) were taken using the 5x objective. For the quantification of resorption pits images were saved as gray value JPG files. Image analysis was carried out using a proprietary application based on a commercially available machine vision software library (Halcon9.0.2, MVTec Software GmbH, Munich). Bright areas were segmented using a locally defined threshold. Analysis parameters including the number of resorption pits, their area, and mean intensity were recorded.

2.3.6. *In vivo* studies

2.3.6.1. IgE-induced passive cutaneous anaphylaxis

Male iSYKKO or WT mice were treated with either vehicle or tamoxifen according to the induction protocol for short-term SYK deletion as mentioned above. Twelve days after the last p.o. application animals were anaesthetized with isoflurane (3-4% in pressurized air) flushed into a perspex box. 20 ng anti-DNP IgE (concentration: 4 ng/ μ l in PBS, application volume: 5 μ l) was injected intradermally into the right ear and PBS into the left ear of each animal by means of a 32G needle (Hamilton Company, Reno, NV) attached to a 10 μ l syringe. 24 hours later 1 mg DNP-BSA diluted in 0.9% NaCl with 1% Evans blue was injected into the tail vein. Thirty minutes after the challenge animals were sacrificed by cervical dislocation and ear tissue (8 mm diameter) was punched out from both ears. Evans blue was extracted by incubation in 0.35 μ l of formamide at 65°C overnight. The absorbance was

measured in the supernatant at 620 nm using a spectrophotometer. To test BAY61-3606 male BALB/c mice were treated with the SYK inhibitor dissolved in 0.5% (w/v) natrosol by oral gavage (p.o.) 30 minutes prior to DNP-BSA application.

2.3.6.2. Ovalbumin-induced pulmonary eosinophilia

In the therapeutic setup mice were immunized by injection of 200 μ l ovalbumin (i.p. 0.1 mg/ml) (Serva, Heidelberg, Germany) absorbed to Imject Alum (Thermo Scientific) in PBS on day 0, 14 and 21. Control animals received PBS. For knockout and control experiments iSYKKO and WT mice were treated with vehicle or tamoxifen from day 28 to 32 as above. Mice were challenged by whole body exposure to nebulised ovalbumin (1% in PBS) in a perspex box with a constant air stream of 2.5 l/min for 20 minutes on days 42 and 43. In the prophylactic setup mice were treated with either vehicle or tamoxifen on day 0 to 4 according to the protocol for short-term SYK deletion as mentioned above. On day 17, 31 and 38 animals were immunized by injection of 200 μ l ovalbumin (i.p. 0.1 mg/ml) absorbed to Imject Alum in PBS and on day 44 and 45 mice were challenged with nebulised OVA as mentioned in the therapeutic setup. To test the SYK inhibitor, BAY61-3606, female BALB/c mice were immunized on day 0, 14 and 21 and challenged with ovalbumin on days 26 and 27. BAY61-3606 (3, 10 and 30 mg/kg) dissolved in 10% hydroxypropyl- β -cyclodextrin containing 3.2% glucose and 10 mM NaOH was injected intraperitoneally 1 hour before, 3 and 6 hours after OVA-challenge. To analyze effects of long-term SYK deletion on the ovalbumin-induced pulmonary eosinophil accumulation animals were treated with either vehicle or tamoxifen on days 0 to 4, 44 to 46 and 85-87. On days 105, 119 and 128 mice were immunized with ovalbumin absorbed to Imject Alum in PBS as mentioned above and on day 133 and 134 animals were challenged with nebulised ovalbumin. In all experimental setups animals were euthanized by pentobarbital injection (i.p. 400 mg/kg Narcoren) 24 hours after the last OVA challenge, and lungs were lavaged two times with 0.8 ml Hanks solution containing EDTA (0.6 mM) and protease inhibitor (Complete Protease Inhibitor Cocktail Tablets, Roche).

2.3.6.3. Thioglycollate-induced sterile peritonitis

Male iSYKKO mice were treated with either vehicle or tamoxifen as mentioned above. Twelve days later mice received a single intraperitoneal injection of 1 ml of 4% (w/v) sterile thioglycollate (Sigma-Aldrich, St. Louis, MO). Mice were euthanized by pentobarbital injection (i.p. 400 mg/kg Narcoren) 4 hours after the thioglycollate application. Peritoneal exudates were collected by flushing the peritoneum with 4 mL of PBS containing 1% (w/v) BSA.

2.3.6.4. Lipopolysaccharid-induced pulmonary inflammation

24 days after the last p.o. treatment with either vehicle or tamoxifen according to the induction protocol for short-term SYK deletion iSYKKO mice were short-term anaesthetized with isoflurane (3-4 %) as described before and fixed in supine position by a wire sling attached to a rodent operating table tilted by 45 degree. 50 µl of LPS from E. coli serotype O111:B4 (Sigma-Aldrich) (100 µg/mL in 0.9 % NaCl) or NaCl were administered intratracheally by means of a 22G feeding needle (B. Braun, Melsungen, Germany) attached to a 1 mL syringe. 4 hours after intratracheal application animals were euthanized by pentobarbital injection (i.p. 400 mg/kg Narcoren) and lungs were lavaged two times with 0.8 mL Hanks solution containing EDTA (0.6 mM).

2.3.6.5. Cigarette smoke-induced pulmonary inflammation

Mice were treated with tamoxifen or vehicle according to the short-term deletion protocol as mentioned above. Exposure to cigarette smoke or room air was started ten days after the last application of vehicle or tamoxifen, respectively.

In both, the acute and chronic model, exposure to the smoke of each cigarette lasted for 15 min followed by an 8 min exposure with fresh room air (15 l/min). Every second cigarette animals were allowed to breathe fresh air (15 l/min) for 24 minutes prior to the next cigarette. Control animals were exposed to room air. In the acute model mice were exposed to cigarette smoke for a total of 4 days in a whole body exposure box as described

previously (85). Briefly, on day one and two mice were exposed to the mainstream smoke of 6 cigarettes (Roth-Händle without filters, tar 10 mg, nicotine 1.0 mg, carbonmonoxide 6 mg, Badische Tabakmanufaktur Roth-Händle[®], Lahr, Germany), on day 3 to 8 cigarettes, and on day 4 to 10 cigarettes. In the chronic model animals were exposed to smoke for a total of 3 weeks. In week one and two animals were exposed to the mainstream smoke of 5 cigarettes on 5 consecutive days followed by a two day recovery period. In week three animals were exposed to the smoke of 5 cigarettes on 4 consecutive days. In both setups the animals were euthanized by pentobarbital injection (i.p. 400 mg/kg Narcoren) 18 h after the final cigarette smoke exposure and the lungs were lavaged two times with 0.8 ml Hanks solution containing EDTA (0.6 mM).

2.3.6.6. MCP-1-induced lung inflammation

Wild type and inducible SYK knockout mice were treated according to the short-term SYK deletion protocol. Ten days after the last vehicle or tamoxifen application animals were short-term anaesthetized by inhalation of isoflurane (3–4%) as described before, were fixed in supine position by a wire sling attached to a rodent operating table tilted by 45 degree and received 10 µg human MCP-1 (PeproTech, Rocky Hill, NJ) in PBS containing 0.1% (w/v) BSA and 10 ng LPS (E. coli serotype O111:B4) in a total volume of 50 µl by intratracheal application as described before. Control animals were intratracheally administered with 50 µl PBS containing 0.1% (w/v) BSA. 48 hours after intratracheal application animals were euthanized by pentobarbital injection and lungs were lavaged twice using 0.8 ml Hanks solution containing EDTA (0.6 mM).

2.3.6.7. Treatment of animals for bone analysis

Wild type and inducible SYK knockout mice were included into the study at the age of 12 weeks. Each group consisted of ten mice (five of each gender). Animals were treated with vehicle or tamoxifen according to the induction protocol for long-term SYK deletion as described above. At the age of 30 weeks animals were euthanized by pentobarbital injection (i.p. 400 mg/kg Narcoren) and samples including femora, tibiae and vertebrae were collected.

2.3.7. Bone analysis

Tartrate-resistant acid phosphatase and alkaline phosphatase staining of humeri was performed in collaboration with the toxicological department at Boehringer Ingelheim Pharma GmbH & Co. KG (Biberach, Germany) under supervision of Dr. Florian Colbatzky.

The cortical and trabecular measurements, as well as the mechanical tests described here were performed in collaboration with the Institute of Biomechanics (Trauma Center Murnau, Germany) under the supervision of Prof. Peter Augat.

2.3.7.1. Tartrate-resistant acid phosphatase and alkaline phosphatase staining of humeri

For analyses of osteoclasts and osteoblasts, humeri were obtained from 30-week-old wild type and inducible SYK knockout mice 18 weeks after the first vehicle or tamoxifen administration. Samples were fixed in cacodylate-buffered paraformaldehyde (4% w/v) and embedded in plastic as described in Colbatzky & Hermanns 1987 (86). Longitudinal sections (2 μ m thickness) of the humeri were prepared and stained for TRAP to visualize osteoclasts and for alkaline phosphatase to visualize osteoblasts. Both methods were carried out according to Lojda *et al.* (87). Images were taken using a 40x objective (Fig. 41).

2.3.7.2. Microcomputed tomography (μ CT) analysis of cortical and trabecular bone

Femora and L1 vertebrae were isolated from wild type and inducible SYK knockout mice 18 weeks after the first vehicle or tamoxifen. Isolated bones were stored in 4% (w/v) paraformaldehyde and scanned using a Scanco's μ CT-80 (Scanco Medical AG, Bruettisellen, Switzerland). Each specimen was scanned at a spatial resolution of 10 μ m (70 kV energy, 114 mA intensity, and 500 ms integration time). For cortical bone analysis of the femur, 50 slices were scanned distally from the centre point of the femur, which was defined as the halfway point between the top surface of the femoral head and the bottom surface of the femoral condyles. For trabecular bone analysis of the femur, 371 slices were scanned proximally from just below the top surface of the femoral condyles. For trabecular bone analysis in the L1 vertebrae all samples were scanned from just above the T13-L1 disk to just below the L1-L2 disc (approximately 350-400 slices). All samples were contoured using an automatic script from Buie *et al.* (88), which separates the cortical and trabecular bone regions accurately and separately. For the cortical bone in the femur, all 50 slices were selected for segmentation. The volumes of interest were analyzed for cortical thickness, cortical volume and polar moment of inertia. For trabecular bone in the femur, 120 slices preceding the first slice with visible growth plate were segmented. For trabecular bone in the L1 vertebrae, all slices without visible growth plate were selected. The trabecular volumes were analyzed for bone volume fraction (BV/TV), trabecular number (Tb. N.), trabecular thickness (Tb. Th.), trabecular separation (Tb. Sp.), relative bone surface (BS/BV) as well as apparent and material density.

2.3.7.3. Mechanical tests

Mechanical tests were performed on the contralateral femora of the female inducible SYK knockout mice after vehicle or tamoxifen treatment (n=5). Mechanical tests were carried out with an electromechanical testing machine (Z010, Zwick/Roell, Ulm-Einsingen, Germany). The femurs were kept frozen at -20°C and were thawed at room temperature prior to mechanical testing. The bones were accurately aligned and embedded with poly

methyl methacrylate (Technovit 3040, Heraeus Kulzer, Wertheim, Germany) at both ends. The samples were loaded in torsion to failure at a loading rate of 0,1 deg/sec. From the torsion tests, the torsional stiffness, maximum torsion, and energy to failure were evaluated.

2.3.8. Total and differential cell count

Total and differential cell counts in BALF, peritoneal fluid and blood were determined by means of a Sysmex XT1800 iVet cell analyzer (Sysmex Europe GmbH, Norderstedt, Germany) utilizing customised settings that were validated with cytopsin preparations (data not shown).

2.3.9. Statistical analysis

All data are presented as means \pm S.E.M. of n analyses. All figures, apart from figure 13B, 16, 17, 18, 21, 24 and 34, were analyzed using GraphPad Prism (version 5.02) and statistical analysis was performed as mentioned in the figure legends. Statistical evaluation of figures 13B, 16, 17, 18, 21, 24 and 34 was prepared using the software package SAS Version 9.2 (SAS Institute Inc., Cary, North Carolina, USA). For figures 13B, 16, 17, 21 and 34 one-factorial analyses of variance (ANOVA) with heteroscedastic variances were applied. For figures 18 and 24 homogeneous variances were assumed. The error terms of the ANOVA were taken as estimates for the variability in the following selected pair wise comparisons of the different experimental groups. To adjust for multiple testing the method of Bonferroni-Holm was used. Statistical significance was accepted at $p < 0.05$.

3. RESULTS

3.1. Generation of tamoxifen-inducible SYK knockout mice

3.1.1. Principle and proof of concept

To circumvent the perinatal lethality of conventional SYK knockout mice (37,38) and to provide an *in vivo* model to explore possible effects and adverse effects of a long-term pharmacotherapy targeting SYK, a tamoxifen-inducible SYK knockout mouse strain (iSYKKO) was generated by crossing *Rosa26CreER^{T2}* mice (89) with mice carrying an exon 2 of the *Syk* gene flanked by loxP sites (21) (Fig 3).

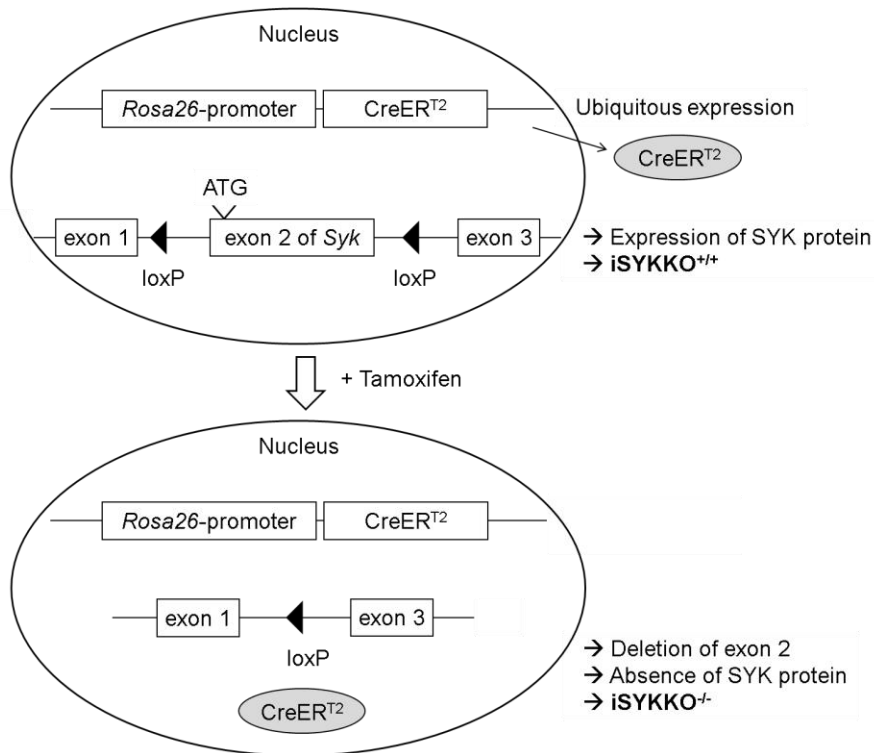


Fig. 3: Schematic drawing of the tamoxifen-induced deletion of SYK using the CreER^{T2} system. In the iSYKKO mouse strain exon 2 of the *Syk* gene which contains the start codon is flanked by loxP sites. Furthermore, a chimeric protein, consisting of the Cre recombinase fused to a mutated form of the ligand binding domain of the oestrogen receptor (CreER^{T2}), is ubiquitously expressed under the control of the *Rosa26*-promoter. Addition of tamoxifen induces the nuclear translocation of the fusion protein and with it the subsequent deletion of exon 2 of the *Syk* gene.

3.1.2. Establishment of a tamoxifen treatment protocol for short-term SYK deletion

To achieve a prominent knockout of SYK, but at the same time to keep tamoxifen exposure as low as possible, different tamoxifen doses and treatment periods were tested in a first set of experiments (data not shown). This led to the establishment of a “standard deletion protocol” in which the knockout was induced by the oral administration of 20 mg/kg tamoxifen on 5 consecutive days. To assess the efficacy and the tissue distribution of the knockout, the deletion of SYK was analyzed 10 days after the last tamoxifen administration by genomic PCR (Fig. 4) and Western blotting (Fig. 5). PCR analysis of DNA from different organs showed the successful deletion of exon 2 in all organs analyzed (Fig. 4).

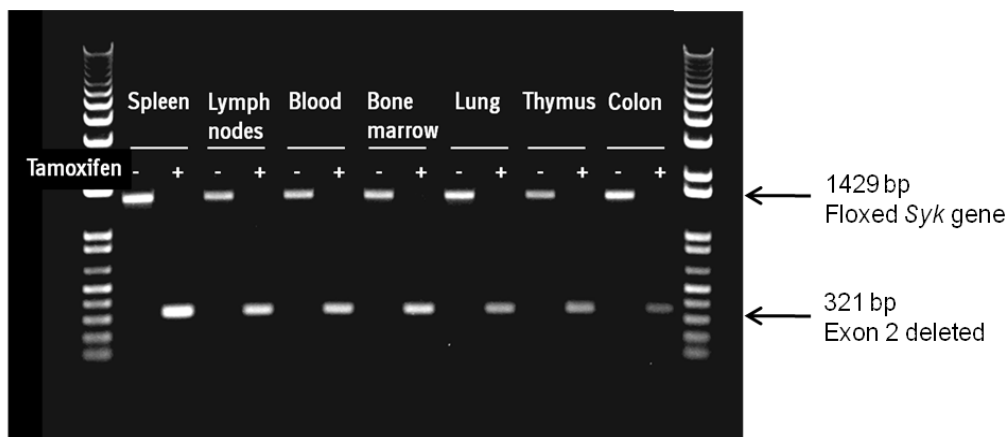


Fig. 4: PCR analysis of genomic DNA isolated from different organs of vehicle- (-) or tamoxifen-treated (+) iSYKKO mice. DNA was isolated from different organs of iSYKKO mice ten days after the last of five vehicle or tamoxifen applications. To detect the excision of exon 2 DNA was analyzed by PCR using primers that amplify a gene segment comprising exon 2. Amplification of the floxed gene segment resulted in a PCR product of 1429 bp whereas amplification of the gene locus after the deletion of exon 2 resulted in a PCR product of 321 bp. Shown is a representative agarose gel of different organs of one out of three experiments performed analogously.

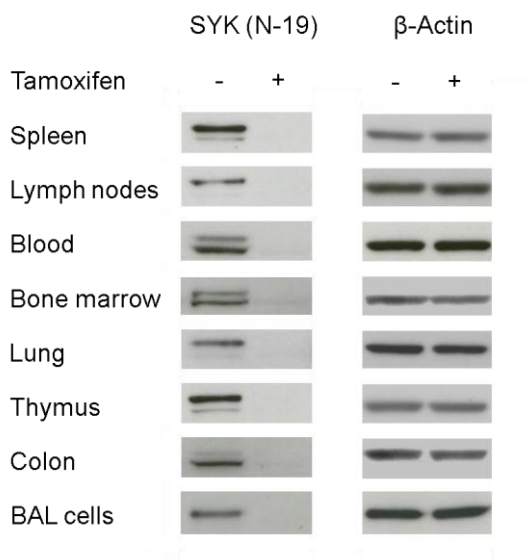


Fig. 5: Western blot analysis of protein extracts from various organs of vehicle- (-) or tamoxifen-treated (+) iSYKKO mice. SYK and β -Actin expression was sampled by Western blot analysis ten days after the last of five vehicle or tamoxifen applications. Shown are representative images of different organs of one out of three experiments performed analogously.

Furthermore, deletion of exon 2 led to undetectable levels of SYK protein as determined by Western blot analysis using an antibody raised against the N-terminus of SYK (Fig. 5), suggesting that the iSYKKO mouse strain represents a suitable model to address the function of SYK in *in vivo* models. Tamoxifen treatment of wild type animals had no detectable influence on SYK expression (data not shown).

3.1.3. Short-term SYK deletion has no negative impact on the health status of iSYKKO mice

Conventional germ-line deleted *Syk*^{-/-} mice display a petechiated *in utero* appearance and die perinatally, indicating an essential function of SYK during embryogenesis (37,38). Therefore, in a first set of analyses several physiological parameters were assessed reflecting the health status of adult (13-week old) mice ten days after SYK deletion.

	iSYKKO ^{+/+} (n = 8)	iSYKKO ^{-/-} (n = 8)
Body weight [g]	24.5 ± 1.6	26.5 ± 1.5
Spleen weight [mg]	89.4 ± 4.4	91.2 ± 8.7
WBC count in blood [x 10 ⁶ cells/ml]	6.50 ± 0.80	6.78 ± 0.55
B lymphocyte count in blood [x 10 ⁶ cells/ml]	2.75 ± 0.47	2.82 ± 0.31

Table I. Physiological parameters of iSYKKO mice after vehicle or tamoxifen treatment. Inducible SYK knockout mice (13-week old) were treated with either vehicle (iSYKKO^{+/+}) or 20 mg/kg of tamoxifen (iSYKKO^{-/-}) on 5 consecutive days. Spleen weight and blood cell counts were determined ten days after last tamoxifen application. Blood samples were withdrawn by puncture of the retrobulbar venous plexus. White blood cell count was determined by a Sysmex XT1800 iVet cell analyzer. CD45R/B220-positive B cell count was determined by flow cytometry. Data are presented as the mean ± SEM of eight animals.

As shown in table I, there were no significant differences in body weight, spleen weight, white blood cell count or B lymphocyte count in blood between the vehicle-treated iSYKKO^{+/+} and the tamoxifen-treated iSYKKO^{-/-} groups. These data suggest that the short-term deletion of SYK does not lead to a general health impairment.

3.1.4. SYK expression recurs with time – Development of a tamoxifen-treatment protocol for long-term SYK deletion

The treatment of iSYKKO mice with 20 mg/kg tamoxifen on 5 consecutive days resulted in the reduction of SYK protein below detection levels as sampled by Western blot analysis (Fig. 5). The next step was to confirm whether treatment of animals according to the short-term protocol would also lead to a sustained deletion of the target protein. Western blot analysis of spleen samples showed that expression of the SYK protein recurred with time (data not shown). To further explore the kinetics of this process a time-course study was performed in which the blood of tamoxifen-treated mice was sampled for SYK mRNA levels

at different time points after tamoxifen administration. Real-time PCR revealed that expression levels of SYK mRNA were reduced below 1% ten days after the last tamoxifen application. However, SYK mRNA expression recurred over time and 12 weeks after initial treatment SYK mRNA levels were back to approximately 5% of the initially measured value before starting the tamoxifen administration (Fig. 6).

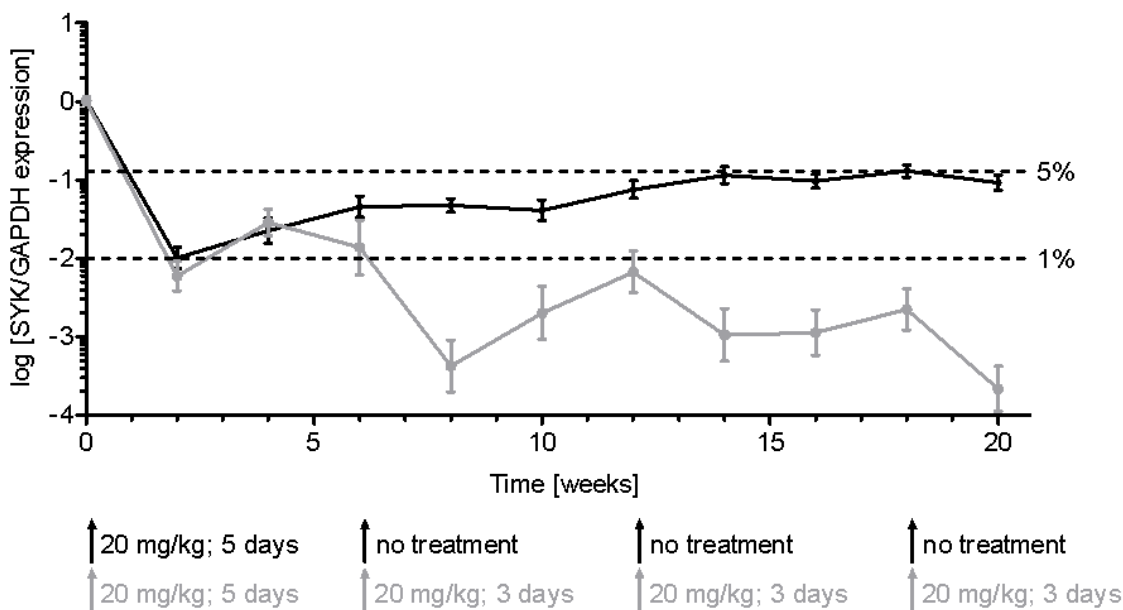


Fig. 6: Relative SYK expression in blood of iSYKKO mice. SYK and GAPDH mRNA levels were determined in blood of iSYKKO mice at different time points after tamoxifen treatment. Bold black line: Relative SYK mRNA expression in blood of inducible SYK knockout mice after treatment of animals with 20 mg/kg of tamoxifen on five consecutive days. Bold grey line: Relative SYK mRNA expression in blood of inducible SYK knockout mice after treatment of animals with 20 mg/kg of tamoxifen on five consecutive days followed by administration of 20 mg/kg of tamoxifen on three consecutive days every sixth week. Error bars represent the mean \pm SEM of six independent analyses.

To achieve a sustained deletion of SYK but again keeping the tamoxifen dose as low as possible, a protocol was established in which animals were initially treated with 20 mg/kg tamoxifen on 5 consecutive days followed by subsequent tamoxifen administration every 6 weeks for 3 consecutive days. According to figure 6 this treatment scheme led to a sustained reduction of SYK mRNA below 1% over a period of 20 weeks.

3.2. Function of SYK in B cells

3.2.1. Long-term SYK deletion leads to a gradual reduction of B lymphocytes in blood

SYK is a key mediator downstream of the B cell receptor (BCR) leading to the activation, differentiation and proliferation of B cells. SYK-deficient B cells do not respond to BCR aggregation (90) and B cell development in germ-line deleted SYK knockout mice is blocked (37,38). However, the effect of SYK deletion on B cell counts in full-grown mice has not been examined. As shown in table I, B lymphocyte counts in the blood of *iSYKKO*^{-/-} mice are unaffected ten days after the last vehicle or tamoxifen application compared to B cell counts in vehicle-treated control animals. To verify that SYK protein was actually prominently reduced in the B cells of *iSYKKO*^{-/-} mice B cells were isolated from the spleens of *iSYKKO*^{+/+} and *iSYKKO*^{-/-} mice ten days after the last tamoxifen application and SYK levels were determined by flow cytometry using a fluorescent-labelled anti-SYK antibody. Figure 7 shows that SYK expression was heavily reduced, confirming the data that showed the reduction of SYK protein below detection limit in spleen samples using Western blot analysis (Fig. 5).

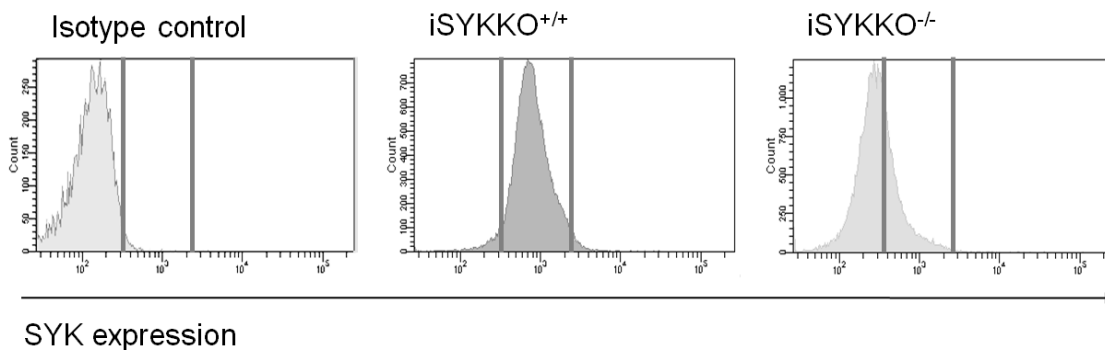


Fig. 7: SYK expression in splenic B cells isolated from *iSYKKO* mice. Spleens of *iSYKKO* mice were sampled for SYK expression in CD45R/B220 positive cells (B lymphocytes) by flow cytometry ten days after the last vehicle or tamoxifen administration. Shown are representative images of splenic B cells stained with either PE-conjugated isotype control or PE-conjugated anti-SYK antibody of one out of eight experiments performed analogously.

Knowing that SYK is essential for B cell development and maturation it was suspected that long-term SYK deletion would eventually result in reduced B cell counts. To evaluate the kinetics of this process, 14-week old *iSYKKO* mice were treated with vehicle or tamoxifen according to the induction protocol for long-term SYK deletion with repeated tamoxifen applications every six weeks on 3 consecutive days. Using CD45R/B220 and CD3 antibodies to detect B and T lymphocytes, respectively, the blood of vehicle and tamoxifen-treated mice was sampled at different time points after the induction of SYK deletion.

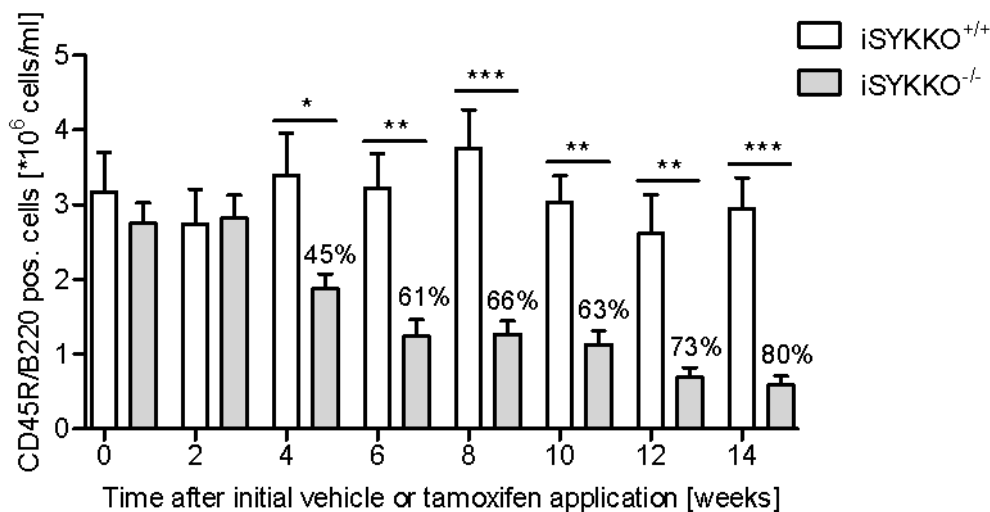


Fig. 8: CD45R/B220 positive cell counts in whole blood of *iSYKKO* mice at different time points after initial vehicle or tamoxifen treatment. B cell counts in whole blood were sampled by FACS analysis using PE-Cy™7-conjugated CD45R/B220 antibody. Error bars represent the mean \pm SEM of eight independent analyses. One-way analysis of variances with Bonferroni post test was performed to test for statistical significance. *: $p < 0.05$, **: $p < 0.01$, ***: $p < 0.001$

Figure 8 shows that long-term SYK deletion led to a gradual reduction in blood B cell counts. Fourteen weeks after the initial tamoxifen treatment B lymphocytes in *iSYKKO*^{-/-} mice ($0.59 \pm 0.12 \times 10^6$ cells/ ml) were reduced by 80% compared to the vehicle-treated control group ($2.95 \pm 0.41 \times 10^6$ cells/ ml). Of note, tamoxifen treatment alone did not influence B cell counts in blood of wild type mice (data not shown).

While SYK is indispensable for B cell development, signalling through SYK is thought to be dispensable for T cell maturation. Therefore, CD3 expression levels in the whole blood of the same mice were quantified using flow cytometry. Over the entire experimental period the number of CD3 positive T cells in the blood of vehicle-treated *iSYKKO*^{+/+} mice was comparable to the number of CD3 positive cells in blood of tamoxifen-treated *iSYKKO*^{-/-} mice (Fig. 9). Thus, the data confirm the specificity of the observed phenomenon and show that the reduced B cell counts are not simply an indicator for a generally compromised health status of *iSYKKO* mice after long-term SYK deletion.

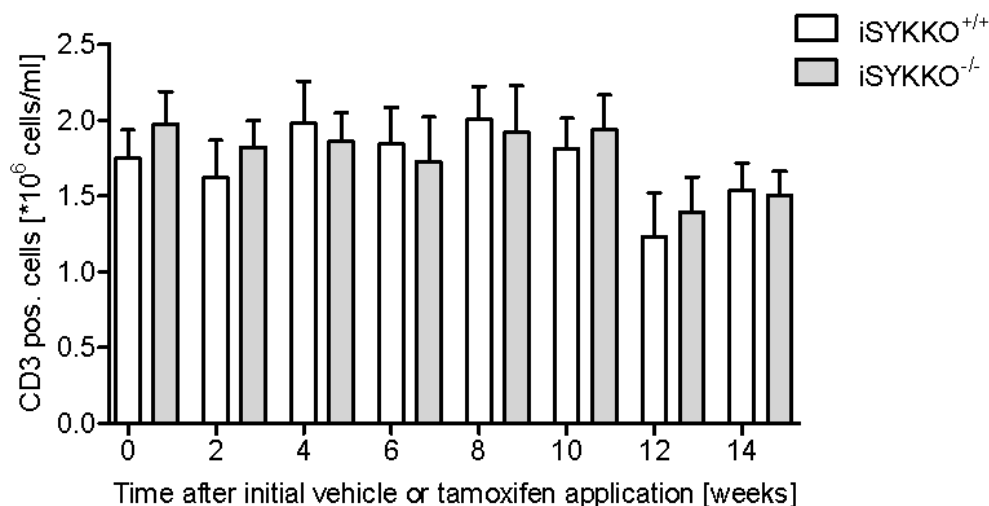


Fig. 9: CD3 positive cell counts in whole blood of *iSYKKO* mice at different time points after initial vehicle or tamoxifen treatment. T cell counts in whole blood were sampled by FACS analysis using APC-conjugated CD3e antibody. Error bars represent the mean \pm SEM of eight independent analyses.

3.2.2. Calcium signalling in B cells is dependent on the activity of SYK

Activation of the B cell receptor initiates the release of calcium from intracellular stores. To test the functionality of B cells in the absence of SYK B cells were isolated from the spleens of *iSYKKO*^{+/+} and *iSYKKO*^{-/-} mice ten days after the last vehicle or tamoxifen application and stimulated with increasing concentrations of goat anti-mouse IgM to crosslink the BCR.

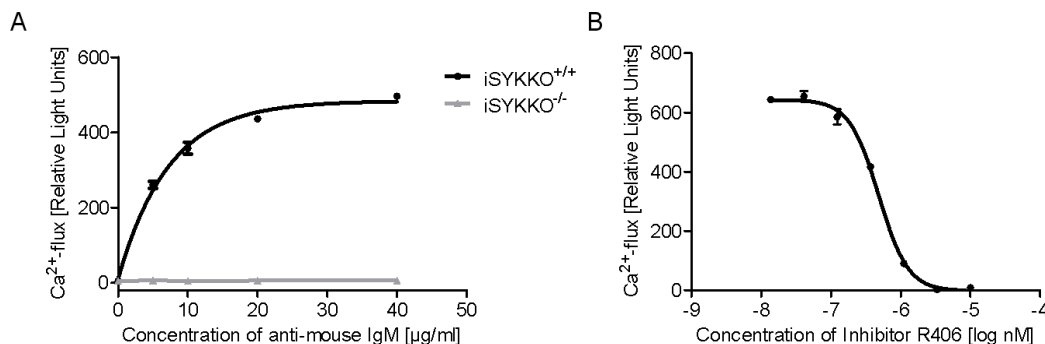


Fig. 10: Anti-mouse IgM stimulated calcium flux into B cells. Calcium release was measured as a surrogate parameter for B cell activation. (A) Stimulation of splenic B cells isolated from iSYKKO^{+/+} and iSYKKO^{-/-} mice with goat anti-mouse IgM. (B) Stimulation of splenic B cells isolated from iSYKKO^{+/+} mice with goat anti-mouse IgM after pre-treatment of cells with increasing concentrations of R406. Error bars represent the mean \pm SEM of three independent analyses.

B cells isolated from iSYKKO^{+/+} mice showed a concentration-dependent increase in calcium release while B cells isolated from iSYKKO^{-/-} were defective in calcium signalling independent of the amount of stimulus used (Fig. 10A). To verify that calcium signalling in B cells is dependent on the kinase activity of SYK the small molecule SYK inhibitor R406 was used (91). Cells isolated from the spleen of iSYKKO^{+/+} animals were pre-incubated with increasing concentrations of R406. Subsequently, calcium release was induced by the treatment of cells with 20 µg/ml of goat anti-mouse IgM. R406 concentration-dependently inhibited the release of calcium from intracellular stores with an IC₅₀ of 486 nM (Fig. 10B).

3.2.3. CD69 and CD25 expression is inhibited in SYK negative B cells *in vitro*

CD25 and CD69 are lymphoid activation antigens which are transiently expressed on activated T and B cells. Their rapid expression within hours after stimulation makes them ideal surrogate parameters for the early detection of B cell activation. To induce B cell activation B lymphocytes isolated from the spleens of iSYKKO^{+/+} and iSYKKO^{-/-} mice were stimulated with goat anti-mouse IgM antibody. After 18 hours in culture CD19-positive B cells were stained for CD25 and CD69 surface expression (Fig. 11A and 11B).

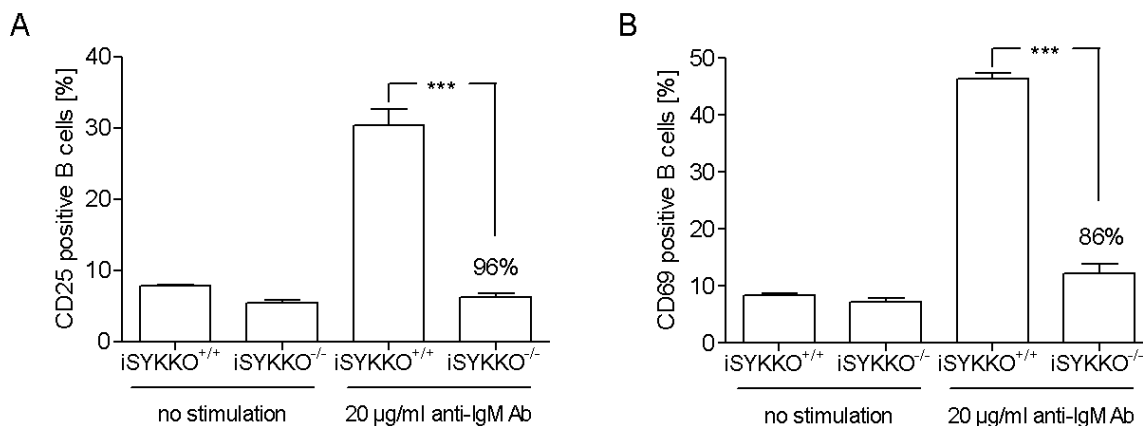


Fig. 11: Anti-mouse IgM stimulated CD25 and CD69 surface expression on B cells. Splenic B cells were isolated from iSYKKO^{+/+} and iSYKKO^{-/-} mice. Surface expression of (A) CD25 and (B) CD69 on primary B cells was measured by FACS analysis. Error bars represent the mean \pm SEM of eight independent analyses. One-way analysis of variances with Bonferroni post test was performed to test for statistical significance. ***: $p < 0.001$

Consistent with the inability of SYK negative cells to release calcium in response to BCR aggregation, the expression of both surface antigens, CD25 and CD69, was heavily compromised in response to BCR activation in B cells isolated from iSYKKO^{-/-} mice (Fig. 11).

3.3. Function of SYK in mast cells

3.3.1. SYK deleted bone marrow cells differentiate normally into mature BMDCs *in vitro* but do not respond to Fc ϵ RI cross-linking

Bone marrow cells were isolated from the long-bones of SYK positive and SYK deleted iSYKKO mice 10 days after the last vehicle or tamoxifen application. After 4-week culture with IL-3, surface expression levels of Fc ϵ RI and c-Kit were measured by flow cytometry (Fig 12A) and the expression of SYK was determined by Western blotting (Fig 12B). mBMDCs cultured from iSYKKO^{-/-} mice were devoid of SYK protein but displayed equivalent Fc ϵ RI and c-Kit expression levels (93%) as cells isolated from iSYKKO^{+/+} mice (90%), indicating that SYK is not necessary for the maturation of mBMDCs *in vitro*.

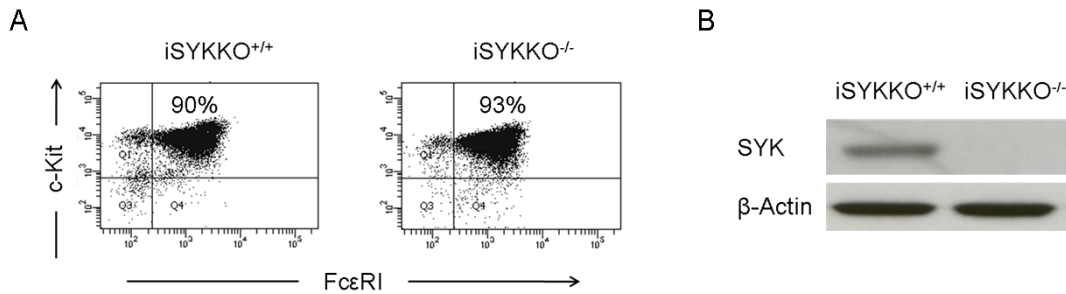


Fig. 12: Analysis of mBMMCs cultured from bone marrow cells of *iSYKKO*^{+/+} and *iSYKKO*^{-/-} mice. (A) Expression levels of FcεRI and c-Kit receptors on *iSYKKO*^{+/+} and *iSYKKO*^{-/-} mBMMCs after 4 weeks of culture with IL-3 as determined by FACS analysis. (B) *iSYKKO*^{+/+} and *iSYKKO*^{-/-} mBMMCs were assayed for SYK and β-Actin expression by Western blot analysis. Shown are representative FACS and Western blot analysis of one out of five experiments performed analogously.

To determine the responsiveness of mBMMCs following FcεRI activation calcium flux and histamine release from mBMMCs were analyzed. As shown in figure 13A, the intracellular calcium concentration of *iSYKKO*^{-/-} mBMMCs did not increase after antigen-induced cross-linking of the high affinity IgE receptor.

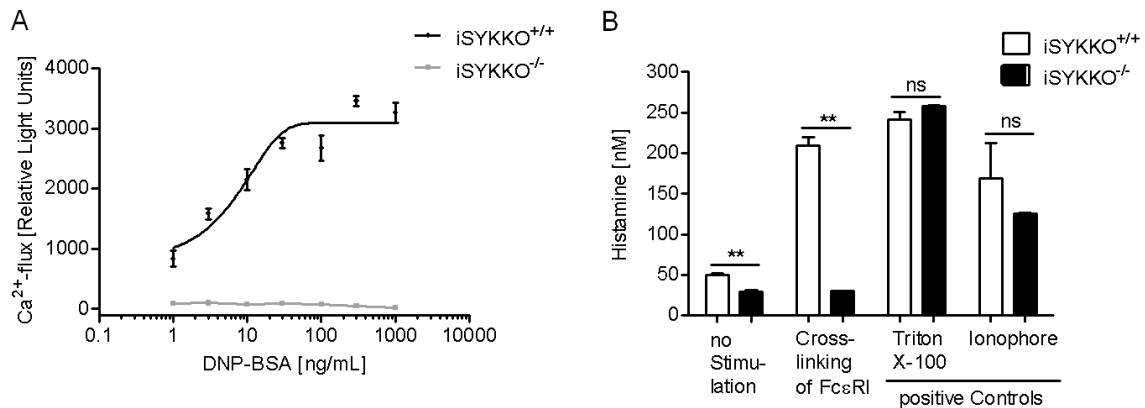


Fig. 13: Calcium and histamine release from *iSYKKO*^{+/+} and *iSYKKO*^{-/-} mBMMCs after cross-linking of FcεRI. (A) Calcium influx into mBMMCs after stimulation with increasing concentrations of DNP-BSA. (B) Histamine release from mBMMCs after stimulation with either DNP-BSA, Triton X-100 or Calcium Ionophore A23187. Error bars represent the mean ± SEM of three independent analyses. For details on statistical analysis see material and methods. *: $p < 0.01$

Consistent with this observation, *iSYKKO^{-/-}* mBMMCs did not release histamine in response to FcεRI cross-linking, but underwent normal histamine degranulation in response to a calcium ionophore. Total intracellular histamine levels, measured following lysis with Triton X-100, were comparable in *iSYKKO^{+/+}* and *iSYKKO^{-/-}* mBMMCs confirming that FcεRI-mediated degranulation absolutely relies on the signalling through SYK (Fig 13B).

3.3.2. Pharmacological inhibition of SYK abrogates FcεRI-triggered signal transduction in mBMMCs

Pharmacological inhibition of SYK kinase activity using the SYK inhibitors BAY61-3606 (92) and R406 (91) showed a concentration-dependent inhibition of calcium influx (IC_{50} of BAY61-3606 = 43 nM; IC_{50} of R406 = 75 nM) and histamine release (IC_{50} of BAY61-3606 = 111 nM; IC_{50} of R406 = 152 nM) after antigen-induced degranulation (Fig 14A and B), suggesting again that the catalytic function of SYK is required for this event.

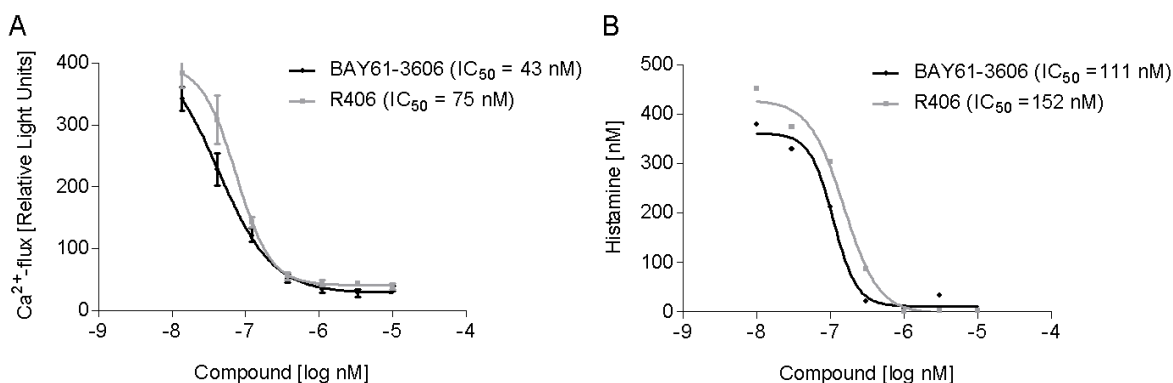


Fig. 14: (A) Concentration-dependent inhibition of calcium flux into murine bone marrow-derived mast cells (mBMMCs) by BAY61-3606 and R406 after cross-linking of high-affinity IgE receptor (FcεRI). Error bars represent the mean \pm SEM of three independent analyses. (B) Concentration-dependent inhibition of antigen-mediated histamine release from mBMMCs by BAY61-3606 or R406. Graph shows the mean of two experiments performed in parallel.

To visualize the blockade of downstream signalling events *iSYKKO^{+/+}* and *iSYKKO^{-/-}* mBMMCs were stimulated by receptor cross-linking in the absence or presence of BAY61-3606 and R406 and analyzed by Western blot analysis. Both pharmacological inhibition and deletion of SYK inhibited the FcεRI-induced phosphorylation of SYK binding partners PLCγ1 and SLP-76 and downstream proteins LAT, ERK, AKT and p38 (Fig. 15).

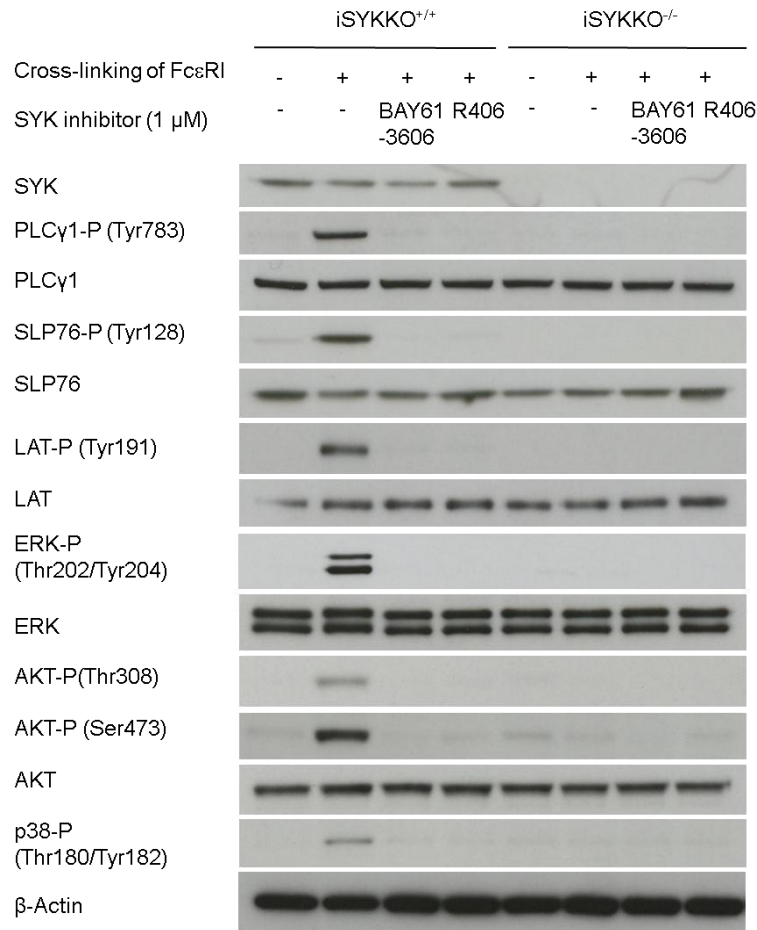


Fig. 15: Analysis of downstream phosphorylation events in *iSYKKO^{+/+}* and *iSYKKO^{-/-}* mBMMCs after cross-linking of the FcεRI as determined by Western blot analysis. Representative Western blots comparing the effect of the induced deletion and pharmacological inhibition of SYK on downstream signalling events in mBMMCs. Shown are representative images of Western blots of one out of three experiments performed analogously.

3.3.3. Deletion and pharmacological inhibition of SYK reduces the IgE-induced passive cutaneous anaphylaxis (PCA) reaction

To address the function of SYK in mast cells *in vivo* iSYKKO^{+/+} and iSYKKO^{-/-} mice were tested in a model of DNP-BSA-induced passive cutaneous anaphylaxis. In this model animals are first injected intradermally with PBS and anti-DNP IgE into the left and right ear, respectively. 24 hours later oedema formation in ear tissue after intravenous injection of DNP-BSA with Evans blue is analyzed. In this experimental setup mast cells are the main effector cells inducing vascular dilatation and oedema formation through the release of histamine and other mediators. Thus, inhibited mast cell degranulation should lead to reduced oedema formation. As such, Evans blue dye leakage is used as a surrogate parameter for mast cell degranulation and subsequent oedema formation.

Testing iSYKKO^{+/+} and wild type mice in this model intravenous injection of DNP-BSA elicited an oedema in DNP-BSA sensitized ears. As shown in figure 16A, the PCA reaction was reduced by 34% in iSYKKO^{-/-} animals in two independent experiments confirming the involvement of SYK in FcεRI mediated mast cell degranulation *in vivo*. Tamoxifen alone had no effect on the PCA reaction in wild type animals (Fig. 16B).

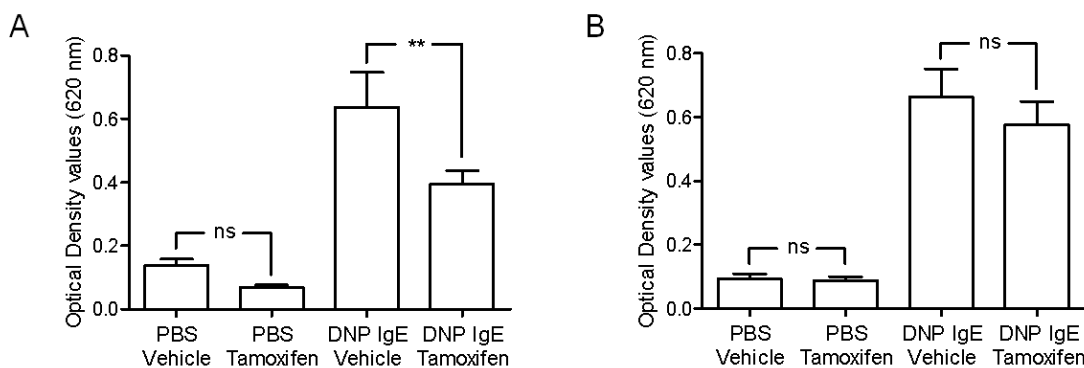


Fig. 16: Amount of dye leakage into ear tissue 30 minutes after DNP-BSA challenge measured colorimetrically at 620 nm in (A) inducible SYK knockout mice and (B) wild type animals after vehicle- or tamoxifen-treatment. Error bars represent the mean ± SEM of seven to nine animals. For details on statistical analysis see material and methods. **: $p < 0.01$

To address whether the effect observed in *iSYKKO*^{-/-} mice was due to the absence of SYK protein or was dependent on the catalytic activity of SYK, the SYK inhibitor BAY61-3606 was tested in the PCA-model. As shown in figure 17, BAY61-3606 dose-dependently inhibited the PCA reaction with an ED₅₀ of 20.6 mg/kg and a maximum effect of 53% at 30 mg/kg (p.o.), indicating that the effect is dependent on the catalytic activity of SYK.

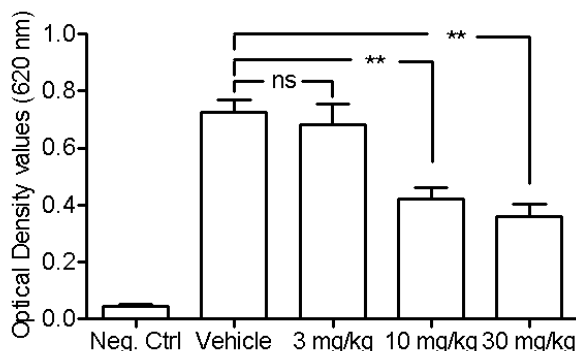


Fig. 17: Evans blue dye leakage into ear tissue of animals pre-treated with BAY61-3606 30 minutes after DNP-BSA challenge. Error bars represent the mean \pm SEM of five independent analyses. For details on statistical analysis see material and methods. **: $p < 0.01$

3.3.4. SYK deletion reduces pathology in a model of ovalbumin-induced pulmonary eosinophilia in a therapeutic and prophylactic setting

Ovalbumin-induced allergic airway inflammation in mice is widely used as a model of airway eosinophilia, pulmonary inflammation and elevated serum IgE levels found in human asthmatics. To get an insight into the role of SYK in this process *iSYKKO* and WT mice were tested in a model of ovalbumin-induced pulmonary eosinophilic lung inflammation in two different settings. In a first set of experiments the consequences of SYK deletion were analyzed in a therapeutic setup by first immunizing the animals with ovalbumin and by inducing the deletion of SYK just before the OVA-challenge. In a second set of experiments the effect of SYK deletion was tested prophylactically by the deletion of SYK before the start of the OVA-immunization. In both setups the allergic response was assessed by eosinophil numbers, IL-4 and IL-5 levels in the BALF and OVA-specific IgE and IgG1 titres in serum.

3.3.4.1. Therapeutic setup

As shown in figure 18, the inhalation of ovalbumin induces a prominent eosinophilic inflammation in the lungs of *iSYKKO*^{+/+} and WT mice. In the therapeutic setup eosinophil numbers in the BALF of *iSYKKO*^{-/-} mice ($0.54 \pm 0.16 \times 10^5$ cells) were reduced by 83% compared to *iSYKKO*^{+/+} mice ($3.26 \pm 1.23 \times 10^5$ cells) (Fig. 18A). In contrast, neutrophil and monocytic cell numbers were unaffected. Tamoxifen alone had no influence on BALF cell numbers in this experimental setup (Fig. 18B).

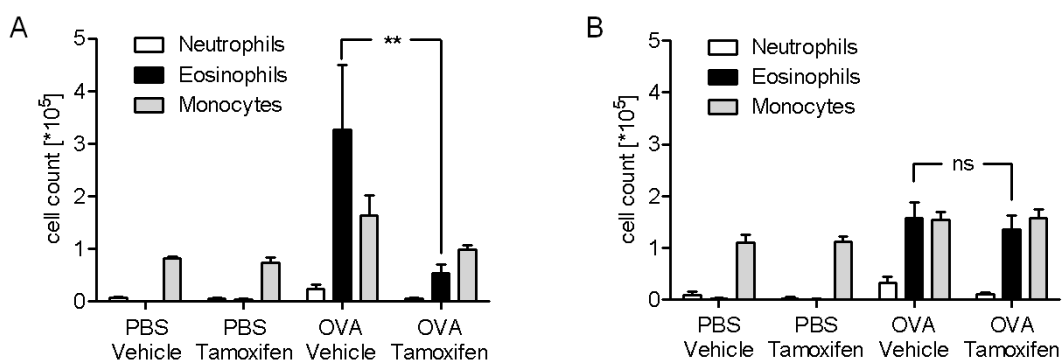


Fig. 18: Neutrophil, eosinophil and monocytic cell counts in the BALF of (A) *iSYKKO* and (B) WT mice in the therapeutic setup 24 hours after second OVA-challenge. Error bars represent the mean \pm SEM of 7 to 8 animals per group. For details on statistical analysis see material and methods. **: $p < 0.01$

The reduced T_H2 response in *iSYKKO*^{-/-} mice was also reflected by decreased IL-4 and IL-5 levels in the BALF of *iSYKKO*^{-/-} mice (28.8 ± 3.4 pg/ml and 78.7 ± 18.0 pg/ml) compared to *iSYKKO*^{+/+} mice (68.1 ± 23.4 pg/ml and 235.4 ± 88.6 pg/ml), respectively (Fig 19A and B). Tamoxifen treatment alone did not affect IL-4 and IL-5 levels in BALF of WT animals (data not shown).

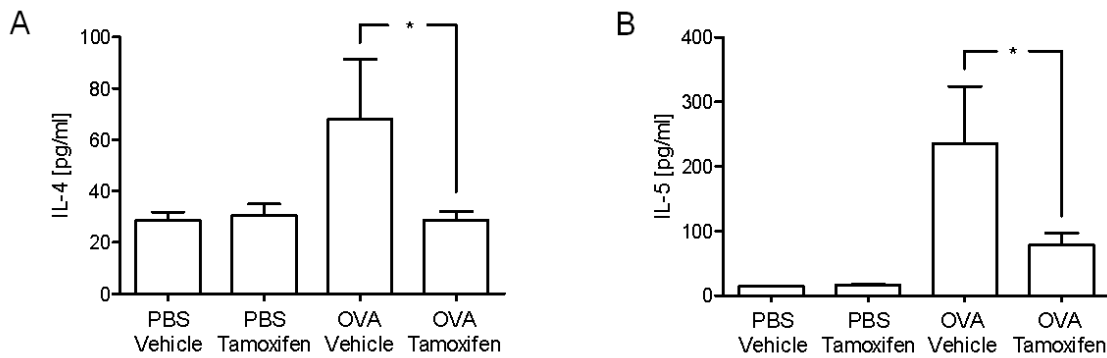


Fig. 19: (A) IL-4 and (B) IL-5 concentrations measured in the BALF of iSYKKO mice 24 hours after second OVA-challenge in the therapeutic model. Error bars represent the mean \pm SEM of 7 to 8 animals. One-way analysis of variances with Bonferroni post test was performed to test for statistical significance. * $p < 0.05$

OVA-specific IgE and IgG1 levels in serum of iSYKKO mice were slightly but non-significantly reduced by the deletion of SYK before the OVA-challenge (Fig. 20A and B).

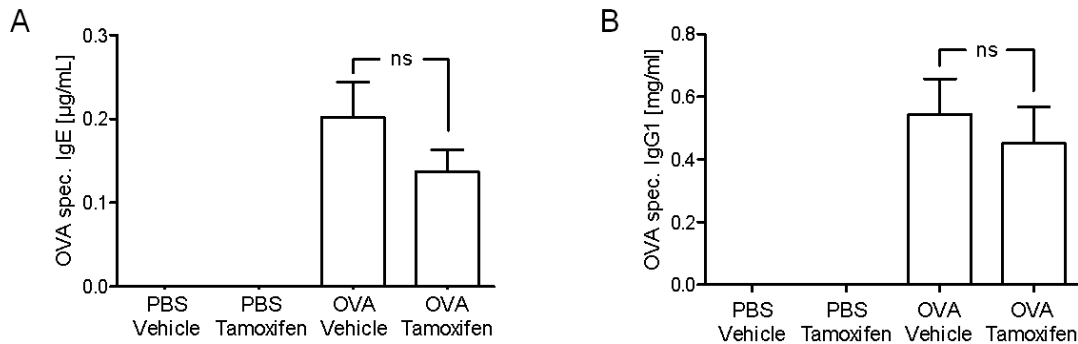


Fig. 20: (A) OVA-specific IgE and (B) IgG1 titres measured in the serum of iSYKKO mice 24 hours after second OVA-challenge in the therapeutic model. Error bars represent the mean \pm SEM of 7 to 8 animals. Unpaired t-test was performed to test for statistical significance.

3.3.4.2. Prophylactic setup

To get an insight into the role of SYK during the immunization process animals were initially treated with tamoxifen to induce the deletion of SYK. Afterwards animals were immunized and challenged with ovalbumin. As shown in figure 21, the deletion of SYK before the immunization did not further improve the outcome. Consistent with the therapeutic model eosinophil numbers in the BALF of *iSYKKO^{-/-}* mice ($0.58 \pm 0.13 \times 10^5$ cells) were reduced by 71% compared to *iSYKKO^{+/+}* mice ($2.00 \pm 0.52 \times 10^5$ cells) (Fig 21A). Again, tamoxifen itself had no influence on BALF cell numbers in wild type mice in the therapeutic setup (Fig. 21B).

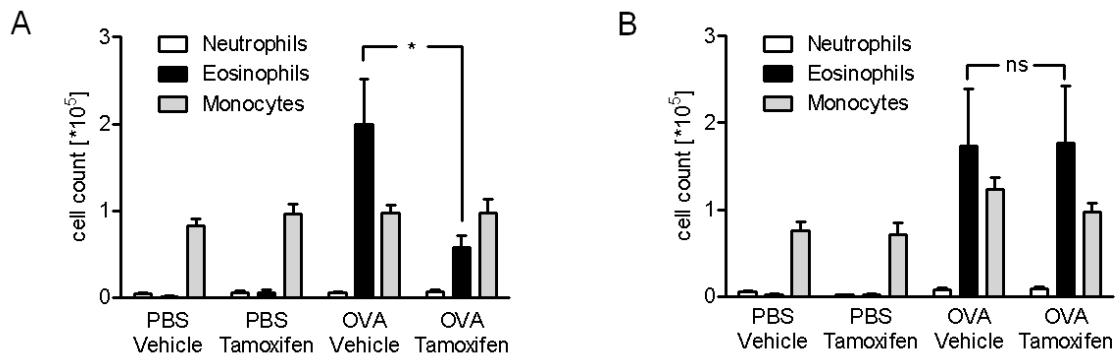


Fig. 21: Neutrophil, eosinophil and monocytic cell counts in the bronchoalveolar lavage of (A) inducible SYK knockout and (B) wild type mice in the prophylactic setup 24 hours after second OVA-challenge. Error bars represent the mean \pm SEM of 7 to 8 animals per group. For details on statistical analysis see material and methods. *: $p < 0.05$

IL-4 and IL-5 cytokine levels in the BALF of *iSYKKO^{-/-}* mice (4.79 ± 0.90 pg/ml and 44.9 ± 13.3 pg/ml) were slightly but, due to the high variability, not significantly reduced compared to cytokine levels in the BALF of *iSYKKO^{+/+}* mice (8.93 ± 2.36 pg/ml and 99.0 ± 38.3 pg/ml) (Fig. 22A and B).

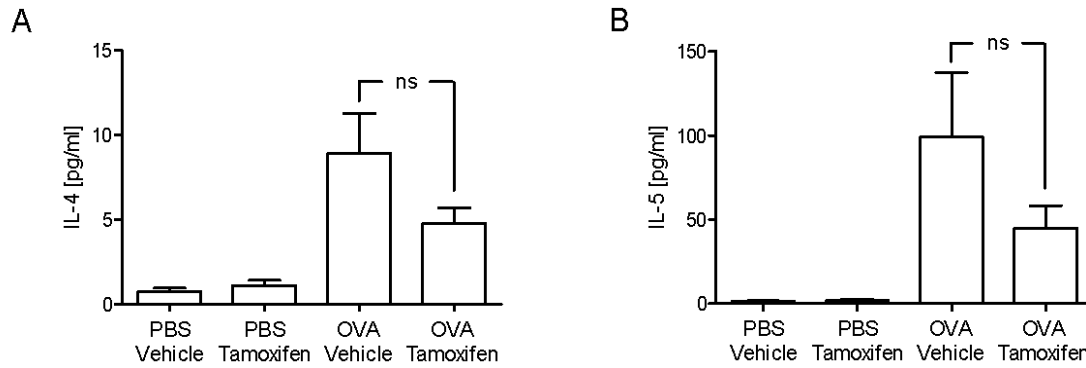


Fig. 22: (A) IL-4 and (B) IL-5 concentrations measured in the BALF of iSYKKO mice 24 hours after second OVA-challenge in the prophylactic model. Error bars represent the mean \pm SEM of 7 to 8 animals. One-way analysis of variances with Bonferroni post test was performed to test for statistical significance.

In contrast to the unaffected OVA-specific antibody levels in the therapeutic setup, a statistically significant increase in OVA specific IgE levels and a statistically significant decrease in OVA-specific IgG1 levels in the serum of iSYKKO^{-/-} mice was found (Fig. 23A and B).

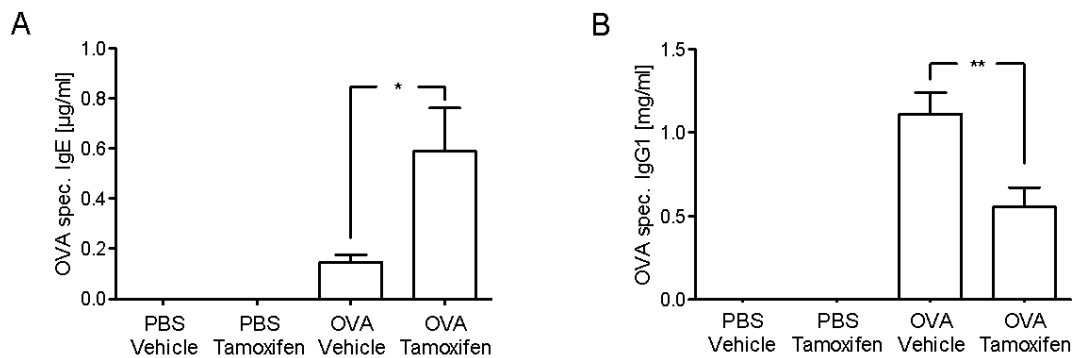


Fig. 23: (A) OVA-specific IgE and (B) IgG1 titres measured in the serum of iSYKKO mice 24 hours after second OVA-challenge in the prophylactic model. Error bars represent the mean \pm SEM of 7 to 8 animals. Unpaired t-test was performed to test for statistical significance. * $p < 0.05$, ** $p < 0.01$

3.3.5. Pharmacological inhibition of SYK reduces ovalbumin-induced pulmonary eosinophilic inflammation in a therapeutic setup

To test whether the effect observed in *iSYKKO*^{-/-} mice was due to the absence of SYK protein or was dependent on the catalytic activity of SYK the effect of the SYK inhibitor BAY61-3606 on BALF cell counts was tested in the OVA-model. In this therapeutic experimental setup BAY61-3606 was intraperitoneally injected 1 hour before, 3 and 6 hours after OVA challenge. The SYK inhibitor significantly decreased the pulmonary eosinophil accumulation by 70% at 30 mg/kg, but had no significant effect on the accumulation of neutrophils or monocytes in the BALF (Fig. 24).

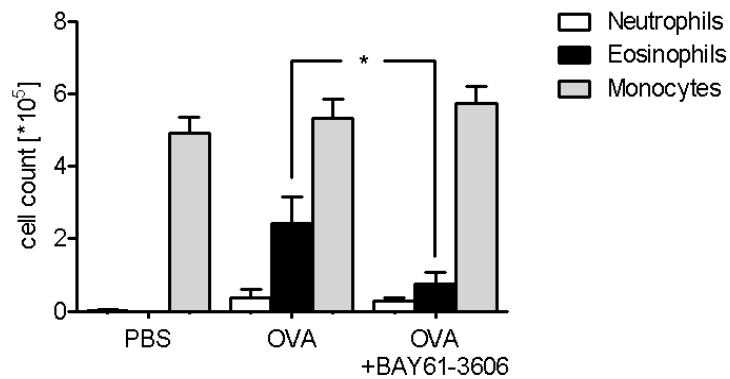


Fig. 24: Neutrophil, eosinophil and monocytic cell numbers in the bronchoalveolar lavage fluid of BALB/c mice after treatment with BAY61-3606 (n = 8 animals per group). Error bars represent the mean \pm SEM of 8 animals per group. For details on statistical analysis see material and methods. *: $p < 0.05$

3.4. Combined effect of reduced B cell counts and inhibition of mast cell function

3.4.1. Long-term SYK deletion improves pathology but leads to increased IgE levels in a model of ovalbumin-induced lung eosinophilia

Having shown that B cell activation is impaired in SYK negative cells *in vitro*, that B cell numbers gradually decrease after long-term SYK deletion *in vivo*, and that SYK deletion impairs mast cell function both *in vitro* and *in vivo*, the next goal was to get an insight into the implications of long-term SYK deletion on allergic parameters in a model of ovalbumin-induced lung eosinophilia.

In this experimental setup animals were treated with vehicle or tamoxifen according to the long-term deletion protocol as detailed in figure 6. After 15 weeks of SYK deletion animals were immunized with ovalbumin and five days after the last of three immunizations animals were challenged with aerosolized ovalbumin. B cell counts in blood and spleen were analyzed by means of flow cytometry. The absolute number of CD45R/B220 positive cells was reduced by 86% in the blood and by 78% in the spleen of iSYKKO^{-/-} mice compared to B cell counts in the vehicle-treated control groups (Fig. 25A and B).

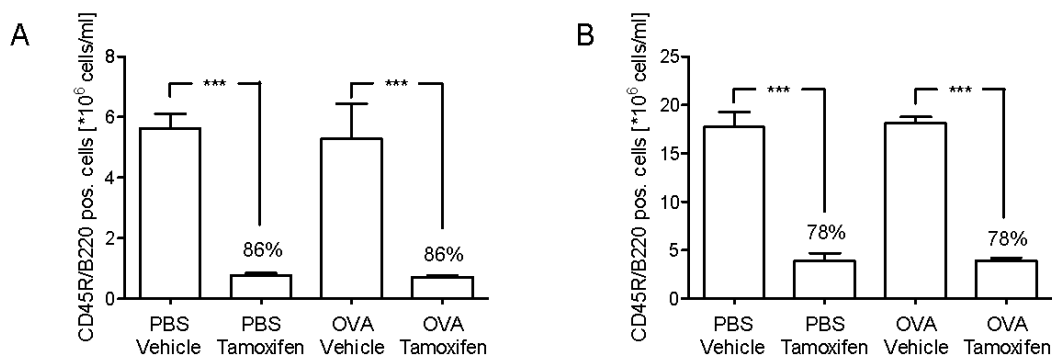


Fig. 25: Number of CD45R/B220 positive cells in (A) blood and (B) spleen of inducible SYK knockout mice after 19 weeks of repeated treatment with either vehicle or tamoxifen. Error bars represent the mean \pm SEM of 6 to 8 animals. One-way analysis of variances with Bonferroni post test was performed to test for statistical significance. *** $p < 0.001$

To evaluate whether reduced B cell counts in combination with inhibited mast cell function further reduce the accumulation of eosinophils in the lung after challenge with nebulized ovalbumin the differential BALF cell count was analyzed. In accordance with the prophylactic and therapeutic model eosinophil numbers in the BALF of *iSYKKO*^{-/-} mice ($1.18 \pm 0.28 \times 10^5$ cells) were reduced again by 74% compared to *iSYKKO*^{+/+} mice ($4.54 \pm 1.70 \times 10^5$ cells) (Fig. 26A). Tamoxifen itself had no influence on BALF cell numbers in wild type mice in the therapeutic setup (Fig. 26B).

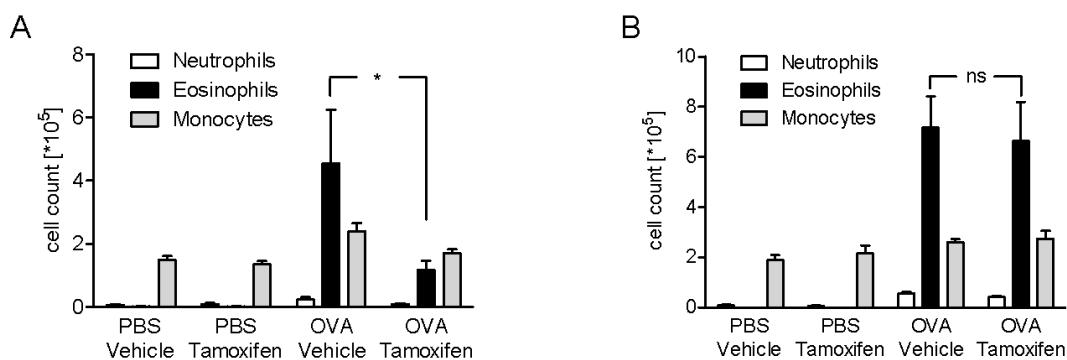


Fig. 26: Neutrophil, eosinophil and monocytic cell counts after long-term SYK deletion in the bronchoalveolar lavage of (A) *iSYKKO* and (B) WT mice 24 hours after second OVA-challenge. Error bars represent the mean \pm SEM of 6 to 8 animals per group. One-way analysis of variances with Bonferroni post test was performed to test for statistical significance. * $p < 0.05$

To rule out that long-term SYK deletion did lead to a reduction in blood eosinophil counts per se the whole blood of all animals included in the study was analyzed for eosinophils. As shown in figure 27, eosinophil numbers in the blood of long-term SYK deleted mice ($0.48 \pm 0.06 \times 10^6$ cells/ml) were undistinguishable from eosinophil numbers in blood of vehicle-treated control mice ($0.49 \pm 0.13 \times 10^6$ cells/ml) after 19 weeks of SYK deletion. These data suggest that the reduced eosinophil numbers in the BALF did not simply reflect a general reduction of eosinophils.

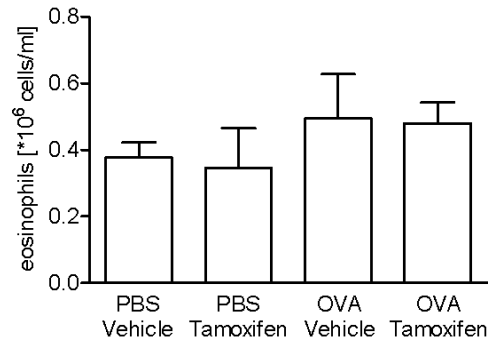


Fig. 27: Eosinophil numbers in blood of iSYKKO mice after treatment of animals with either vehicle or tamoxifen for 19 weeks. Error bars represent the mean \pm SEM of 6 to 8 animals per group.

Having shown that eosinophil accumulation is not further inhibited in the BALF of iSYKKO mice after long-term SYK deletion, the next step was to evaluate the impact of long-term SYK deletion on cytokine levels in BALF and OVA-specific antibody levels in serum. IL-4 levels in the BALF of vehicle-treated mice were considerably induced by the application of ovalbumin and this induction was statistically significantly reduced by 63% after long-term SYK deletion (Fig. 28A). IL-5 levels were not induced by the application of ovalbumin in this setup and no significant changes of IL-5 levels were detectable after long-term SYK deletion (Fig. 28B).

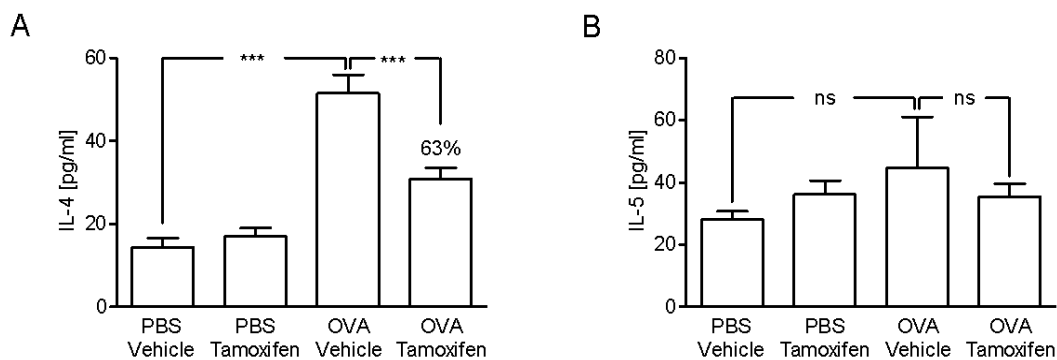


Fig. 28: (A) IL-4 and (B) IL-5 levels in BALF of iSYKKO mice 24 hours after second OVA-challenge after treatment of mice with either vehicle or tamoxifen for 19 weeks. Error bars represent the mean \pm SEM of 7 to 8 animals. One-way analysis of variances with Bonferroni post test was performed to test for statistical significance. *** $p < 0.001$

In accordance with the findings made in the prophylactic setup, ovalbumin-treatment resulted in a statistically significant increase of OVA-specific IgE levels in the serum of long-term SYK deleted mice compared to the vehicle-treated control animals ($0.133 \pm 0.027 \mu\text{g/ml}$ vs. $0.268 \pm 0.045 \mu\text{g/ml}$) (Fig. 29A) and in a decrease in OVA-specific IgG1 levels ($0.59 \pm 0.06 \text{ mg/ml}$ vs. $0.11 \pm 0.04 \text{ mg/ml}$) (Fig. 29B).

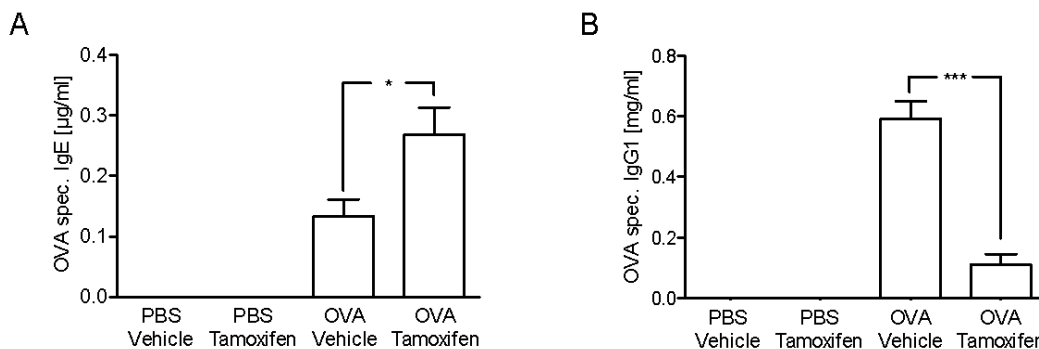


Fig. 29: (A) OVA-specific IgE and (B) IgG1 titres measured in the serum of iSYKKO mice 24 hours after second OVA-challenge after pre-treatment of animals with vehicle or tamoxifen for 19 weeks. Error bars represent the mean \pm SEM of 6 to 8 animals. Unpaired t-test was performed to test for statistical significance. * $p < 0.05$; *** $p < 0.001$

3.4.2. Total CD23 expression on spleen cells is reduced after long-term SYK deletion

CD23, the low-affinity receptor for IgE (Fc ϵ RII), is an important regulator of IgE synthesis. *In vivo* studies showed that mice lacking CD23 exhibit increased IgE production whereas mice overexpressing CD23 show strongly suppressed IgE responses (93,94). CD23 is expressed on B cells and treatment of B cells with IL-4 leads to the up-regulation of CD23 (95). To test the hypothesis that reduced CD23 expression might be the reason for the increased IgE titres in the serum of SYK deleted mice, spleen cells were isolated from iSYKKO and wild type mice 19 weeks after the initiation of vehicle or tamoxifen treatment. Single cell suspensions of the spleens were stained using fluorescent-labelled CD45R/B220 and CD23 antibodies and analyzed using a BD LSR II flow cytometer. OVA-treatment significantly increased the number of CD23^{high} CD45R/B220 positive cells in the spleens of both, iSYKKO^{+/+} and wild

type mice (Fig. 30A and B). Deletion of SYK for 19 weeks resulted in a statistically significant increase in the percentage of CD23 positive B cells in the spleen of *iSYKKO*^{-/-} mice (data not shown). However, the reduced B cell count in the spleens of long-term SYK deleted mice resulted in a significant reduction of the total number of CD23^{high} CD45R/B220 positive cells (Fig. 30A). Tamoxifen treatment of wild type animals did also lead to an increase in the percentage of CD23 positive B cells but had no detectable influence on the total number of CD23 positive B cells in the spleens of these animals (Fig. 30B).

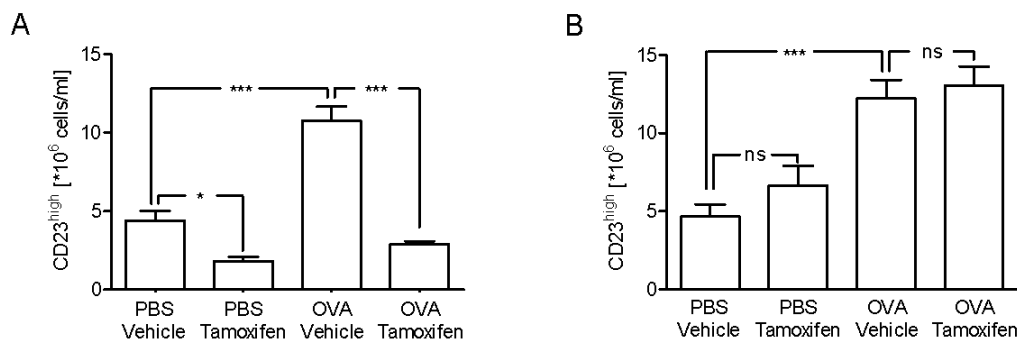


Fig. 30: Number of CD23^{high} CD45R/B220 positive splenic B cells in (A) *iSYKKO* or (B) wild type mice after 19 weeks of treatment with either vehicle or tamoxifen as measured by flow cytometry. Error bars represent the mean ± SEM of 6 to 8 animals. One-way analysis of variances with Bonferroni post test was performed to test for statistical significance. * p < 0.05; *** p < 0.001

3.5. Function of SYK in splenocytes

3.5.1. IL-3-induced cytokine production from primary splenocytes is defective after deletion or pharmacological inhibition of SYK

Mast cells are involved in the promotion of T_H2 responses through the release of a host of different mediators. Since the deletion of SYK leads to a functional impairment of mast cells T_H2 responses are dampened in *iSYKKO*^{-/-} mice. However, little is known about the cell types involved in the initiation of T_H2 responses. A recent study identified basophils as the cell type that can be directly targeted by protease allergens leading to the induction of T_H2 differentiation *in vivo* through the production of T_H2-promoting cytokines such as IL-4 (96).

Basophils express the IL-3 receptor on their surface, which in response to IL-3 induces the production of a variety of cytokines that amongst others promote T_H2 differentiation (28). SYK was shown to be involved in signalling events downstream of the IL-3 receptor in basophils (28). To verify the role of SYK in this process the ability of splenocytes to release cytokines in response to IL-3 was sampled after pharmacological inhibition or deletion of SYK. In a first set of experiments splenocytes from iSYKKO^{+/+} mice were incubated for 24 hours with IL-3 and the expression of IL-4 was measured in the supernatants. Figure 31 shows that IL-3 concentration-dependently induced the release of IL-4 from spleen cells and that the SYK inhibitor R406 concentration-dependently inhibited the release of IL-4. DMSO alone had no influence on the IL-3-induced IL-4 release.

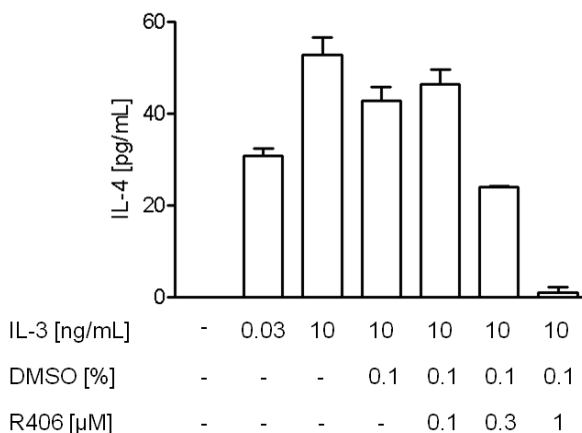


Fig. 31: IL-3-induced IL-4 expression from spleen cells isolated from an iSYKKO^{+/+} mouse. Spleen cells were treated with IL-3 for 24 hours in the absence or presence of the SYK inhibitor R406. Error bars represent the mean \pm SEM of three independent analyses.

As a next step it was evaluated whether the IL-3-induced cytokine release is also inhibited in cells isolated from iSYKKO^{-/-}. For this purpose single cell suspensions from the spleens of iSYKKO^{+/+} and iSYKKO^{-/-} mice were prepared and stimulated with IL-3 for 72 hours. IL-3-induced a prominent release of both IL-4 and IL-6 from iSYKKO^{+/+} spleen cells, which was abrogated when SYK activity was inhibited by R406 (Fig. 32A and B). Cells isolated from the spleen of iSYKKO^{-/-} animals completely lacked their ability to release IL-4 or IL-6 in response to ligation of the IL-3 receptor.

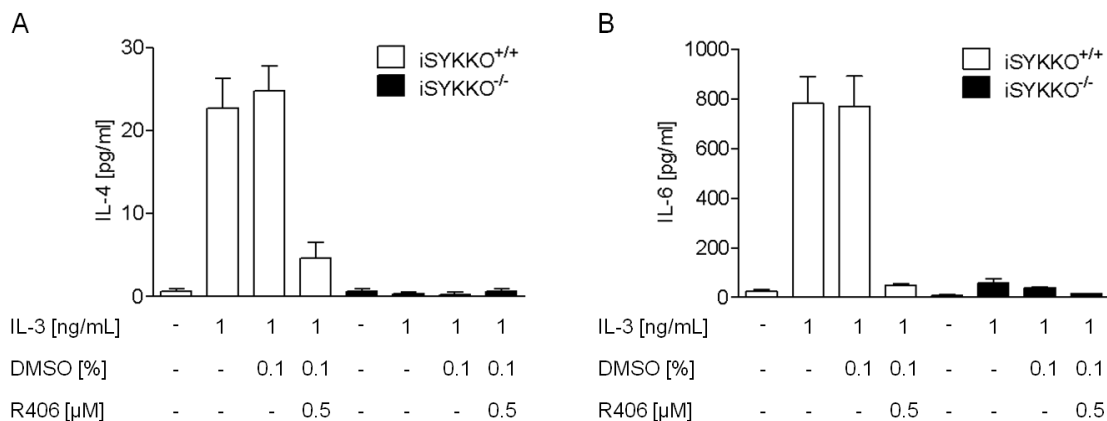


Fig. 32: IL-3-induced expression of (A) IL-4 and (B) IL-6 from splenocytes isolated from iSYK^{+/+} or iSYK^{-/-} mice, respectively. Spleen cells were treated with IL-3 for 72 hours in the absence or presence of the SYK inhibitor R406. Error bars represent the mean \pm SEM of three independent analyses.

3.6. Function of SYK in neutrophils

3.6.1. SYK deletion results in increased chemotactic activity of SYK negative neutrophils *in vitro*

The recruitment of neutrophils to the site of tissue damage or infection constitutes the first line of host defence against invading organisms. Neutrophils exhibit a strong directional migration towards increasing concentrations of chemokines or bacterial peptides. Thus, the capability of neutrophils to migrate in response to a variety of chemoattractants plays a pivotal role in setting the early stages of inflammation. To get an insight into the role of SYK in the *in vitro* migration of primary neutrophils iSYK^{+/+} and iSYK^{-/-} mice were stimulated intraperitoneally with thioglycollate. Peritoneal exudates, which predominantly contained neutrophils, were extracted four hours after i.p. treatment and seeded in the upper compartment of a 96-well cell migration system with a 5.0 μ m porous polycarbonate membrane. The lower compartments contained different concentrations of the murine neutrophil chemokine KC. Figure 33 shows that the migration of iSYK^{-/-} neutrophils

towards KC was increased compared to the migration of cells isolated from *iSYKKO*^{+/+} mice. Migration of SYK negative neutrophils reached a maximum at a concentration of 10 nM KC, while the number of migrating SYK positive neutrophils increased gradually up to a concentration of 300 nM KC.

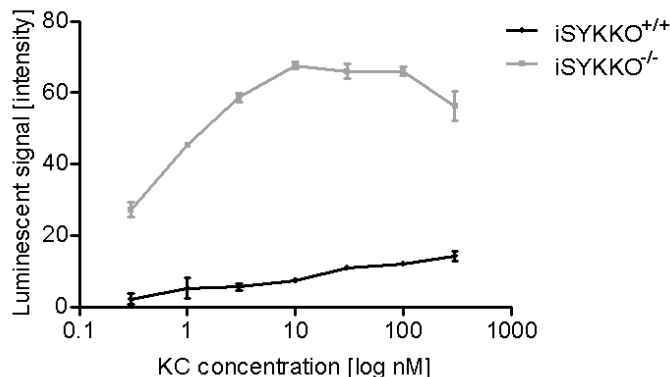


Fig. 33: Migration of primary peritoneal neutrophils towards KC in a 96-well cell migration system with a 5.0 μm porous polycarbonate membrane. The number of migrated cells was measured using a luciferase assay generating a luminescent signal which was proportional to the number of cells present. Error bars represent the mean \pm SEM of three independent analyses

3.6.2. SYK is not required *in vivo* for the migration of neutrophils in models of thioglycollate-induced sterile peritonitis and LPS- or CS-induced pulmonary inflammation

Having shown that SYK deletion does not negatively impact the capability of neutrophils to migrate towards a chemotactic stimulus *in vitro*, disease-related animal models were used to test whether the same holds true for the *in vivo* situation. To explore the function of SYK in the migration of neutrophils *in vivo* *iSYKKO* mice were used in models of thioglycollate-induced sterile peritonitis, lipopolysaccharid- and cigarette smoke-induced pulmonary inflammation.

In the thioglycollate-induced sterile peritonitis model, administration of thioglycollate resulted in the influx of predominantly neutrophils into the peritoneum of *iSYKKO*^{+/+} and *iSYKKO*^{-/-} mice. Deletion of SYK had no impact on neutrophil numbers, since the WBC and

neutrophil cell count in the peritoneal lavage fluid of *iSYKKO*^{-/-} mice was similar or slightly higher compared to the cell count in *iSYKKO*^{+/+} animals (Fig. 34A). Direct instillation of LPS into the lung or inhalation of cigarette smoke also induces a prominent pulmonary neutrophilic inflammation. Again, deletion of SYK had no effect on neutrophil cell numbers in BALF in both experimental setups (Fig. 34B and C).

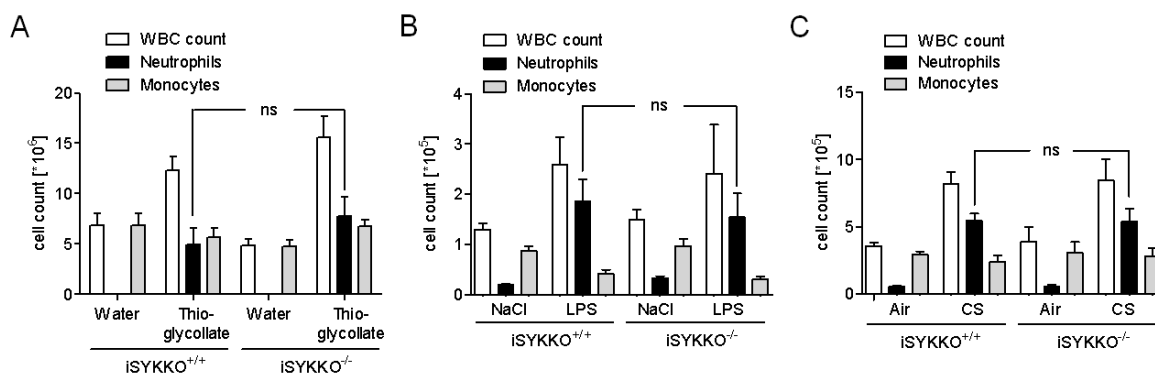


Fig. 34: WBC, neutrophil and monocytic cell count in *iSYKKO*^{+/+} and *iSYKKO*^{-/-} mice in animal models of thioglycollate-induced sterile peritonitis and lipopolysaccharid- or cigarette smoke-induced pulmonary inflammation. Cell counts in *iSYKKO*^{+/+} and *iSYKKO*^{-/-} mice in the (A) peritoneal lavage fluid four hours after thioglycollate application (n=6 animals per group), (B) bronchoalveolar lavage fluid four hours after LPS challenge (n=8 animals per group) and (C) bronchoalveolar lavage fluid 18 hours after last cigarette smoke exposure. (n=5-7 animals per group). Error bars represent the mean \pm SEM of n animals. For details on statistical analysis see material and methods.

3.7. Function of SYK in macrophages

3.7.1. SYK deletion has no influence on cell recruitment in models of MCP-1 and cigarette smoke-induced monocytic lung inflammation

SYK has been shown to be essential for the CX3CL1-induced chemotaxis of monocytes/macrophages *in vitro* (69). Furthermore, SYK has been implicated in MCP-1-induced receptor-mediated signal transduction by activating the p38 pathways eventually leading to monocytic transendothelial migration (47). To get an insight into the role of SYK in the

migration of macrophages *in vivo* the inducible SYK knockout mice were tested in models of MCP-1 and chronic cigarette smoke-induced lung inflammation, both models aiming at the recruitment of macrophages to the lung.

Treatment of mice with MCP-1 (in combination with LPS) led to a prominent monocytic lung inflammation in both inducible SYK knockout and wild type mice. However, neither the SYK deletion in iSYKKO mice, nor the tamoxifen treatment in wild type mice had an influence on total or differential BALF cell counts (Fig. 35A and B).

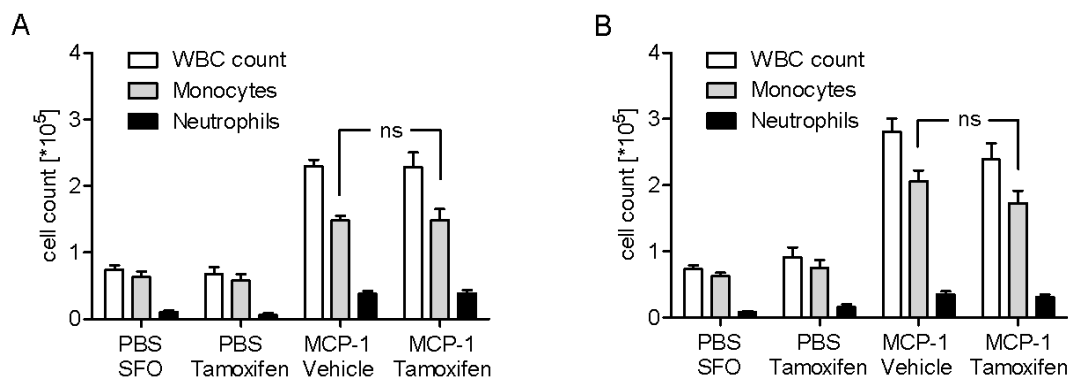


Fig. 35: Total, monocytic and neutrophil cell numbers in the bronchoalveolar lavage fluid of (A) iSYKKO and (B) WT mice treated with either PBS or MCP-1. Error bars represent the mean \pm SEM of 6 to 8 animals. One-way analysis of variances with Bonferroni post test was performed to test for statistical significance.

To confirm that the absence of SYK does not affect macrophage migration *in vivo* and that this observation was not dependent on the experimental model used, the animals were additionally tested in a chronic cigarette smoke model. In this experiment animals were exposed to cigarette smoke over a period of three weeks and 24 hours after the last cigarette smoke exposure the lungs were lavaged. The exposure of iSYKKO and wild type mice to cigarette smoke led to a prominent accumulation of monocytic cells in the lungs of both strains independent if animals were pre-treated with vehicle or tamoxifen. Intriguingly, tamoxifen treatment of both, iSYKKO and wild type mice, led to increased monocytic cell counts compared to the vehicle-treated control groups (Fig. 36A and B).

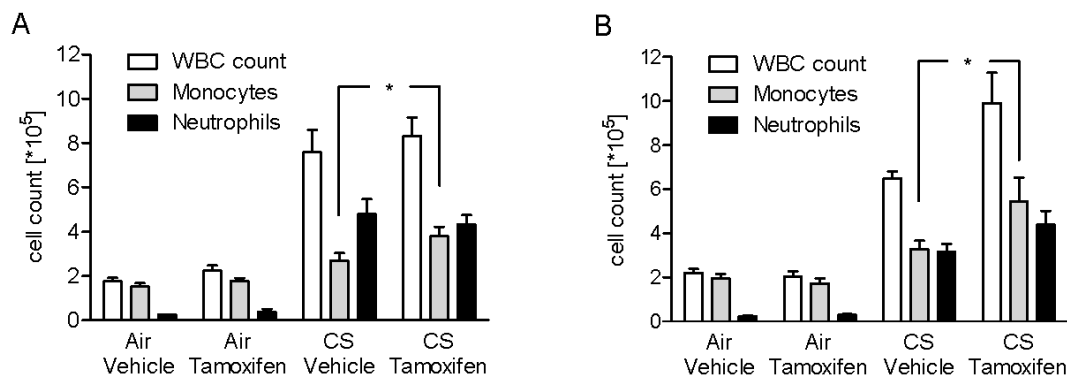


Fig. 36: WBC, monocytic and neutrophil cell numbers in the bronchoalveolar lavage fluid of (A) iSYKKO and (B) WT mice after 3 weeks of exposure to either air or cigarette smoke (CS). Error bars represent the mean \pm SEM of 6 to 8 animals. One-way analysis of variances with Bonferroni post test was performed to test for statistical significance. * $p < 0.05$

3.8. Function of SYK in osteoclasts

3.8.1. *In vitro* differentiation and function is inhibited in SYK negative osteoclasts

To get an insight into the role of SYK during osteoclastogenesis bone marrow cells were isolated from wild type or inducible SYK knockout mice after vehicle or tamoxifen treatment and cultured with M-CSF and RANKL, two well-described mediators of osteoclast differentiation (72). On day 9, cells were fixed and analyzed for tartrate-resistant acid phosphatase (TRAP) activity. Figure 37A shows that only cells isolated from wild type or vehicle-treated iSYKKO mice with functional SYK developed into multinucleated TRAP-positive giant cells. In contrast, cells isolated from iSYKKO^{-/-} mice showed TRAP-staining but were much smaller with an irregular shape. Tamoxifen treatment of wild type animals alone had no effect on osteoclast development *in vitro* (Fig. 37A). Western blot analysis confirmed that SYK protein was reduced below the detection limit in cells generated from the bone marrow of iSYKKO^{-/-} knockout mice concomitant with a lack of phosphorylation of SYK-downstream target molecules, like SLP-76 (Fig. 37B).

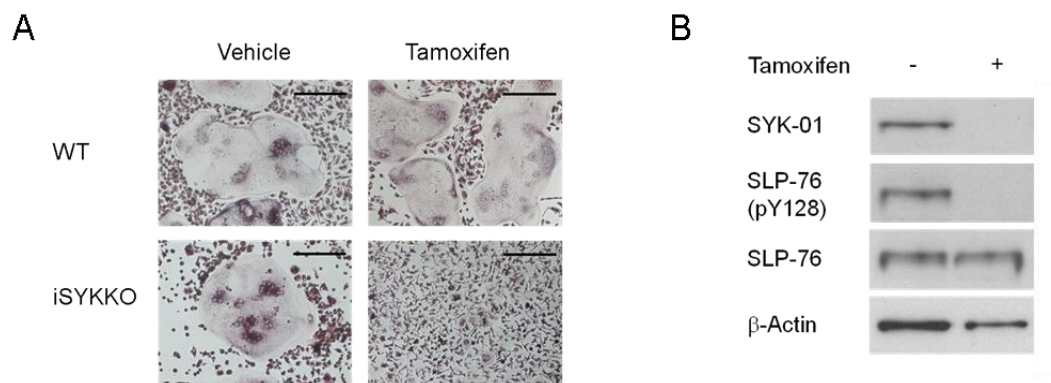


Fig 37: Analysis of osteoclasts generated from the bone marrow of WT or iSYKKO mice after vehicle or tamoxifen treatment. Animals were treated with vehicle or tamoxifen according to the short-term protocol. Ten days after the last p.o. application bone marrow cells were isolated and cultured with M-CSF and RANKL. (A) After 9 days of culture cells were stained for tartrate-resistant acid phosphatase activity. Black bars represent 200 μm. Shown are representative images of one out of seven experiments performed analogously. (B) Cells were lysed in 1 x LDS sample buffer and lysates were subjected to Western blot analysis. Antibodies used are indicated.

To further evaluate the impact of SYK deletion on osteoclast function, cells were grown on calcium phosphate-coated quartz slides mimicking the *in vivo* bone surface. After nine days of culture cells were removed and the remaining calcium phosphate surface was visualized using von Kossa staining. Only SYK positive cells resorbed the calcium phosphate layer while SYK negative osteoclasts completely lacked their resorptive capacity (Fig. 38A). Osteoclasts isolated from tamoxifen-treated wild type animals showed no functional abnormalities (Fig. 38A). To quantify the functional impairment after deletion of SYK osteoclasts generated from the bone marrow of seven individual mice per group were grown on calcium phosphate and the number of resorption pits was quantified. Figure 38B shows that SYK negative osteoclasts completely failed to resorb the calcium phosphate surface.

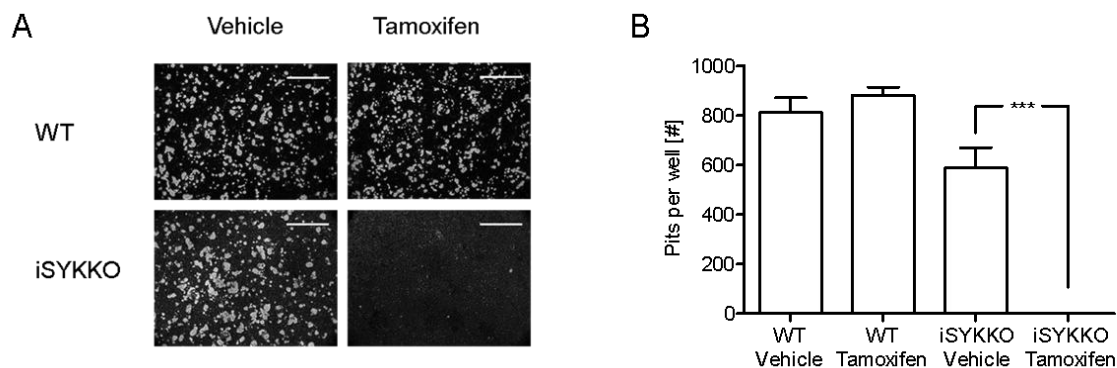


Fig. 38: Evaluation of resorption capacity of osteoclasts cultured on calcium phosphate-coated quartz slides. After 9 days cells were removed and the remaining calcium phosphate was visualized using von Kossa staining. (A) Representative images of the von Kossa-stained calcium phosphate surface. White bars represent 400 μm . Shown are representative images of one out of seven experiments performed analogously. (B) The number of resorption pits per well was quantified. Error bars represent the mean \pm SEM of seven independent analyses. Unpaired t-test was performed to test for statistical significance. *** $p < 0.001$

3.8.2. Pharmacological inhibition of SYK activity concentration-dependently inhibits osteoclast differentiation and function *in vitro*

The pharmacological SYK inhibitor R406 was used to address whether the defects in osteoclast differentiation and function observed in SYK negative cells were due to the lack of its kinase activity or a consequence of a potential missing adapter function of the SYK protein. As shown in figure 39A, treatment of bone marrow cells with R406 concentration-dependently inhibited osteoclastogenesis *in vitro*. Furthermore, increasing concentrations of R406 led to decreasing numbers of multinucleated TRAP-positive cells. At a concentration of 1 μM R406 TRAP-staining was completely absent.

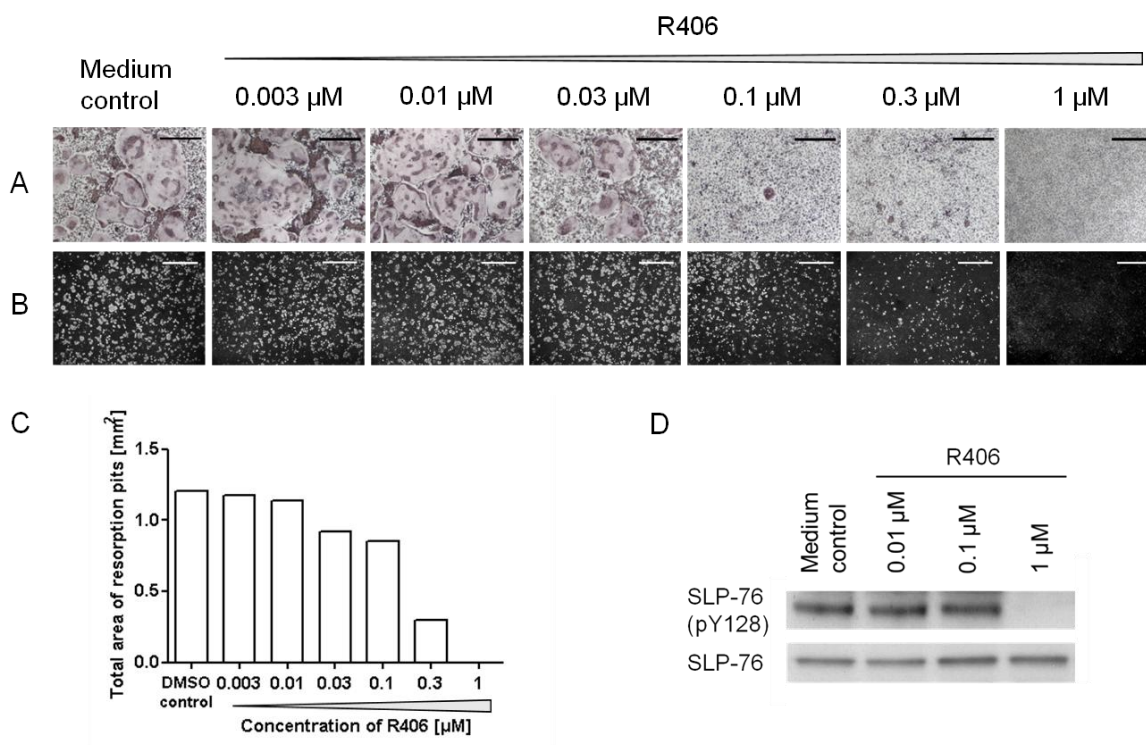


Fig. 39: Effect of the pharmacological inhibition of SYK on osteoclast differentiation and function *in vitro*. Bone marrow cells isolated from BALB/c mice were cultured for 9 days with M-CSF and RANKL in the presence of increasing concentrations of the SYK inhibitor R406. (A) Cells were stained for tartrate-resistant acid phosphatase activity. Black bars represent 100 μm . (B) Cells were grown on calcium phosphate-coated quartz slides. After 9 days cells were removed and the remaining calcium phosphate was visualized using von Kossa staining. White bars represent 400 μm . (A+B) Shown are representative images of one out of two independent experiments. (C) Total area of resorption pits was analyzed. Bars represent mean values of two parallel determinations. (D) Bone marrow cells cultured for 9 days with M-CSF and RANKL in the presence of the SYK inhibitor R406 were lysed and subjected to Western blot analysis.

Consistent with the concentration-dependent inhibition of osteoclast differentiation, osteoclast function was also inhibited. Treatment with R406 concentration-dependently blocked the ability of cells to resorb the calcium phosphate surface with an IC_{50} value of 0.28 μM . At a concentration of 1 μM R406 osteoclast function was completely absent (Fig. 39B and C). The concentration-dependent inhibition of SYK by R406 was confirmed by Western blot analysis showing that the phosphorylation of the downstream target molecule SLP-76 was absent at 1 μM R406 (Fig. 39D).

3.8.3. SYK deletion leads to reduced TRACP 5b and CTX-I levels in the serum of SYK knockout mice

Having shown that SYK plays a pivotal role in osteoclast development and function *in vitro* the following experiments were performed to get an insight into the effect of SYK deletion on osteoclast numbers and resorption activity *in vivo*. For this purpose WT or iSYKKO animals were treated with vehicle or tamoxifen according to the treatment protocol for long-term SYK deletion. Eighteen weeks after the first p.o. administration serum samples were collected. To quantify osteoclast numbers TRACP 5b (tartrate-resistant acid phosphatase, isoform 5b) levels were determined. TRACP 5b is an enzyme that is expressed in high amounts by osteoclasts.

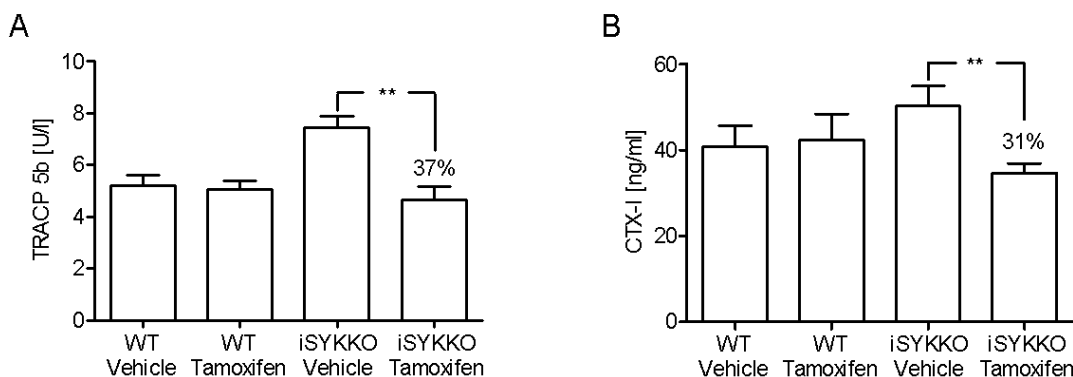


Fig. 40: Serum markers of osteoclast number and resorption activity are significantly reduced in SYK deleted animals. Eighteen weeks after the first administration of vehicle or tamoxifen blood was taken from wild type (WT) or inducible SYK knockout mice (iSYKKO) and (A) osteoclast-derived tartrate-resistant acid phosphatase form 5b (TRACP 5b) or (B) C-telopeptide of type I collagen (CTX-I) were quantified by ELISA. Error bars represent the mean \pm SEM of six to eight animals. Unpaired t-test was performed to test for statistical significance. ** $p < 0.01$

TRACP 5b was decreased by 37% ($p = 0.001$) in iSYKKO^{-/-} mice compared to the TRACP 5b levels in the serum of iSYKKO^{+/+} mice whereas tamoxifen treatment alone had no effect on TRACP 5b levels in wild type animals (Fig. 40A). To assess bone resorption *in vivo* CTX-I (C-telopeptide of type I collagen) levels were measured in the serum of the same mice. CTX-I is

a degradation product of collagen type I generated by osteoclasts during the resorption of the bone matrix. As shown in figure 40B, CTX-I levels were reduced by 31% ($p = 0.009$) after 18 weeks of SYK deletion.

3.8.4. Osteoblast and osteoclast numbers in humeri are not affected after 18 weeks of SYK deletion

The tartrate-resistant acid phosphatase and alkaline phosphatase stainings of humeri were performed in collaboration with the toxicological department at Boehringer Ingelheim Pharma GmbH & Co. KG (Biberach, Germany) under supervision of Dr. Florian Colbatzky.

Since all the parameters evaluated *in vitro* and the TRACP 5c and CTX-I levels measured in serum of iSYKKO^{-/-} mice pointed towards a defect in osteoclast development and function, alkaline phosphatase- and TRAP-stained sections of humeri, which were isolated from mice after 18 weeks of SYK deletion, were analyzed as a measure of osteoblast and osteoclast numbers, respectively.

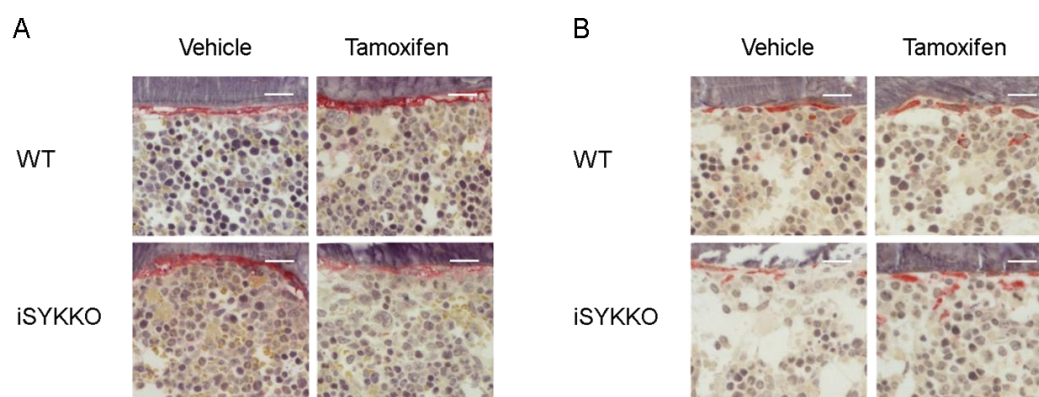


Fig. 41: Sections of humeri stained for alkaline phosphatase or tartrate-resistant acid phosphatase activity. WT and iSYKKO mice were treated with vehicle or tamoxifen according to the treatment protocol for long-term SYK deletion. Eighteen weeks after the initiation of p.o. treatment humeri were removed, fixed in paraformaldehyde and embedded in plastic. Longitudinal sections (2 μm thickness) of the humeri were stained for (A) alkaline phosphatase or (B) tartrate-resistant acid phosphatase to visualize osteoblasts or osteoclasts, respectively. White bars represent 40 μm . Shown are representative images of one out of ten experiments performed analogously.

Figure 41A illustrates that the number of alkaline phosphatase-positive osteoblasts in humeri of iSYKKO^{+/+} and iSYKKO^{-/-} was comparable. Tamoxifen-treatment of wild type mice did also not influence osteoblast numbers. Furthermore, the number of TRAP-positive osteoclasts was not significantly reduced in the humeri of iSYKKO^{-/-} compared to the number of TRAP-positive cells in the humeri of iSYKKO^{+/+} mice. Tamoxifen-treatment of WT animals did neither affect the number nor the appearance of TRAP-positive cells (Fig. 41B).

3.8.5. Cortical thickness of femora is increased in female mice after 18 weeks of SYK deletion

The morphometric analysis of the cortical and trabecular bone architecture, as well as the mechanical tests described here were performed in collaboration with the Institute of Biomechanics (Trauma Center Murnau, Germany) under the supervision of Prof. Peter Augat.

To assess the consequences of long-term SYK deletion on bone strength a quantitative evaluation of cortical bone architecture was carried out by means of μ CT analysis. Bones were isolated 18 weeks after the first vehicle or tamoxifen administration. Evaluation parameters included cortical thickness, cortical volume and polar moment of inertia. To be able to detect potential gender differences data for male and female mice were analyzed separately. Male iSYKKO mice showed no significant change in any cortical parameter evaluated (Fig. 42). For the femora isolated from female iSYKKO^{-/-} mice a 12% increase in cortical thickness compared to female iSYKKO^{+/+} mice was observed (0.269 ± 0.008 mm vs. 0.241 ± 0.004 mm, $p = 0.01$, Fig. 42A). However, no significant effects on cortical volume (Fig. 42B) or polar moment of inertia (Fig. 42C) were detectable in female iSYKKO^{-/-} mice. Tamoxifen treatment alone had no significant effects on cortical parameters of the femora of wild type mice (data not shown).

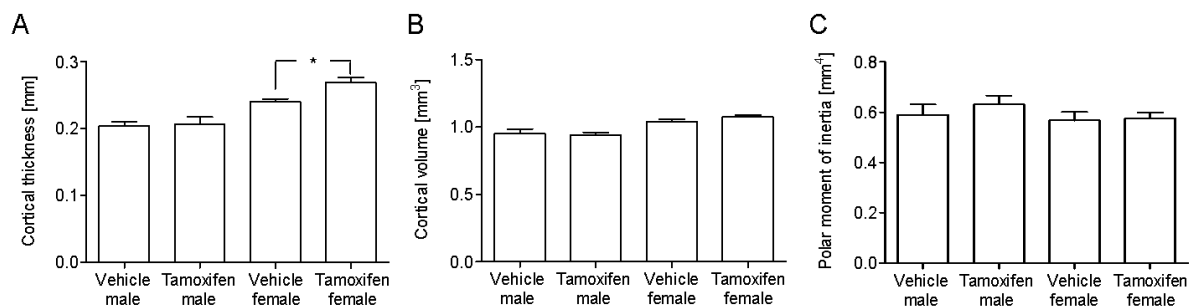


Fig. 42: Quantitative evaluation of cortical thickness, cortical volume and polar moment of inertia measured by means of μ CT analysis. Inducible SYK knockout mice were treated with vehicle or tamoxifen according to the treatment protocol for long-term SYK deletion. Eighteen weeks after the initiation of p.o. treatment femora were removed and cortical bone parameters including (A) cortical thickness, (B) cortical volume and (C) polar moment of inertia were determined by means of μ CT analysis (n=10 animals per group, 5 of each gender). Error bars represent the mean \pm SEM. Unpaired t-test was performed to test for statistical significance. * $p < 0.05$

3.8.6. Changes in trabecular parameters are only seen in female SYK knockout mice after 18 weeks of SYK deletion

To further assess bone quality after long-term SYK deletion the trabecular structure of the femora and L1 vertebrae was analyzed.

In accordance with the cortical analysis most of the changes seen in trabecular bone after SYK deletion were restricted to the female SYK knockout mice. For the femora of the female $iSYK^{KO-/-}$ mice a significant increase in relative bone volume, connectivity density, trabecular number, trabecular thickness, and apparent density together with a significant decrease in the structural model index, trabecular separation and relative bone surface were observed (Table II).

Femora	Female		Male	
	Vehicle	Tamoxifen	Vehicle	Tamoxifen
Relative bone volume (BV/TV) [%]	4.18 ± 1.44	12.5 ± 2.7*** (↑)	9.67 ± 4.37	10.2 ± 3.6
Connectivity density (Conn. D.) [1/mm ³]	20.1 ± 12.9	61.4 ± 21.8** (↑)	60.7 ± 50.7	66.2 ± 24.5
Structure model index (SMI) [-]	3.12 ± 0.31	1.56 ± 0.32*** (↓)	2.08 ± 0.36	2.32 ± 0.48
Trabecular number (Tb. N.) [1/mm]	2.58 ± 0.24	3.10 ± 0.29* (↑)	3.27 ± 1.00	3.70 ± 0.30
Trabecular thickness (Tb. Th.) [mm]	0.048 ± 0.003	0.054 ± 0.002* (↑)	0.051 ± 0.006	0.049 ± 0.007
Trabecular separation (Tb. Sp.) [mm]	0.39 ± 0.03	0.33 ± 0.03* (↓)	0.32 ± 0.11	0.27 ± 0.02
Apparent density [mgHA/cm ³]	139 ± 19	227 ± 25*** (↑)	186 ± 46	202 ± 34
Material density [mgHA/cm ³]	1040 ± 35	1020 ± 30	1008 ± 16	1016 ± 31
Relative bone surface (BS/BV) [1/mm]	61.1 ± 4.0	45.3 ± 1.4*** (↓)	51.5 ± 7.3	54.8 ± 8.5

Table II: Analysis of the trabecular structure of femora isolated from inducible SYK knockout mice. Data are expressed as the mean of $n = 5 \pm$ standard deviation. Arrows indicate increased (↑) or decreased (↓) values compared to vehicle controls. Unpaired t-test was performed to test for statistical significance. * $p < 0.05$, ** $p < 0.01$, *** $p < 0.001$

Consistent with these observations a significant increase in the connectivity density and in trabecular number, as well as a significant decline in the structural model index, in trabecular separation and in the material density of the L1 vertebrae of the female *iSYKKO*^{-/-} mice was found (Table III). For the male *iSYKKO*^{-/-} mice no significant effects were observed in the femora (Table II). In the L1 vertebrae of the male *iSYKKO*^{-/-} mice a decrease in connectivity density and an increase in material density were the only significant effects (Table III).

L1 vertebrae	Female		Male	
	Vehicle	Tamoxifen	Vehicle	Tamoxifen
Relative bone volume (BV/TV) [%]	26.3 ± 2.9	34.1 ± 8.5	20.2 ± 6.0	21.2 ± 2.1
Connectivity density (Conn. D.) [1/mm ³]	107 ± 31	305 ± 140* (↑)	178 ± 30	142 ± 19* (↓)
Structure model index (SMI) [-]	0.050 ± 0.250	-0.43 ± 0.34* (↓)	0.85 ± 0.55	0.69 ± 0.20
Trabecular number (Tb. N.) [1/mm]	4.68 ± 0.20	5.85 ± 1.06* (↑)	4.83 ± 0.57	4.81 ± 0.35
Trabecular thickness (Tb. Th.) [mm]	0.061 ± 0.011	0.053 ± 0.009	0.044 ± 0.004	0.046 ± 0.001
Trabecular separation (Tb. Sp.) [mm]	0.20 ± 0.01	0.17 ± 0.03* (↓)	0.20 ± 0.03	0.20 ± 0.02
Apparent density [mgHA/cm ³]	324 ± 48	392 ± 78	271 ± 52	288 ± 21
Material density [mgHA/cm ³]	1028 ± 20	960 ± 45* (↓)	972 ± 19	1011 ± 13** (↑)
Relative bone surface (BS/BV) [1/mm]	36.3 ± 4.1	40.5 ± 7.1	51.4 ± 6.5	47.8 ± 1.6

Table III: Analysis of the trabecular structure of L1 vertebrae isolated from inducible SYK knockout mice. Data are expressed as the mean of $n = 5 \pm$ standard deviation. Arrows indicate increased (↑) or decreased (↓) values compared to vehicle controls. Unpaired t-test was performed to test for statistical significance. * $p < 0.05$, ** $p < 0.01$

Since tamoxifen treatment may influence the cortical and trabecular bone parameters (97) the femora and L1 vertebrae of wild type mice treated with vehicle or tamoxifen were measured, too. Female wild type mice showed only minor effects on trabecular parameters after tamoxifen treatment (Table IV). An increase in apparent density in the femora, as well as a decrease in relative bone volume and an increase in the structural model index in the L1 vertebrae were the only alterations observed at a significant level (Table V).

Femora	Female		Male	
	Vehicle	Tamoxifen	Vehicle	Tamoxifen
Relative bone volume (BV/TV) [%]	2.54 ± 1.13	3.43 ± 1.17	10.2 ± 1.1	7.15 ± 1.68** (↓)
Connectivity density (Conn. D.) [1/mm ³]	9.32 ± 6.35	10.5 ± 5.4	88.2 ± 35.3	35.0 ± 6.6* (↓)
Structure model index (SMI) [-]	3.55 ± 0.27	3.53 ± 0.41	2.11 ± 0.14	2.79 ± 0.32** (↑)
Trabecular number (Tb. N.) [1/mm]	2.35 ± 0.08	2.31 ± 0.18	3.86 ± 0.33	3.30 ± 0.25* (↓)
Trabecular thickness (Tb. Th.) [mm]	0.048 ± 0.012	0.059 ± 0.006	0.046 ± 0.004	0.050 ± 0.004
Trabecular separation (Tb. Sp.) [mm]	0.43 ± 0.02	0.43 ± 0.03	0.25 ± 0.02	0.30 ± 0.02** (↑)
Apparent density [mgHA/cm ³]	102 ± 13	133 ± 10** (↑)	179 ± 10	172 ± 16
Material density [mgHA/cm ³]	1024 ± 34	1053 ± 28	988 ± 12	1019 ± 9** (↑)
Relative bone surface (BS/BV) [1/mm]	72.0 ± 17.2	56.2 ± 9.0	57.4 ± 4.0	56.8 ± 7.4

Table IV: Analysis of the trabecular structure of femora isolated from wild type mice. Data are expressed as the mean of $n = 5 \pm$ standard deviation. Arrows indicate increased (↑) or decreased (↓) values compared to vehicle controls. Unpaired t-test was performed to test for statistical significance. * $p < 0.05$, ** $p < 0.01$

However, as shown in table IV, tamoxifen had more extensive implications on trabecular parameters of the femora of male wild type mice. A significant decline in relative bone volume, connectivity density and trabecular number as well as a significant augmentation in structural model index, trabecular separation and material density was observed. Additionally, a decrease in connectivity density and relative bone surface was found, together with an increase in trabecular thickness in the L1 vertebrae (Table V).

L1 vertebrae	Female		Male	
	Vehicle	Tamoxifen	Vehicle	Tamoxifen
Relative bone volume (BV/TV) [%]	25.7 ± 2.6	20.9 ± 3.6* (↓)	23.9 ± 1.5	24.2 ± 3.9
Connectivity density (Conn. D.) [1/mm ³]	122 ± 22	115 ± 33	199 ± 22	150 ± 24** (↓)
Structure model index (SMI) [-]	0.24 ± 0.09	0.67 ± 0.31* (↑)	0.40 ± 0.18	0.49 ± 0.32
Trabecular number (Tb. N.) [1/mm]	4.48 ± 0.42	3.93 ± 0.39	5.31 ± 0.16	4.96 ± 0.54
Trabecular thickness (Tb. Th.) [mm]	0.056 ± 0.003	0.054 ± 0.002	0.045 ± 0.001	0.049 ± 0.002** (↑)
Trabecular separation (Tb. Sp.) [mm]	0.22 ± 0.02	0.25 ± 0.03	0.18 ± 0.01	0.19 ± 0.03
Apparent density [mgHA/cm ³]	324 ± 28	284 ± 32	301 ± 14	314 ± 36
Material density [mgHA/cm ³]	1024 ± 15	1007 ± 14	996 ± 4	1001 ± 6
Relative bone surface (BS/BV) [1/mm]	39.4 ± 1.9	42.0 ± 2.2	48.0 ± 1.4	44.3 ± 2.9* (↓)

Table V: Analysis of the trabecular structure of L1 vertebrae isolated from wild type mice. Data are expressed as the mean of $n = 5 \pm$ standard deviation. Arrows indicate increased (↑) or decreased (↓) values compared to vehicle controls. Unpaired t-test was performed to test for statistical significance. * $p < 0.05$, ** $p < 0.01$

3.8.7. Maximum torsional strength and energy to failure are increased in the femora of female iSYKKO^{-/-} mice

We next examined whether the changes seen in the bones of female iSYKKO^{-/-} mice were associated with altered mechanical properties. Evaluation parameters included bone stiffness, maximum strength and energy to failure. The femora of female iSYKKO^{-/-} mice demonstrated no significant increase in stiffness compared to the femora of iSYKKO^{+/+} mice (Fig. 43A). However, the data for the femora indicated a significant increase in maximum torsional strength for the bones isolated from female iSYKKO^{-/-} mice compared to vehicle-treated control animals (58.8 ± 1.9 N·mm vs. 46.3 ± 3.4 N·mm, $p=0.018$, Fig. 43B) and a non-significant trend towards an increase in energy to failure (307 ± 27 N·mm·deg vs. 201 ± 34 N·mm·deg, $p=0.052$, Fig. 43C).

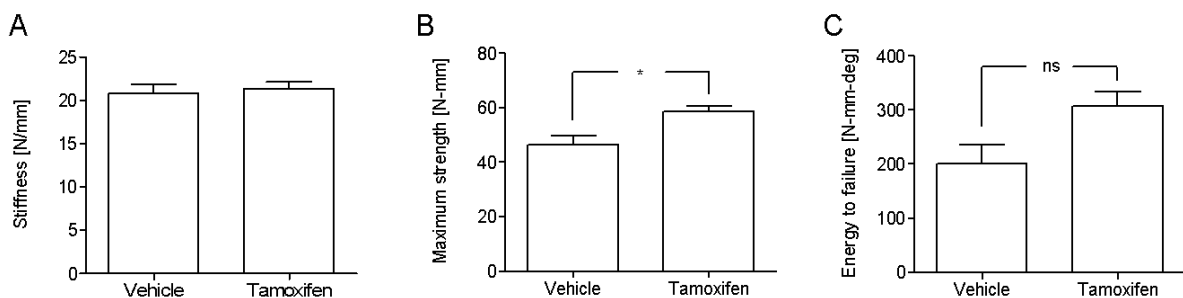


Fig. 43: Mechanical properties of femora isolated from female iSYKKO mice 18 weeks after first vehicle or tamoxifen treatment. Error bars represent the mean \pm SEM of five animals. Unpaired t-test was performed to test for statistical significance. * $p<0.05$

4. DISCUSSION

4.1. Tamoxifen-inducible SYK deletion

In this thesis a tamoxifen-inducible SYK knockout mouse strain was used to overcome the perinatal lethality seen in conventional germ-line deleted SYK knockout mice (37,38) and to get an insight into the function of SYK in physiological processes as well as in a variety of disease-related animal models. Besides its advantages working with inducible knockout strains always holds the risk that the induced deletion of a target gene might not be complete and that the inducing agent might influence the outcome of the study. Thus, it was important on the one hand to thoroughly determine knockout efficiency and on the other hand to include tamoxifen-treated wild type animals in each experiment to be able to identify tamoxifen-triggered effects. In preliminary experiments the dose of tamoxifen was carefully titrated with the aim to achieve a prominent knockout of SYK while keeping the tamoxifen exposure as low as possible. SYK expression levels were determined by PCR to verify deletion of exon 2 of SYK in genomic DNA and by Western blot analysis to verify SYK deletion on the protein level. The short-term deletion protocol established resulted in the deletion of SYK in all tissues analyzed including spleen, lymph nodes, blood, bone marrow, lung, thymus and colon. As a first novel finding it was observed that the short-term deletion of SYK had no overt effects on basic body functions as assessed by body weight, spleen weight, blood cell counts and B cell counts 10 days after the last tamoxifen administration. All animals exhibited a normal behaviour and were healthy.

However, long-term studies revealed that the standard deletion protocol resulted in the reappearance of SYK expression over time. Thus, it was necessary to establish a second protocol that allowed a prominent and sustained deletion of SYK over longer periods of time. As shown by quantitative real-time PCR of total RNA isolated from the blood of tamoxifen-treated mice repeated applications of tamoxifen every six weeks fulfilled these criteria.

The observation that SYK expression recurred with time may challenge the validity of this

iSYKKO stain. However, this apparent issue can also be seen as an advantage. Since one of the goals was to address the impact of short- and long-term treatment with a pharmacological small molecule SYK inhibitor on general physiological parameters and on disease outcomes in disease-related animal models. It is assumed as unlikely that a small molecule inhibitor of SYK will lead to a complete inhibition of its kinase activity over a long-period of time. In this respect, the apparent disadvantage of the model system may indeed be regarded as an advantage since the prominent reduction of SYK observed reflects more closely the properties of a small molecule inhibitor than a complete 100% deletion. Nevertheless, considering the strong reduction of SYK mRNA to levels below 1 % of control levels in the blood of tamoxifen-treated mice as quantified by real-time PCR and considering the effective reduction of SYK protein below the detection limit in a variety of tissues as measured by Western blot analysis, the term “SYK deletion” does appropriately describe the *in vivo* situation.

4.2. Function of SYK in B cells

SYK is essential for signal transduction downstream of the B cell receptor (BCR) leading to B cell activation and maturation (98). As such, SYK negative bone marrow chimera show a block in B cell development at the pro-B to pre-B cell transition (38). However, whether SYK plays a role in the antigen-independent tonic signalling events downstream of the BCR, which are necessary for B cell survival, remained undefined (99). To get an insight in the impact of SYK deletion on B cell numbers in adult mice inducible SYK knockout mice were treated with tamoxifen according to the established protocols. B cells, isolated from the spleens of mice treated according to the standard protocol for short-term SYK deletion, showed a prominent reduction of SYK protein compared to vehicle-treated control animals as assayed by flow cytometry. Having shown that SYK is strongly reduced in splenic B cells after tamoxifen treatment the blood of vehicle- and tamoxifen-deleted mice was sampled for the expression of the B cell surface antigen CD45R/B220 at different time points after the induction of SYK deletion (100). Since B cells have a half-life of 5-6 weeks an observation

period of 14 weeks was chosen, sufficiently long to observe changes resulting from a block in B cell development (101). B cell counts in the blood of SYK deleted mice gradually decreased by 80% after 14 weeks of SYK deletion. The kinetics of this process pointed towards the fact that SYK is not involved in the survival of B cells by transmitting tonic survival signals because in this case SYK deletion would have been expected to result in the immediate apoptosis and as such, in the sudden depletion of all circulating B cells. The steady reduction of B cells rather indicated that the development and replenishment of B cells is inhibited after SYK deletion. According to the expectations no differences in the expression of CD3 antigen, which is part of the T cell receptor, were found indicating that the development of T cells is normal in SYK deleted animals.

To confirm that B cells isolated from $iSYKKO^{-/-}$ mice are defective in signalling events downstream of the BCR splenic B cells were tested for their capability to release calcium in response to anti-IgM-induced BCR ligation. Consistent with data published by Takata *et al.*, SYK negative B cells completely lacked their ability to release calcium in response to BCR ligation (90). Furthermore, the SYK inhibitor R406 concentration-dependently inhibited the release of calcium from intracellular stores indicating that the process relies on the kinase activity of SYK. In accordance with these findings, the ability of SYK negative B cells to induce the expression of two activation markers, CD69 and CD25, after cross-linking of the BCR was heavily compromised.

In summary the results confirm that SYK is necessary for B cell activation and development and provide strong evidence that SYK is not involved in the transduction of survival signals downstream of the BCR. However, long-term SYK deletion leads to a gradual reduction of B cells *in vivo* reflecting a block in the replenishment of aging B lymphocytes.

4.3. Function of SYK in mast cells

SYK is known to play an important role in signalling events downstream of the high-affinity IgE receptor (FcεRI) on mast cells (44). It was shown that the development of mast cells, generated from the bone marrow of $iSYKKO^{-/-}$ animals, was not impaired. This confirms a

previous study that showed normal differentiation of mast cells from SYK-deficient foetal liver cells (44). However, FcεRI-induced calcium release and mast cell degranulation were abrogated in mBMMCs derived from iSYKKO^{-/-} mice. Furthermore, treatment of SYK positive mBMMCs with the SYK inhibitors, BAY61-3606 and R406, concentration-dependently reduced calcium influx and histamine release. Consistent with these findings the deletion or pharmacological inhibition of SYK resulted in the abrogated phosphorylation of SYK binding partners and downstream proteins involved in FcεRI signalling, like PLCγ1, SLP-76, LAT, ERK, AKT and p38.

The *in vitro* experiments showed that mast cell functions downstream of the FcεRI are inhibited in cells isolated from iSYKKO^{-/-} mice. Thus, the next aim was to confirm the role of SYK in mast cell functions *in vivo*. In the mast cell-dependent passive cutaneous anaphylaxis (PCA) model SYK deletion significantly reduced mast cell-dependent inflammation. Additionally, treatment of BALB/c mice with BAY61-3606 resulted in a comparable inhibition of the PCA reaction, suggesting that the catalytic activity of SYK is required in this process.

Mediator release from mast cells plays an important role in the pathophysiology of asthma (102). To further confirm the role of SYK in mast cell-driven immune responses *in vivo* the effect of SYK deletion was determined in a model of ovalbumin-induced eosinophil accumulation in two different setups. In a therapeutic setup animals were first immunized with OVA and then SYK deletion was induced before the OVA-challenge. Analysis of this experiment revealed that both, OVA-induced eosinophil numbers and T_H2 cytokines (IL-4 and IL-5) were significantly reduced in the BALF of iSYKKO^{-/-} mice. However, OVA-specific IgE and IgG1 levels in the serum of iSYKKO^{-/-} mice were unaffected which is in accordance with the normal amounts of SYK protein present during the immunization period. In a prophylactic setting mice were initially treated with vehicle or tamoxifen and ten days after the termination of vehicle or tamoxifen treatment immunization with ovalbumin was initiated. Knowing that SYK is important for the activation of B cells it was suspected that the deletion of SYK during immunization might lead to reduced OVA-specific antibody levels in the serum of iSYKKO^{-/-} mice which in turn could further reduce T_H2 responses including

eosinophil accumulation and cytokine release. However, eosinophil numbers in the BALF of iSYK^{-/-} mice treated according to the prophylactic setting were reduced to a similar extent as eosinophil numbers in the BALF of iSYK^{-/-} mice treated according to the therapeutic scheme. Furthermore, IL-4 and IL-5 levels in BALF were slightly but non-significantly reduced. Analysis of OVA-specific antibody levels in the serum of iSYK^{-/-} mice, treated according to the prophylactic setup, only showed a prominent reduction of OVA-specific IgG1 levels. Surprisingly, OVA-specific IgE titres were significantly increased. These observations suggest that SYK deletion during immunization leads to reduced B cell activation and with it to diminished antibody levels as seen in reduced OVA-specific IgG1 antibody titres. However, the tight control of IgE antibody production seems to be deregulated after SYK deletion. Additionally, these data indicate that the augmentation of OVA-specific IgE does not negatively impact disease outcome since signalling events downstream of the high-affinity IgE receptor are still blocked when SYK is deleted.

In accordance with the PCA model the SYK inhibitor BAY61-3606 led to a prominent reduction of eosinophil numbers in the BALF when tested in the OVA-induced pulmonary eosinophilia model. These observations confirm findings made in an OVA-induced pulmonary inflammation model in rats using the SYK inhibitor BAY61-3606 (92,103). Furthermore, the SYK inhibitor R406 has also been reported to inhibit OVA-induced pulmonary eosinophilia, as well as AHR and goblet cell metaplasia in mice (103,104). However, since R406 is a potent inhibitor of multiple proteins including SYK, Flt3, Ret, c-Kit, Lck, Jak 1/3 and the adenosine receptor (105) it is difficult to ascertain which effects observed with this compound are attributable to SYK inhibition.

Taken together the results confirm and complement the consensus that SYK is a suitable target for mast cell-driven allergic diseases including asthma and allergic rhinitis.

4.4. Combined effect of reduced B cell counts and inhibition of mast cell function

Having shown that SYK deletion leads to the gradual reduction of B cell counts in blood and inhibits mast cell functions both, *in vitro* and *in vivo*, the next goal was to determine how the

combined effect after long-term SYK deletion impacts disease outcome in a model of ovalbumin-induced lung eosinophilia. The rationale for this experiment was the assumption that reduced B cell counts might lead to reduced OVA-specific IgE and IgG1 antibody titres resulting in a reduced IgE-mediated allergic response. For this purpose animals were treated with vehicle or tamoxifen for 15 weeks before starting OVA-treatment. To make sure that B cell counts were effectively reduced CD45R/B220 positive cells were quantified in the blood and spleen of tamoxifen-treated mice showing that B cell counts were reduced by 86% and 78%, respectively. Eosinophil counts and IL-4 levels in the BALF were assayed as surrogate parameters for the OVA-elicited T_H2 response. Eosinophils in the BALF of iSYKKO^{-/-} mice were reduced by 74% compared to eosinophil numbers in the BALF of iSYKKO^{+/+} mice. This reduction can not be attributed to a systemic reduction of eosinophils after long-term SYK deletion, since eosinophil counts in the blood of long-term SYK deleted mice were comparable to eosinophil numbers in the blood of vehicle-treated control animals. Reduced IL-4 levels measured in the BALF of iSYKKO^{-/-} mice also reflected the suppressed T_H2-response. The reduction in both, BALF eosinophils and IL-4, was comparable to the reduction observed in the therapeutic and prophylactic models as mentioned above and as such, reduced B cell counts did not further improve disease outcome. Furthermore, OVA-specific antibody titres measured in the blood of long-term SYK deleted mice showed a similar effect as in the prophylactic model. OVA-specific IgG1 levels were significantly reduced while, surprisingly, OVA-specific IgE levels were augmented. This might imply that the 20% of B cells remaining after long-term SYK deletion produced about double the amount of OVA-specific IgE compared to B cells from mice harbouring SYK. Thus, the data suggest that SYK might play a so far unexplored role in the regulation of IgE synthesis. CD23, the low-affinity receptor for IgE (FcεRII) was identified as a possible link between SYK and the regulation of IgE synthesis. CD23 is an important regulator of IgE synthesis and is mainly expressed on B cells. *In vivo* studies showed that mice lacking CD23 exhibit increased IgE production whereas mice overexpressing CD23 show strongly suppressed IgE responses (93,94). Unexpectedly, the deletion of SYK resulted in an increase in the percentage of CD23

positive B cells in the spleen of *iSYKKO^{-/-}* mice. However, due to the reduced B cell count in the spleens of long-term SYK deleted mice the total number of CD23^{high} CD45R/B220 positive cells was significantly reduced.

Summing up, the reduced B cell counts found after long-term SYK deletion do not further attenuate allergic responses by reducing IgE titres. Instead OVA-specific IgE titres in the blood increase after SYK deletion possibly due to reduced numbers of CD23 positive B cells which are involved in the regulation of IgE synthesis.

4.5. Function of SYK in splenocytes

Recently, three groups identified the major histocompatibility complex class II positive IL-4-producing basophil as the antigen-presenting cell that is both necessary and sufficient for the generation of type 2 immunity (106-108). Furthermore, basophils have been identified as the primary source of IL-4 which is known to be essential for T_H2 differentiation (109). Basophils produce IL-4 in response to various stimuli, including allergen and IL-3 (28,96). The ITAM-containing adapter, FcR γ , is a constitutive component of the IL-3 receptor which is expressed on the surface of basophils (28). Thus, activation of the IL-3 receptor leads to the phosphorylation of the tyrosine residues contained in the ITAM-motif of the FcR γ chain which in turn leads to the recruitment of SYK. As such, SYK is supposed to be involved in the IL-3-induced IL-4 production and in supporting T_H2 differentiation by basophils. To verify the involvement of SYK in this process spleen cells from *iSYKKO^{+/+}* mice were isolated and treated with increasing concentrations of the SYK inhibitor R406 which concentration-dependently inhibited the release of IL-4. Accordingly, spleen cells isolated from *iSYKKO^{-/-}* mice lacked their ability to release IL-4 and IL-6 in response to stimulation of the IL-3 receptor. In summary, these experiments confirm that SYK is an integral component in the signalling cascade downstream of the IL-3 receptor. However, whether basophils are the only cell type in the spleen producing IL-4 and IL-6 in response to IL-3 can be challenged. Thus, to confirm and further elucidate the role of SYK in basophils additional experiments using basophil-enriched spleen or bone marrow samples should be conducted.

4.6. Function of SYK in neutrophils

Neutrophils constitute the first line of host defence against invading organisms. As such, the directional migration towards chemoattractant gradients, a prerequisite for neutrophil accumulation at the sites of inflammation, is indispensable for the initiation of inflammation. However, neutrophils also play an important role under pathological conditions by driving inflammation through antigen presentation and secretion of cytokines, chemokines, prostaglandins and leukotrienes. For example, in COPD neutrophils are the most abundant inflammatory cell type present in the bronchial wall, bronchial lumen, lung parenchyma, and submucosal glands (60). Furthermore, in patients with rheumatoid arthritis high numbers of neutrophils appear within the rheumatoid joint leading to tissue, bone and cartilage damage via the secretion of proteases and toxic oxygen metabolites (110). Thus, inhibiting the migratory ability of neutrophils is expected to improve disease outcome in a variety of malignancies with a prominent neutrophilic component. With respect to the function of SYK in the *in vivo* migration of neutrophils a couple of conflicting studies have been published (54,57,59,111). Therefore, the aim of the neutrophil experiments, performed here, was to elucidate the role of SYK in the migration of neutrophils using inducible SYK knockout mice.

In a first set of experiments the *in vitro* migration of thioglycollate-elicited peritoneal neutrophils was analyzed. Migration of neutrophils, isolated from $iSYKKO^{-/-}$ mice, towards the murine neutrophil chemokine KC was increased compared to the migration of cells isolated from $iSYKKO^{+/+}$ mice. This is in accordance with data published by Mocsai *et al.* which showed that transmigration of SYK negative neutrophils through a fibrinogen-coated transwell membrane in response to the bacterial peptide fMLP was slightly increased at higher concentrations of the stimulus (54).

To analyze the role of SYK in the *in vivo* migration of neutrophils inducible SYK knockout mice were tested in three different disease-related animal models including a model of thioglycollate-induced neutrophilic peritonitis and models of LPS- and cigarette smoke-induced pulmonary neutrophilia. Thioglycollate-induced neutrophilic peritonitis was unaltered in the $iSYKKO^{-/-}$ mice compared to control animals. This finding is in agreement

with experiments showing that lethally irradiated recipient mice reconstituted with *Syk*^{-/-} bone marrow cells have unaltered peritoneal neutrophil numbers in the thioglycollate model (54). However, the observations made in the course of this study contrast recent findings suggesting that the CD95-Src-family-SYK-axis has a pivotal function in the migration of neutrophils in the same model (112).

Normal neutrophil migration in the absence of SYK was also observed in an *in vivo* LPS-induced pulmonary neutrophilia model and it was demonstrated for the first time that the absence of SYK does not protect mice from cigarette smoke-induced pulmonary neutrophilic inflammation.

On first sight these findings are in contrast to the reduced neutrophil accumulation elicited by the reverse-passive Arthus reaction in bone marrow chimera carrying a SYK-deficient hematopoietic system and also contradict the reduced leukocyte counts found in the joints of mice carrying a SYK-deficient hematopoietic system after the injection of arthritogenic K/BxN serum (59,105). However, it is known from the literature that mast cells make an important contribution to the reverse-passive Arthus reaction (113) and as such it is reasonable to speculate that the reduced neutrophil accumulation observed in SYK-deficient mice is not due to a direct defect in neutrophil migration but rather results from the inhibition of mast cell activity. Likewise, the inhibition of leukocyte infiltration, observed in *SYK*^{-/-} bone marrow chimera in the K/BxN arthritis model, may not reflect a neutrophil migration defect, too. Also in this model, induction of disease development is dependent on mast cells as seen by the fact that mast cell-deficient mice are resistant to K/BxN serum transfer arthritis (114). As such, in both experimental setups reduced neutrophil accumulation is most likely a consequence of attenuated onset of pathological alterations reflecting inhibited mast cell activity as a result of SYK deletion.

In sum, the results demonstrate that SYK is dispensable for the *in vivo* migration of neutrophils.

4.7. Function of SYK in macrophages

Like neutrophils macrophages are involved in host defence against invading pathogens. They are attracted to the site of inflammation or tissue damage by directional migration towards a chemoattractant stimulus. At the site of inflammation macrophages are involved in the phagocytosis of perturbing organisms and the presentation of antigens. Apart from their role in the uptake of pathogens macrophages are important sources of pro- and anti-inflammatory cytokines. However, under pathological conditions macrophages can become hyperresponsive, resulting in dysregulated release of mediators that exacerbate acute tissue injury. Thus, interfering with the ability of macrophages to migrate to the site of inflammation might be a way to attenuate disease severity in malignancies with an underlying chronic inflammation.

SYK has been implicated in MCP-1-induced receptor-mediated signal transduction eventually leading to monocytic transendothelial migration (47). Furthermore, SYK was demonstrated to be involved in the CX3CL1-induced chemotaxis of monocytes/macrophages *in vitro* (69) which may be of clinical relevance since CX3CL1 has been implicated in the pathogenesis of a number of diseases, including rheumatoid arthritis (115,116) and atherosclerosis (117-119).

To elucidate the role of SYK in the migration of macrophages *in vivo* the inducible SYK knockout mice were tested in models of MCP-1 and chronic cigarette smoke-induced lung inflammation. However, SYK deletion had no influence on the migration of macrophages in either model, indicating that SYK is not involved in the transendothelial migration of macrophages in response to either MCP-1 or cigarette smoke-induced chemokines *in vivo*.

4.8. Function of SYK in osteoclasts

SYK has been implicated in the regulation of signal transduction during osteoclast development and function, making SYK a potential target for the treatment of rheumatoid arthritis and osteoporosis (120). Several studies have been published that examined the

effect of SYK deletion on osteoclasts *in vitro* (73,75,76,121), but due to the perinatal lethality of conventional SYK knockout mice little is known about how these effects translate into the *in vivo* situation (37,38).

Several studies have reported that SYK^{-/-} bone marrow cells cultured with M-CSF and RANKL *in vitro* failed to differentiate normally and that these cells had severe functional defects (73,75,76,121). Experiments performed in the course of this study showed that the same holds true for bone marrow cells isolated from iSYKKO^{-/-} mice. SYK deleted cells displayed TRAP staining but were smaller with less nuclei and an irregular shape and failed to digest an artificial calcium phosphate substrate. Signalling events downstream of SYK were also inhibited as shown by the absence of phosphorylation of SLP-76 at tyrosine 128. Furthermore, the effect of the SYK inhibitor R406 on cells isolated from wild type mice was evaluated. According to the knockout situation a defect in both osteoclast development and function was found, indicating that the defects seen are not due to a possible adapter function of SYK, but relate to the missing kinase activity which is in accordance with data published by Koga *et al.* (74).

To further analyze the effects of SYK deletion *in vivo* two serological markers, tartrate-resistant acid phosphatase form 5b (TRACP 5b) and C-telopeptide of type I collagen (CTX-I) were measured as surrogate parameters of *in vivo* osteoclast number and function, respectively. After 18 weeks of SYK deletion both markers were significantly reduced reflecting that the defects seen *in vitro* translate at least partially into the *in vivo* situation. In contrast, staining of histological sections of humeri revealed that osteoclast numbers in SYK deleted mice are indistinguishable from that of wild type mice after 18 weeks of SYK deletion, confirming the findings made in SYK^{-/-} bone marrow chimera (76). These data show that the absence of SYK does not result in a complete block of osteoclast development *in vivo* as would have been expected from the *in vitro* findings.

To quantify the effect of SYK deletion on bone morphology a detailed μ CT analysis was performed. Surprisingly, effects on bone parameters were present only in female SYK deleted mice. Cortical parameters of the femora of female mice revealed a significant

increase in cortical thickness after SYK deletion. Consistent with these observations changes of trabecular parameters were found in the femora and L1 vertebrae of the female SYK deleted mice, pointing towards an increase in bone density. The data observed in female mice support earlier findings made by Zou *et al.*, who observed increased bone density in SYK^{-/-} embryos (76). On the contrary, bones of SYK deleted male mice were indistinguishable from bones of vehicle-treated control animals.

To exclude that the effects observed in the female inducible knockout animals were not due to the tamoxifen treatment, μ CT analysis was also performed on the femora and L1 vertebrae of wild type mice after tamoxifen treatment. In wild type mice no changes on cortical parameters were observed. Interestingly, the changes on trabecular parameters of wild type mice were almost exclusively restricted to the male animals and were pointing towards a decrease in trabecular bone. These findings were rather unexpected since it has been shown by Starnes *et al.* that C57BL/6J mice exhibit an increase in both cortical and trabecular bone after bi-weekly intraperitoneal injections of 0.1 mg 4-hydroxytamoxifen dissolved in corn oil for 12 weeks (starting at the age of 5 weeks) and these effects were more pronounced in female mice (97). These contradictory findings might be due to strain differences, to the different age of animals at the beginning of the study or to the different tamoxifen doses and administration protocols used. However, the findings might also be an explanation why the changes in bone morphology after SYK deletion were restricted to female mice. Since it was observed that SYK deletion leads to an increase in cortical and trabecular bone parameters and that tamoxifen treatment reduces trabecular bone in male wild type mice, it might be possible that the two effects counterbalance each other leading to the absence of a phenotype in male inducible SYK knockout animals.

Since significant changes in cortical and trabecular parameters were only seen in the bones of female iSYKKO^{-/-} mice, mechanical analyses were restricted to the femora of those animals. The measurements taken during mechanical testing demonstrated that the femora of female iSYKKO^{-/-} mice have increased mechanical properties compared to vehicle-treated

control mice. This results in functionally improved bones, as the maximum strength was increased by 27% and the energy to failure load was more than doubled in the femora of female *iSYKKO^{-/-}* mice.

Taken together, the study demonstrated that the distinct effects on osteoclast development and function seen *in vitro*, do not translate into a pathological phenotype *in vivo*, but rather lead to a functional improvement in bone quality, reflecting diminished osteoclast activity. Therefore, it is most likely that signalling through SYK is important but not the sole regulator of osteoclast differentiation and function *in vivo*. In conclusion, the osteoclast and bone analyses support the *in vitro* studies already published by others, and further reveal that SYK deletion results in increased mechanical bone properties *in vivo*.

5. SUMMARY

Spleen tyrosine kinase (SYK), a cytoplasmic non-receptor tyrosine kinase, is a key mediator of immunoreceptor signalling. SYK is expressed in cells of the hematopoietic lineage such as B cells, mast cells, basophils, neutrophils, macrophages, and osteoclasts, but is also present in cells of non-hematopoietic origin such as epithelial cells, hepatocytes, fibroblasts, neuronal cells, and vascular endothelial cells. Thus, SYK appears to play a general physiological function in a wide variety of cells. SYK functions downstream of ITAM-containing antigen- and Fc-receptor complexes and transduces signals leading to a host of effector functions including altered gene expression, cytokine production, cell differentiation and proliferation. Since SYK signalling downstream of the B cell receptor is necessary for B cell development and maturation, SYK is discussed as a candidate for the treatment of certain B cell lymphomas, which are characterized by uncontrolled SYK-dependent growth, like the B cell non-Hodgkin lymphoma. Abnormal signalling through SYK is further associated with different antibody-mediated autoimmune diseases and allergic disorders including rheumatoid arthritis, asthma and allergic rhinitis, making SYK an attractive pharmacological target for the treatment of these diseases. Due to the involvement of SYK in numerous diseases with high unmet medical need extensive efforts have been made to further characterize the role of SYK in preclinical models *in vivo*. Since conventional germ-line deleted SYK knockout mice suffer from severe haemorrhaging and die perinatally efforts to generate a mouse model allowing the characterization of SYK have been unsuccessful. To circumvent these difficulties, a tamoxifen-inducible SYK knockout strain was generated, allowing to knockout SYK in adult mice and thus to evaluate the effect of SYK deletion on physiological parameters and in various disease-related animal models. Short-term SYK deletion had no negative impact on health status of adult mice. After long-term SYK deletion reduced B cell counts and slight improvements on bone morphology were observed. SYK deletion proved to be efficacious in mast cell-driven animal models including a model of passive cutaneous anaphylaxis and a model of ovalbumin-induced lung

eosinophilia. However, SYK deletion did not impact the migration of neutrophils or macrophages after the application of inflammatory stimuli including lipopolysaccharid, thioglycollate, cigarette smoke or MCP-1. As such, the tamoxifen-inducible SYK knockout mice provide a appropriate tool to examine the role of SYK in various disease-related animal models.

6. ZUSAMMENFASSUNG

Die Milz-Tyrosin-Kinase (*spleen tyrosine kinase*) SYK, eine zytoplasmatische nicht-Rezeptor-Tyrosin-Kinase, ist ein wichtiger Modulator der immunologischen Signalübertragung. SYK wird nicht nur in hämatopoetischen Zellen wie B-Zellen, Mastzellen, Basophilen, Neutrophilen, Makrophagen und Osteoklasten exprimiert, sondern auch in Zellen mit nicht-hämatopoetischem Hintergrund wie Epithelzellen, Hepatozyten, Fibroblasten, neuronalen Zellen und vaskulären Endothelzellen. Demnach ist anzunehmen, dass SYK eine generelle physiologische Rolle in einer Vielzahl von unterschiedlichen Zelltypen spielt. Die Hauptfunktion von SYK ist die Signaltransduktion von Antigen- und Fc-Rezeptoren, die sogenannte ITAM-Sequenzen enthalten. Die durch SYK vermittelte Signalübertragung führt in den Zellen letztendlich zu zahlreichen Effektorfunktionen, wie zu einer veränderten Genexpression, Zytokinproduktion, Zelldifferenzierung und -proliferation. In B-Zellen ist die Signalübertragung durch SYK als Folge der Aktivierung des B-Zellrezeptors für die Entwicklung und Reifung notwendig. B-Zell-Lymphome zeichnen sich durch ein unkontrolliertes Wachstum der B-Zellen aus, welches teilweise durch SYK vermittelt wird. Deshalb wird SYK als Target für die Behandlung von bestimmten B-Zell-Lymphomen wie dem Non-Hodgkin B-Zell-Lymphom diskutiert. Störungen in der Signalübertragung durch SYK sind außerdem mit antikörpervermittelten Autoimmun- und allergischen Erkrankungen wie rheumatoider Arthritis, Asthma und allergischer Rhinitis assoziiert. Dies macht SYK zu einem möglichen Angriffspunkt für eine pharmakologische Behandlung dieser Krankheiten. Aufgrund der Beteiligung von SYK an der Pathogenese zahlreicher Erkrankungen, für die es momentan noch keine adäquaten Behandlungsmöglichkeiten gibt, wurden in vergangenen Jahren viele Anstrengungen unternommen, um die Rolle von SYK im lebenden Organismus weiter zu charakterisieren. Die Etablierung eines Mausmodells wurde jedoch dadurch erschwert, dass konventionelle Keimbahn-knockout-Mäuse an schwerwiegenden inneren Blutungen leiden und perinatal sterben. Um diese Schwierigkeiten zu umgehen, wurde im Rahmen der vorgelegten Doktorarbeit eine, durch Tamoxifen induzierbare, SYK knockout

Mauslinie charakterisiert, welche die Deletion von SYK im adulten Organismus ermöglicht. Die induzierbare knockout Mauslinie eröffnete dadurch die Möglichkeit die Auswirkungen der SYK-Deletion auf physiologische Parameter, sowie auf die Pathogenese in unterschiedlichen krankheitsrelevanten Tiermodellen zu untersuchen. Die kurzfristige SYK-Deletion hatte keinen negativen Einfluss auf den Gesundheitsstatus der adulten Mäuse. Als Folge der langfristigen SYK-Deletion konnten jedoch eine Abnahme der B-Lymphozytenzahl im Blut und eine geringfügige Verbesserung der Knochenqualität beobachtet werden. Die SYK-Deletion zeigte außerdem einen inhibitorischen Effekt in mastzellabhängigen Tiermodellen, wie z. B. einem Modell der passiven kutanen Anaphylaxie und einem Modell der Ovalbumin-induzierten Lungeneosinophilie. Im Tierversuch konnte jedoch keine Hemmwirkung der SYK-Deletion auf die Neutrophilen- bzw. Makrophagenmigration, ausgelöst durch die Applikation von Entzündungsreizen wie Lipopolysaccharid, Thioglykolat, Zigarettenrauch oder MCP-1, beobachtet werden. Zusammenfassend haben sich die SYK knockout Mäuse als geeignetes Modellsystem zur Untersuchung der *in vivo* Funktion von SYK in zahlreichen krankheitsrelevanten Tiermodellen erwiesen.

7. REFERENCES

1. Sada, K., T. Takano, S. Yanagi, and H. Yamamura. 2001. Structure and function of Syk protein-tyrosine kinase. *J. Biochem.* 130: 177-186.
2. Reth, M. 1989. Antigen receptor tail clue. *Nature* 338: 383-384.
3. Kumaran, S., R. A. Grucza, and G. Waksman. 2003. The tandem Src homology 2 domain of the Syk kinase: a molecular device that adapts to interphosphotyrosine distances. *Proc. Natl. Acad. Sci. U. S. A* 100: 14828-14833.
4. Mocsai, A., J. Ruland, and V. L. Tybulewicz. 2010. The SYK tyrosine kinase: a crucial player in diverse biological functions. *Nat. Rev. Immunol.* 10: 387-402.
5. Furlong, M. T., A. M. Mahrenholz, K. H. Kim, C. L. Ashendel, M. L. Harrison, and R. L. Geahlen. 1997. Identification of the major sites of autophosphorylation of the murine protein-tyrosine kinase Syk. *Biochim. Biophys. Acta* 1355: 177-190.
6. Keshvara, L. M., C. Isaacson, M. L. Harrison, and R. L. Geahlen. 1997. Syk activation and dissociation from the B-cell antigen receptor is mediated by phosphorylation of tyrosine 130. *J. Biol. Chem.* 272: 10377-10381.
7. Zhang, Y., H. Oh, R. A. Burton, J. W. Burgner, R. L. Geahlen, and C. B. Post. 2008. Tyr130 phosphorylation triggers Syk release from antigen receptor by long-distance conformational uncoupling. *Proc. Natl. Acad. Sci. U. S. A* 105: 11760-11765.
8. Yankee, T. M., L. M. Keshvara, S. Sawasdikosol, M. L. Harrison, and R. L. Geahlen. 1999. Inhibition of signaling through the B cell antigen receptor by the protooncogene product, c-Cbl, requires Syk tyrosine 317 and the c-Cbl phosphotyrosine-binding domain. *J. Immunol.* 163: 5827-5835.
9. Moon, K. D., C. B. Post, D. L. Durden, Q. Zhou, P. De, M. L. Harrison, and R. L. Geahlen. 2005. Molecular basis for a direct interaction between the Syk protein-tyrosine kinase and phosphoinositide 3-kinase. *J. Biol. Chem.* 280: 1543-1551.
10. Deckert, M., S. Tartare-Deckert, C. Couture, T. Mustelin, and A. Altman. 1996. Functional and physical interactions of Syk family kinases with the Vav proto-oncogene product. *Immunity.* 5: 591-604.
11. Law, C. L., K. A. Chandran, S. P. Sidorenko, and E. A. Clark. 1996. Phospholipase C-gamma1 interacts with conserved phosphotyrosyl residues in the linker region of Syk and is a substrate for Syk. *Mol. Cell Biol.* 16: 1305-1315.

12. Rowley, R. B., J. B. Bolen, and J. Fargnoli. 1995. Molecular cloning of rodent p72Syk. Evidence of alternative mRNA splicing. *J. Biol. Chem.* 270: 12659-12664.
13. Au-Yeung, B. B., S. Deindl, L. Y. Hsu, E. H. Palacios, S. E. Levin, J. Kuriyan, and A. Weiss. 2009. The structure, regulation, and function of ZAP-70. *Immunol. Rev.* 228: 41-57.
14. Wang, L., L. Duke, P. S. Zhang, R. B. Arlinghaus, W. F. Symmans, A. Sahin, R. Mendez, and J. L. Dai. 2003. Alternative splicing disrupts a nuclear localization signal in spleen tyrosine kinase that is required for invasion suppression in breast cancer. *Cancer Res.* 63: 4724-4730.
15. Latour, S., J. Zhang, R. P. Siraganian, and A. Veillette. 1998. A unique insert in the linker domain of Syk is necessary for its function in immunoreceptor signalling. *EMBO J.* 17: 2584-2595.
16. Baldock, D., B. Graham, M. Akhlaq, P. Graff, C. E. Jones, and K. Menear. 2000. Purification and characterization of human Syk produced using a baculovirus expression system. *Protein Expr. Purif.* 18: 86-94.
17. Zhang, J., M. L. Billingsley, R. L. Kincaid, and R. P. Siraganian. 2000. Phosphorylation of Syk activation loop tyrosines is essential for Syk function. An in vivo study using a specific anti-Syk activation loop phosphotyrosine antibody. *J. Biol. Chem.* 275: 35442-35447.
18. Zeitlmann, L., T. Knorr, M. Knoll, C. Romeo, P. Sirim, and W. Kolanus. 1998. T cell activation induced by novel gain-of-function mutants of Syk and ZAP-70. *J. Biol. Chem.* 273: 15445-15452.
19. Fu, C., C. W. Turck, T. Kurosaki, and A. C. Chan. 1998. BLNK: a central linker protein in B cell activation. *Immunity.* 9: 93-103.
20. Latour, S., and A. Veillette. 2001. Proximal protein tyrosine kinases in immunoreceptor signaling. *Curr. Opin. Immunol.* 13: 299-306.
21. Saijo, K., C. Schmedt, I. H. Su, H. Karasuyama, C. A. Lowell, M. Reth, T. Adachi, A. Patke, A. Santana, and A. Tarakhovsky. 2003. Essential role of Src-family protein tyrosine kinases in NF-kappaB activation during B cell development. *Nat. Immunol.* 4: 274-279.
22. Barker, S. C., D. B. Kassel, D. Weigl, X. Huang, M. A. Luther, and W. B. Knight. 1995. Characterization of pp60c-src tyrosine kinase activities using a continuous assay: autoactivation of the enzyme is an intermolecular autophosphorylation process. *Biochemistry* 34: 14843-14851.

23. Thomas, S. M., and J. S. Brugge. 1997. Cellular functions regulated by Src family kinases. *Annu. Rev. Cell Dev. Biol.* 13: 513-609.
24. Kimura, T., H. Sakamoto, E. Appella, and R. P. Siraganian. 1996. Conformational changes induced in the protein tyrosine kinase p72syk by tyrosine phosphorylation or by binding of phosphorylated immunoreceptor tyrosine-based activation motif peptides. *Mol. Cell Biol.* 16: 1471-1478.
25. rias-Palomo, E., M. A. Recuero-Checa, X. R. Bustelo, and O. Llorca. 2009. Conformational rearrangements upon Syk auto-phosphorylation. *Biochim. Biophys. Acta* 1794: 1211-1217.
26. Jakus, Z., S. Fodor, C. L. Abram, C. A. Lowell, and A. Mocsai. 2007. Immunoreceptor-like signaling by beta 2 and beta 3 integrins. *Trends Cell Biol.* 17: 493-501.
27. Kerrigan, A. M., and G. D. Brown. 2010. Syk-coupled C-type lectin receptors that mediate cellular activation via single tyrosine based activation motifs. *Immunol. Rev.* 234: 335-352.
28. Hida, S., S. Yamasaki, Y. Sakamoto, M. Takamoto, K. Obata, T. Takai, H. Karasuyama, K. Sugane, T. Saito, and S. Taki. 2009. Fc receptor gamma-chain, a constitutive component of the IL-3 receptor, is required for IL-3-induced IL-4 production in basophils. *Nat. Immunol.* 10: 214-222.
29. Mocsai, A., C. L. Abram, Z. Jakus, Y. Hu, L. L. Lanier, and C. A. Lowell. 2006. Integrin signaling in neutrophils and macrophages uses adaptors containing immunoreceptor tyrosine-based activation motifs. *Nat. Immunol.* 7: 1326-1333.
30. Feldman, A. L., D. X. Sun, M. E. Law, A. J. Novak, A. D. Attygalle, E. C. Thorland, S. R. Fink, J. A. Vrana, B. L. Caron, W. G. Morice, E. D. Remstein, K. L. Grogg, P. J. Kurtin, W. R. Macon, and A. Dogan. 2008. Overexpression of Syk tyrosine kinase in peripheral T-cell lymphomas. *Leukemia* 22: 1139-1143.
31. Krishnan, S., Y. T. Juang, B. Chowdhury, A. Magilavy, C. U. Fisher, H. Nguyen, M. P. Nambiar, V. Kytтары, A. Weinstein, R. Bahjat, P. Pine, V. Rus, and G. C. Tsokos. 2008. Differential expression and molecular associations of Syk in systemic lupus erythematosus T cells. *J. Immunol.* 181: 8145-8152.
32. Coopman, P. J., M. T. Do, M. Barth, E. T. Bowden, A. J. Hayes, E. Basyuk, J. K. Blancato, P. R. Vezza, S. W. McLeskey, P. H. Mangeat, and S. C. Mueller. 2000. The Syk tyrosine kinase suppresses malignant growth of human breast cancer cells. *Nature* 406: 742-747.

33. Elkak, A., S. W. Al, and K. Mokbel. 2005. SYK expression in human breast cancer. *J. Carcinog.* 4: 7.
34. Dal Porto, J. M., S. B. Gauld, K. T. Merrell, D. Mills, A. E. Pugh-Bernard, and J. Cambier. 2004. B cell antigen receptor signaling 101. *Mol. Immunol.* 41: 599-613.
35. Flaswinkel, H., and M. Reth. 1994. Dual role of the tyrosine activation motif of the Ig- α protein during signal transduction via the B cell antigen receptor. *EMBO J.* 13: 83-89.
36. Rolli, V., M. Gallwitz, T. Wossning, A. Flemming, W. W. Schamel, C. Zurn, and M. Reth. 2002. Amplification of B cell antigen receptor signaling by a Syk/ITAM positive feedback loop. *Mol. Cell* 10: 1057-1069.
37. Cheng, A. M., B. Rowley, W. Pao, A. Hayday, J. B. Bolen, and T. Pawson. 1995. Syk tyrosine kinase required for mouse viability and B-cell development. *Nature* 378: 303-306.
38. Turner, M., P. J. Mee, P. S. Costello, O. Williams, A. A. Price, L. P. Duddy, M. T. Furlong, R. L. Geahlen, and V. L. Tybulewicz. 1995. Perinatal lethality and blocked B-cell development in mice lacking the tyrosine kinase Syk. *Nature* 378: 298-302.
39. Gururajan, M., C. D. Jennings, and S. Bondada. 2006. Cutting edge: constitutive B cell receptor signaling is critical for basal growth of B lymphoma. *J. Immunol.* 176: 5715-5719.
40. Lin, T. S. 2010. New agents in chronic lymphocytic leukemia. *Curr. Hematol. Malig. Rep.* 5: 29-34.
41. Jumaa, H., R. W. Hendriks, and M. Reth. 2005. B cell signaling and tumorigenesis. *Annu. Rev. Immunol.* 23: 415-445.
42. Tsokos, G. C. 2004. B cells, be gone--B-cell depletion in the treatment of rheumatoid arthritis. *N. Engl. J. Med.* 350: 2546-2548.
43. Blank, U., C. Ra, L. Miller, K. White, H. Metzger, and J. P. Kinet. 1989. Complete structure and expression in transfected cells of high affinity IgE receptor. *Nature* 337: 187-189.
44. Costello, P. S., M. Turner, A. E. Walters, C. N. Cunningham, P. H. Bauer, J. Downward, and V. L. Tybulewicz. 1996. Critical role for the tyrosine kinase Syk in signalling through the high affinity IgE receptor of mast cells. *Oncogene* 13: 2595-2605.
45. Bischoff, S. C. 2007. Role of mast cells in allergic and non-allergic immune responses: comparison of human and murine data. *Nat. Rev. Immunol.* 7: 93-104.

46. Woolley, D. E., and L. C. Tetlow. 2000. Mast cell activation and its relation to proinflammatory cytokine production in the rheumatoid lesion. *Arthritis Res.* 2: 65-74.
47. Cambien, B., M. Pomeranz, M. A. Millet, B. Rossi, and A. Schmid-Alliana. 2001. Signal transduction involved in MCP-1-mediated monocytic transendothelial migration. *Blood* 97: 359-366.
48. Shefler, I., and R. Sagi-Eisenberg. 2001. Gi-mediated activation of the Syk kinase by the receptor mimetic basic secretagogues of mast cells: role in mediating arachidonic acid/metabolites release. *J. Immunol.* 167: 475-481.
49. Wan, Y., T. Kurosaki, and X. Y. Huang. 1996. Tyrosine kinases in activation of the MAP kinase cascade by G-protein-coupled receptors. *Nature* 380: 541-544.
50. Wan, Y., K. Bence, A. Hata, T. Kurosaki, A. Veillette, and X. Y. Huang. 1997. Genetic evidence for a tyrosine kinase cascade preceding the mitogen-activated protein kinase cascade in vertebrate G protein signaling. *J. Biol. Chem.* 272: 17209-17215.
51. Hirasawa, N., A. Scharenberg, H. Yamamura, M. A. Beaven, and J. P. Kinet. 1995. A requirement for Syk in the activation of the microtubule-associated protein kinase/phospholipase A2 pathway by Fc epsilon R1 is not shared by a G protein-coupled receptor. *J. Biol. Chem.* 270: 10960-10967.
52. Mocsai, A., Z. Jakus, T. Vantus, G. Berton, C. A. Lowell, and E. Ligeti. 2000. Kinase pathways in chemoattractant-induced degranulation of neutrophils: the role of p38 mitogen-activated protein kinase activated by Src family kinases. *J. Immunol.* 164: 4321-4331.
53. Mocsai, A., H. Zhang, Z. Jakus, J. Kitaura, T. Kawakami, and C. A. Lowell. 2003. G-protein-coupled receptor signaling in Syk-deficient neutrophils and mast cells. *Blood* 101: 4155-4163.
54. Mocsai, A., M. Zhou, F. Meng, V. L. Tybulewicz, and C. A. Lowell. 2002. Syk is required for integrin signaling in neutrophils. *Immunity.* 16: 547-558.
55. Willeke, T., J. Schymeinsky, P. Prange, S. Zahler, and B. Walzog. 2003. A role for Syk-kinase in the control of the binding cycle of the beta2 integrins (CD11/CD18) in human polymorphonuclear neutrophils. *J. Leukoc. Biol.* 74: 260-269.
56. Woodside, D. G., A. Obergfell, A. Talapatra, D. A. Calderwood, S. J. Shattil, and M. H. Ginsberg. 2002. The N-terminal SH2 domains of Syk and ZAP-70 mediate phosphotyrosine-independent binding to integrin beta cytoplasmic domains. *J. Biol. Chem.* 277: 39401-39408.

-
57. Van Ziffle, J. A., and C. A. Lowell. 2009. Neutrophil-specific deletion of Syk kinase results in reduced host defense to bacterial infection. *Blood* 114: 4871-4882.
 58. Kiefer, F., J. Brumell, N. Al-Alawi, S. Latour, A. Cheng, A. Veillette, S. Grinstein, and T. Pawson. 1998. The Syk protein tyrosine kinase is essential for Fc γ receptor signaling in macrophages and neutrophils. *Mol. Cell Biol.* 18: 4209-4220.
 59. Schymeinsky, J., A. Sindrilaru, D. Frommhold, M. Sperandio, R. Gerstl, C. Then, A. Mocsai, K. Scharffetter-Kochanek, and B. Walzog. 2006. The Vav binding site of the non-receptor tyrosine kinase Syk at Tyr 348 is critical for beta2 integrin (CD11/CD18)-mediated neutrophil migration. *Blood* 108: 3919-3927.
 60. Quint, J. K., and J. A. Wedzicha. 2007. The neutrophil in chronic obstructive pulmonary disease. *J. Allergy Clin. Immunol.* 119: 1065-1071.
 61. Sparrow, D., R. J. Glynn, M. Cohen, and S. T. Weiss. 1984. The relationship of the peripheral leukocyte count and cigarette smoking to pulmonary function among adult men. *Chest* 86: 383-386.
 62. Kariyawasam, H. H., M. Aizen, J. Barkans, D. S. Robinson, and A. B. Kay. 2007. Remodeling and airway hyperresponsiveness but not cellular inflammation persist after allergen challenge in asthma. *Am. J. Respir. Crit Care Med.* 175: 896-904.
 63. Bajpai, M., P. Chopra, S. G. Dastidar, and A. Ray. 2008. Spleen tyrosine kinase: a novel target for therapeutic intervention of rheumatoid arthritis. *Expert. Opin. Investig. Drugs* 17: 641-659.
 64. Weinblatt, M. E., A. Kavanaugh, M. C. Genovese, T. K. Musser, E. B. Grossbard, and D. B. Magilavy. 2010. An oral spleen tyrosine kinase (Syk) inhibitor for rheumatoid arthritis. *N. Engl. J. Med.* 363: 1303-1312.
 65. Dale, D. C., L. Boxer, and W. C. Liles. 2008. The phagocytes: neutrophils and monocytes. *Blood* 112: 935-945.
 66. Laskin, D. L., and J. D. Laskin. 2001. Role of macrophages and inflammatory mediators in chemically induced toxicity. *Toxicology* 160: 111-118.
 67. Vines, C. M., J. W. Potter, Y. Xu, R. L. Geahlen, P. S. Costello, V. L. Tybulewicz, C. A. Lowell, P. W. Chang, H. D. Gresham, and C. L. Willman. 2001. Inhibition of beta 2 integrin receptor and Syk kinase signaling in monocytes by the Src family kinase Fgr. *Immunity.* 15: 507-519.
 68. Matsuda, M., J. G. Park, D. C. Wang, S. Hunter, P. Chien, and A. D. Schreiber. 1996. Abrogation of the Fc gamma receptor IIA-mediated phagocytic signal by stem-loop

- Syk antisense oligonucleotides. *Mol. Biol. Cell* 7: 1095-1106.
69. Gevrey, J. C., B. M. Isaac, and D. Cox. 2005. Syk is required for monocyte/macrophage chemotaxis to CX3CL1 (Fractalkine). *J. Immunol.* 175: 3737-3745.
70. Laskin, D. L., V. R. Sunil, C. R. Gardner, and J. D. Laskin. 2010. Macrophages and Tissue Injury: Agents of Defense or Destruction? *Annu. Rev. Pharmacol. Toxicol.*
71. Gorska, K., M. Maskey-Warzechowska, and R. Krenke. 2010. Airway inflammation in chronic obstructive pulmonary disease. *Curr. Opin. Pulm. Med.* 16: 89-96.
72. Boyle, W. J., W. S. Simonet, and D. L. Lacey. 2003. Osteoclast differentiation and activation. *Nature* 423: 337-342.
73. Mocsai, A., M. B. Humphrey, J. A. Van Ziffle, Y. Hu, A. Burghardt, S. C. Spusta, S. Majumdar, L. L. Lanier, C. A. Lowell, and M. C. Nakamura. 2004. The immunomodulatory adapter proteins DAP12 and Fc receptor gamma-chain (FcRgamma) regulate development of functional osteoclasts through the Syk tyrosine kinase. *Proc. Natl. Acad. Sci. U. S. A* 101: 6158-6163.
74. Koga, T., M. Inui, K. Inoue, S. Kim, A. Suematsu, E. Kobayashi, T. Iwata, H. Ohnishi, T. Matozaki, T. Kodama, T. Taniguchi, H. Takayanagi, and T. Takai. 2004. Costimulatory signals mediated by the ITAM motif cooperate with RANKL for bone homeostasis. *Nature* 428: 758-763.
75. Faccio, R., S. L. Teitelbaum, K. Fujikawa, J. Chappel, A. Zallone, V. L. Tybulewicz, F. P. Ross, and W. Swat. 2005. Vav3 regulates osteoclast function and bone mass. *Nat. Med.* 11: 284-290.
76. Zou, W., H. Kitaura, J. Reeve, F. Long, V. L. Tybulewicz, S. J. Shattil, M. H. Ginsberg, F. P. Ross, and S. L. Teitelbaum. 2007. Syk, c-Src, the alphavbeta3 integrin, and ITAM immunoreceptors, in concert, regulate osteoclastic bone resorption. *J. Cell Biol.* 176: 877-888.
77. McHugh, K. P., K. Hodivala-Dilke, M. H. Zheng, N. Namba, J. Lam, D. Novack, X. Feng, F. P. Ross, R. O. Hynes, and S. L. Teitelbaum. 2000. Mice lacking beta3 integrins are osteosclerotic because of dysfunctional osteoclasts. *J. Clin. Invest* 105: 433-440.
78. Zou, W., J. L. Reeve, Y. Liu, S. L. Teitelbaum, and F. P. Ross. 2008. DAP12 couples c-Fms activation to the osteoclast cytoskeleton by recruitment of Syk. *Mol. Cell* 31: 422-431.

-
79. Hirayama, T., L. Danks, A. Sabokbar, and N. A. Athanasou. 2002. Osteoclast formation and activity in the pathogenesis of osteoporosis in rheumatoid arthritis. *Rheumatology. (Oxford)* 41: 1232-1239.
 80. Rajewsky, K., H. Gu, R. Kuhn, U. A. Betz, W. Muller, J. Roes, and F. Schwenk. 1996. Conditional gene targeting. *J. Clin. Invest* 98: 600-603.
 81. Sternberg, N., and D. Hamilton. 1981. Bacteriophage P1 site-specific recombination. I. Recombination between loxP sites. *J. Mol. Biol.* 150: 467-486.
 82. Metzger, D., J. Clifford, H. Chiba, and P. Chambon. 1995. Conditional site-specific recombination in mammalian cells using a ligand-dependent chimeric Cre recombinase. *Proc. Natl. Acad. Sci. U. S. A* 92: 6991-6995.
 83. Feil, R., J. Wagner, D. Metzger, and P. Chambon. 1997. Regulation of Cre recombinase activity by mutated estrogen receptor ligand-binding domains. *Biochem. Biophys. Res. Commun.* 237: 752-757.
 84. Livak, K. J., and T. D. Schmittgen. 2001. Analysis of relative gene expression data using real-time quantitative PCR and the 2(-Delta Delta C(T)) Method. *Methods* 25: 402-408.
 85. Wollin, L., and M. P. Pieper. 2010. Tiotropium bromide exerts anti-inflammatory activity in a cigarette smoke mouse model of COPD. *Pulm. Pharmacol. Ther.*
 86. Colbatzky, F., and W. Hermanns. 1987. Immunohistochemical demonstration of various antigens in tissues embedded in plastic. *Histochem. J.* 19: 589-593.
 87. Lojda, Z., R. Grossau, and T. H. Schiebler. 1979. *Enzyme Histochemistry. A Laboratory Manual.* Springer Verlag, Berlin.
 88. Buie, H. R., G. M. Campbell, R. J. Klinck, J. A. MacNeil, and S. K. Boyd. 2007. Automatic segmentation of cortical and trabecular compartments based on a dual threshold technique for in vivo micro-CT bone analysis. *Bone* 41: 505-515.
 89. Seibler, J., B. Zevnik, B. Kuter-Luks, S. Andreas, H. Kern, T. Hennek, A. Rode, C. Heimann, N. Faust, G. Kauselmann, M. Schoor, R. Jaenisch, K. Rajewsky, R. Kuhn, and F. Schwenk. 2003. Rapid generation of inducible mouse mutants. *Nucleic Acids Res.* 31: e12.
 90. Takata, M., H. Sabe, A. Hata, T. Inazu, Y. Homma, T. Nukada, H. Yamamura, and T. Kurosaki. 1994. Tyrosine kinases Lyn and Syk regulate B cell receptor-coupled Ca²⁺ mobilization through distinct pathways. *EMBO J.* 13: 1341-1349.

91. Braselmann, S., V. Taylor, H. Zhao, S. Wang, C. Sylvain, M. Baluom, K. Qu, E. Herlaar, A. Lau, C. Young, B. R. Wong, S. Lovell, T. Sun, G. Park, A. Argade, S. Jurcevic, P. Pine, R. Singh, E. B. Grossbard, D. G. Payan, and E. S. Masuda. 2006. R406, an orally available spleen tyrosine kinase inhibitor blocks fc receptor signaling and reduces immune complex-mediated inflammation. *J. Pharmacol. Exp. Ther.* 319: 998-1008.
92. Yamamoto, N., K. Takeshita, M. Shichijo, T. Kokubo, M. Sato, K. Nakashima, M. Ishimori, H. Nagai, Y. F. Li, T. Yura, and K. B. Bacon. 2003. The orally available spleen tyrosine kinase inhibitor 2-[7-(3,4-dimethoxyphenyl)-imidazo[1,2-c]pyrimidin-5-ylamino]nicotinamide dihydrochloride (BAY 61-3606) blocks antigen-induced airway inflammation in rodents. *J. Pharmacol. Exp. Ther.* 306: 1174-1181.
93. Yu, P., M. Kosco-Vilbois, M. Richards, G. Kohler, and M. C. Lamers. 1994. Negative feedback regulation of IgE synthesis by murine CD23. *Nature* 369: 753-756.
94. Payet, M. E., E. C. Woodward, and D. H. Conrad. 1999. Humoral response suppression observed with CD23 transgenics. *J. Immunol.* 163: 217-223.
95. Paterson, R. L., R. Or, J. M. Domenico, G. Delespesse, and E. W. Gelfand. 1994. Regulation of CD23 expression by IL-4 and corticosteroid in human B lymphocytes. Altered response after EBV infection. *J. Immunol.* 152: 2139-2147.
96. Sokol, C. L., G. M. Barton, A. G. Farr, and R. Medzhitov. 2008. A mechanism for the initiation of allergen-induced T helper type 2 responses. *Nat. Immunol.* 9: 310-318.
97. Starnes, L. M., C. M. Downey, S. K. Boyd, and F. R. Jirik. 2007. Increased bone mass in male and female mice following tamoxifen administration. *Genesis.* 45: 229-235.
98. Cornall, R. J., A. M. Cheng, T. Pawson, and C. C. Goodnow. 2000. Role of Syk in B-cell development and antigen-receptor signaling. *Proc. Natl. Acad. Sci. U. S. A* 97: 1713-1718.
99. Monroe, J. G. 2004. Ligand-independent tonic signaling in B-cell receptor function. *Curr. Opin. Immunol.* 16: 288-295.
100. Coffman, R. L. 1982. Surface antigen expression and immunoglobulin gene rearrangement during mouse pre-B cell development. *Immunol. Rev.* 69: 5-23.
101. Fulcher, D. A., and A. Basten. 1997. B cell life span: a review. *Immunol. Cell Biol.* 75: 446-455.
102. Bradding, P., A. F. Walls, and S. T. Holgate. 2006. The role of the mast cell in the pathophysiology of asthma. *J. Allergy Clin. Immunol.* 117: 1277-1284.

-
103. Stenton, G. R., M. Ulanova, R. E. Dery, S. Merani, M. K. Kim, M. Gilchrist, L. Puttagunta, S. Musat-Marcu, D. James, A. D. Schreiber, and A. D. Befus. 2002. Inhibition of allergic inflammation in the airways using aerosolized antisense to Syk kinase. *J. Immunol.* 169: 1028-1036.
104. Matsubara, S., G. Li, K. Takeda, J. E. Loader, P. Pine, E. S. Masuda, N. Miyahara, S. Miyahara, J. J. Lucas, A. Dakhama, and E. W. Gelfand. 2006. Inhibition of spleen tyrosine kinase prevents mast cell activation and airway hyperresponsiveness. *Am. J. Respir. Crit Care Med.* 173: 56-63.
105. Jakus, Z., E. Simon, B. Balazs, and A. Mocsai. 2010. Genetic deficiency of Syk protects mice from autoantibody-induced arthritis. *Arthritis Rheum.* 62: 1899-1910.
106. Perrigoue, J. G., S. A. Saenz, M. C. Siracusa, E. J. Allenspach, B. C. Taylor, P. R. Giacomin, M. G. Nair, Y. Du, C. Zaph, R. N. van, M. R. Comeau, E. J. Pearce, T. M. Laufer, and D. Artis. 2009. MHC class II-dependent basophil-CD4⁺ T cell interactions promote T(H)2 cytokine-dependent immunity. *Nat. Immunol.* 10: 697-705.
107. Sokol, C. L., N. Q. Chu, S. Yu, S. A. Nish, T. M. Laufer, and R. Medzhitov. 2009. Basophils function as antigen-presenting cells for an allergen-induced T helper type 2 response. *Nat. Immunol.* 10: 713-720.
108. Yoshimoto, T., K. Yasuda, H. Tanaka, M. Nakahira, Y. Imai, Y. Fujimori, and K. Nakanishi. 2009. Basophils contribute to T(H)2-IgE responses in vivo via IL-4 production and presentation of peptide-MHC class II complexes to CD4⁺ T cells. *Nat. Immunol.* 10: 706-712.
109. Mowen, K. A., and L. H. Glimcher. 2004. Signaling pathways in Th2 development. *Immunol. Rev.* 202: 203-222.
110. Wright, H. L., R. J. Moots, R. C. Bucknall, and S. W. Edwards. 2010. Neutrophil function in inflammation and inflammatory diseases. *Rheumatology. (Oxford)* 49: 1618-1631.
111. Zarbock, A., C. A. Lowell, and K. Ley. 2007. Spleen tyrosine kinase Syk is necessary for E-selectin-induced alpha(L)beta(2) integrin-mediated rolling on intercellular adhesion molecule-1. *Immunity.* 26: 773-783.
112. Letellier, E., S. Kumar, I. Sancho-Martinez, S. Krauth, A. Funke-Kaiser, S. Laudenklos, K. Konecki, S. Klussmann, N. S. Corsini, S. Kleber, N. Drost, A. Neumann, M. Levi-Strauss, B. Brors, N. Gretz, L. Edler, C. Fischer, O. Hill, M. Thiemann, B. Biglari, S. Karray, and A. Martin-Villalba. 2010. CD95-ligand on peripheral myeloid cells activates Syk kinase to trigger their recruitment to the inflammatory site. *Immunity.* 32: 240-252.

113. Zhang, Y., B. F. Ramos, and B. A. Jakschik. 1991. Augmentation of reverse arthus reaction by mast cells in mice. *J. Clin. Invest* 88: 841-846.
114. Nigrovic, P. A., B. A. Binstadt, P. A. Monach, A. Johnsen, M. Gurish, Y. Iwakura, C. Benoist, D. Mathis, and D. M. Lee. 2007. Mast cells contribute to initiation of autoantibody-mediated arthritis via IL-1. *Proc. Natl. Acad. Sci. U. S. A* 104: 2325-2330.
115. Blaschke, S., M. Koziolok, A. Schwarz, P. Benohr, P. Middel, G. Schwarz, K. M. Hummel, and G. A. Muller. 2003. Proinflammatory role of fractalkine (CX3CL1) in rheumatoid arthritis. *J. Rheumatol.* 30: 1918-1927.
116. Nanki, T., Y. Urasaki, T. Imai, M. Nishimura, K. Muramoto, T. Kubota, and N. Miyasaka. 2004. Inhibition of fractalkine ameliorates murine collagen-induced arthritis. *J. Immunol.* 173: 7010-7016.
117. Combadiere, C., S. Potteaux, J. L. Gao, B. Esposito, S. Casanova, E. J. Lee, P. Debre, A. Tedgui, P. M. Murphy, and Z. Mallat. 2003. Decreased atherosclerotic lesion formation in CX3CR1/apolipoprotein E double knockout mice. *Circulation* 107: 1009-1016.
118. Lesnik, P., C. A. Haskell, and I. F. Charo. 2003. Decreased atherosclerosis in CX3CR1^{-/-} mice reveals a role for fractalkine in atherogenesis. *J. Clin. Invest* 111: 333-340.
119. McDermott, D. H., A. M. Fong, Q. Yang, J. M. Sechler, L. A. Cupples, P. W. Wilson, R. B. D'Agostino, C. J. O'Donnell, D. D. Patel, and P. M. Murphy. 2003. Chemokine receptor mutant CX3CR1-M280 has impaired adhesive function and correlates with protection from cardiovascular disease in humans. *J. Clin. Invest* 111: 1241-1250.
120. Kyttaris, V. C., and G. C. Tsokos. 2007. Syk kinase as a treatment target for therapy in autoimmune diseases. *Clin. Immunol.* 124: 235-237.
121. Faccio, R., W. Zou, G. Colaianni, S. L. Teitelbaum, and F. P. Ross. 2003. High dose M-CSF partially rescues the Dap12^{-/-} osteoclast phenotype. *J. Cell Biochem.* 90: 871-883.

8. ACKNOWLEDGEMENTS

First of all I would like to thank Dr. Andreas Schnapp and Dr. Lutz Wollin for their guidance and scientific support and for patiently proof-reading my manuscript drafts and numerous previous versions of this thesis over and over again.

I would like to thank PD Dr. Florian Gantner for providing me the opportunity to accomplish my Ph.D. thesis in the department of respiratory diseases research.

I would like to thank Prof. Alexander Tarakhovsky for providing the *Syk^{fl/+}* animals.

I am grateful to Prof. Peter Augat, Dr. Julia Koerber, Dr. Ahmed Abdulazim and Rainer Penzkofer for the successful collaboration concerning the bone measurements.

I would like to thank Dr. Florian Colbatzky and Anja Krämer for sharing their expertise in the field of bone histology.

I am grateful to Martina Hagel, Sylvia Blum, Eva Zeller, Martina Keck and Heike Ernst. Apart from teaching me everything I know about animal handling and apart from helping me whenever I needed support you became great friends.

I would like to thank Christine Strasser, Margit Ried, Alexandra Franz, Bernd Guilliard and Christine Pischzan for their personal support and most of all for the many good laughs that we had in the lab which sometimes turned a bad day around.

Special thanks go to Matthias Düchs and Tobias Kiechle for the many times that you prepared dinner for me, for encouraging me when I needed motivation, for the distractions when I was working insane hours and for just listening when I was complaining about the same things over and over again.

My deepest thanks go to my family and Basti for their support and patience, for motivating me throughout difficult times, for putting up with my bad moods and most of all for listening to my complaints and worries.

9. PUBLICATIONS

Sanderson, M. P.; Wex, E.; Kono, T.; Uto, K.; Schnapp, A.; (2010) Syk and Lyn mediate distinct Syk phosphorylation events in FcεRI-signal transduction: Implications for regulation of IgE-mediated degranulation. *Mol. Immunol.* 48(1-3): 171-178.

Wex, E.; Bouyssou, T.; Duechs, M.; Erb, K.; Gantner, F.; Sanderson, M.; Schnapp, A.; Stierstorfer, B.; Wollin, L.; (2011) Induced Syk deletion leads to suppressed allergic responses but has no effect on neutrophil or monocyte migration *in vivo*. *Eur. J. Immunol.* 41(11): 3208-3218.

Ozaki, N.; Sato, Y.; Harada, Y.; Tanaka, K.; Wex, E.; Wollin, L.; Schnapp, A.; Kono, T.; Kubo, M.; Kitamura, D.; Encinas, J.; Hara, H.; Suzuki, S.; Yoshida, H.; Syk-dependent signaling pathways are indispensable in the pathogenesis of anti-collagen antibody-induced arthritis. (Manuscript submitted)

Wex, E.; Koerber, J.; Abdulazim, A.; Colbatzky, F.; Penzkofer, R.; Schnapp, A.; Wollin, L.; Gantner, F.; Augat, P.; Long-term deletion of SYK results in slight improvement of mechanical bone properties in adult mice. (Manuscript in preparation)